

Oralloy (93.2²³⁵U) Metal Cylinder with Beryllium Top Reflector

John D. Bess
Leland M. Montierth
Nathan Devine
Fitz Trumble
John T. Mihalczko

September 2010



The INL is a U.S. Department of Energy National Laboratory
operated by Battelle Energy Alliance

Oralloy (93.2²³⁵U) Metal Cylinder with Beryllium Top Reflector

**John D. Bess
Leland Montierth
Nathan Devine¹
Fitz Trumble¹
John T. Mihalcz²**

¹Washington Safety Management Solutions LLC

²Oak Ridge National Laboratory

September 2010

**Idaho National Laboratory
Idaho Falls, Idaho 83415**

<http://www.inl.gov>

**Prepared for the
U.S. Department of Energy
Office of Nuclear Energy
Under DOE Idaho Operations Office
Contract DE-AC07-05ID14517**

**ORALLOY (93.2 ²³⁵U) METAL CYLINDER
WITH BERYLLIUM TOP REFLECTOR**

Evaluator

**John D. Bess
Idaho National Laboratory**

**Internal Reviewer
Leland M. Montierth**

Independent Reviewers

**Nathan Devine
Fitz Trumble
Washington Safety Management Solutions LLC**

**John T. Mihalcz
Oak Ridge National Laboratory**

ORALLOY (93.2 ²³⁵U) METAL CYLINDER WITH BERYLLIUM TOP REFLECTOR

IDENTIFICATION NUMBER: HEU-MET-FAST-069

SPECTRA

KEY WORDS: acceptable, beryllium-moderated, beryllium-reflected, critical experiment, cylinder, fast-spectrum, highly enriched, metal, one-side reflected, oralloy, uranium

1.0 DETAILED DESCRIPTION

1.1 Overview of Experiment

A variety of critical experiments were constructed of enriched uranium metal (oralloy^a) during the 1960s and 1970s at the Oak Ridge Critical Experiments Facility (ORCEF) in support of criticality safety operations at the Y-12 Plant. The purposes of these experiments included the evaluation of storage, casting, and handling limits for the Y-12 Plant and providing data for verification of calculation methods and cross-sections for nuclear criticality safety applications. These included solid cylinders of various diameters, annuli of various inner and outer diameters, two and three interacting cylinders of various diameters, and graphite and polyethylene reflected cylinders and annuli.

Of the hundreds of delayed critical experiments, one experiment was comprised of a stack of approximately 7-inch-diameter metal discs. The bottom of the stack consisted of uranium with an approximate height of 4-1/8 inches. The top of the stack consisted of beryllium with an approximate height of 5-9/16 inches. This experiment was performed on August 20, 1963 by J. T. Mihalczo and R. G. Taylor (Ref. 1) with additional information in its corresponding logbook.^b

Unreflected and unmoderated experiments with the same set of highly enriched uranium metal parts were performed at the Oak Ridge Critical Experiments Facility in the 1960s and are evaluated in [HEU-MET-FAST-051](#). Thin graphite reflected (2 inches or less) experiments also using the same set of highly enriched uranium metal parts are evaluated in [HEU-MET-FAST-071](#). Polyethylene-reflected configurations are evaluated in [HEU-MET-FAST-076](#). Highly enriched metal annuli with beryllium cores are evaluated in [HEU-MET-FAST-059](#).

Both detailed and simplified model specifications are provided in this evaluation. This fast-spectra experiment was determined to be an acceptable benchmark experiment. The calculated eigenvalues for both the detailed and the simple models are within approximately 0.5% of the benchmark values, but exceed the benchmark values by significantly greater than 3 σ from the benchmark value because the uncertainty in the benchmark is very small: ± 0.0003 (1 σ). There is significant variability between results using different neutron cross section libraries, the greatest being a Δk_{eff} of $\sim 0.64\%$.

This benchmark experiment was compared to a similar bare HEU configuration (Appendix D). The reflector mass savings (reduction in critical mass by the addition of the beryllium top reflector to an unreflected cylinder of the same diameter) is 9.922 kg HEU, and the calculated reactivity worth of the beryllium reflector is 10.7 ± 0.5 dollars (\$).

^a Oralloy stands for Oak Ridge Alloy, and consists of HEU metal with an ²³⁵U enrichment of more than 93%.

^b Experimental data for this experiment can be found on pages 135-140 of ORNL logbook 13R (East Cell -- Logbook 2).

1.2 Description of Experimental Configuration

The experiment was performed in the 35 × 35 × 30-ft-high East Cell of the ORCEF, and the uranium assembly was located approximately 11.7 ft from the 5-ft-thick concrete west wall, 12.7 ft from the 2-ft-thick concrete north wall, and 9.2 ft above the concrete floor.

This single top-side-reflected experiment consisted of a stack of four uranium discs with a nominal height of ~4-1/8 inches and a diameter of ~7 inches. The reflector was comprised of five beryllium discs with a combined height of ~5-9/16 inches and diameter of ~7 inches (see Figure 1). A thin stainless steel (SS304) diaphragm separated the two bottommost uranium discs.

Detectors used for reactor period measurements were placed 10 to 15 feet away and consisted of BF₃ boron-lined ionization chambers. The reactivity worth was obtained from the difference in two measurements; one without the change and the other with the change. The inhour equation was then used to convert reactor period to reactivity. A neutron source was near the assemblies for startup only and was withdrawn ~4 feet away into a borated paraffin shield during the measurements. Measurements were performed at fission rates such that the neutrons coming out of the shield from the startup source were insignificant.^a

1.2.1 General Assembly Procedure – The experiment was constructed on a vertical assembly machine (shown in Figure 2), which primarily consisted of a hydraulic lift (22-inch vertical motion) to support the lower section and a stationary upper section (The upper support shown in the Figure 2 was not used in this experiment).

For unreflected experiments (i.e., no significant amounts of reflector material was placed around the periphery of the experiment), the lower support stand held the uranium metal of the lower section in place. The lower section was supported on 0.125-inch-thick aluminum edges, oriented vertically 120 degrees apart (visible in Figure 3). The upper section was supported by four vertical posts, which held a low-mass support consisting of two 30-inch-ID, 2-inch wide, 0.5-inch-thick, aluminum clamping rings bolted together and supported off vertical poles by aluminum tubing; see Figure 3. The 30-inch-diameter clamping rings held a 0.010-inch-thick stainless steel (304L) diaphragm on which the upper uranium metal section was supported. The lower section was supported on a low-mass support stand (sometimes referred to as a support tower) mounted in the vertical position and also shown in Figure 3. The 0.5-inch-thick, 18-inch-diameter aluminum base of this support stand was bolted to the 1-inch-thick, 18-inch-diameter stainless steel table of the vertical lift as shown in Figure 3. The lower surface of the uranium was at a height of 36 inches above the aluminum base. Small aluminum pieces bolted to the 120° vertical members restrained lateral motion of the lower section. These low mass supports were used to minimize the reflection effects of support structure. The aluminum base of the support stand is type Al6061 and the stainless steel table is type 304L.^b Additional structural detail for the lower support stand and diaphragm clamping ring are given in Appendix E.

Experiments were assembled by mounting a fixed height of uranium metal parts on the lower section, after which uranium and reflector materials were added to the upper section until near delayed criticality was achieved. For these experiments, the lower section was raised until it made contact with the diaphragm and actually slightly lifted the upper section of material mounted on the diaphragm. The lifting of the top section slightly by the bottom section was used to compensate for the sag of the diaphragm due to the weight of the upper material. The lifting of the diaphragm was monitored to the nearest 0.001 inches and the lower section was moved up only until the diaphragm was level. Due to the thickness of the smallest uranium parts, the system could rarely be adjusted to exactly delayed criticality. For most assemblies the uranium mass of the upper section was adjusted until a self-sustaining fission chain reaction occurred with a measurable positive stable reactor period. For assemblies that were slightly subcritical, an additional hydrogenous reflector

^a Personal communication with John T. Mihalcz, March 2010.

^b Personal communication with John T. Mihalcz, February 2010.

(small piece of Plexiglas) was added as a reflector to achieve a self-sustaining chain reaction. When the fission rate achieved a value from which a negative reactor period could be measured, the Plexiglas was quickly (within a fraction of a second)^a removed to measure the resulting negative reactor period.

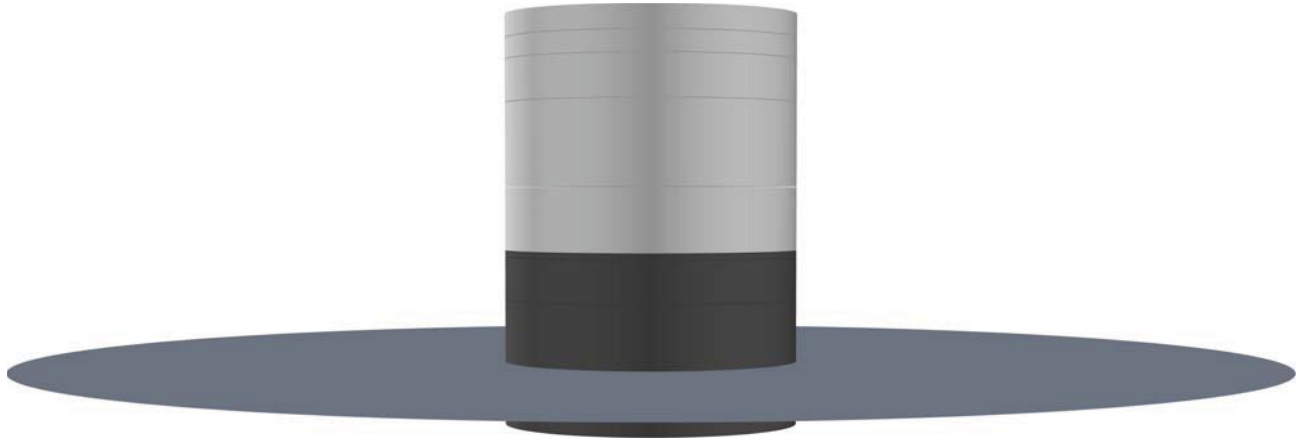


Figure 1.a. Orallo Metal Cylinders with Beryllium Top Reflector.

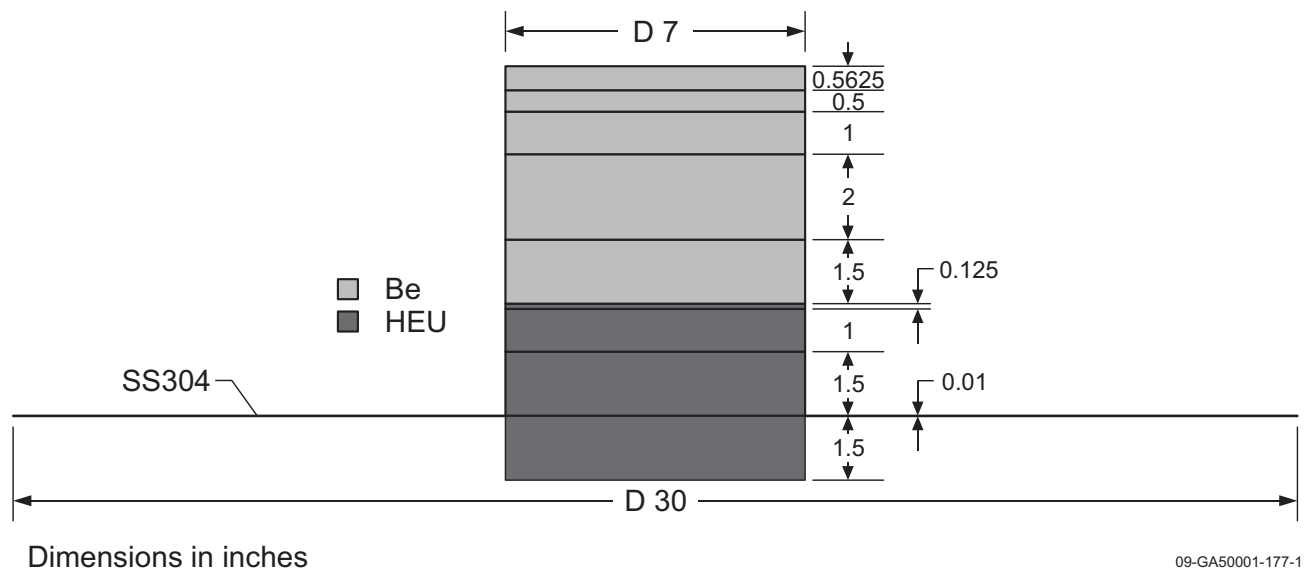


Figure 1.b. Orallo Metal Cylinders with Beryllium Top Reflector (dimensions are nominal).

^a Personal communication with John T. Mihalczo in [HEU-MET-FAST-076](#), June 2006.

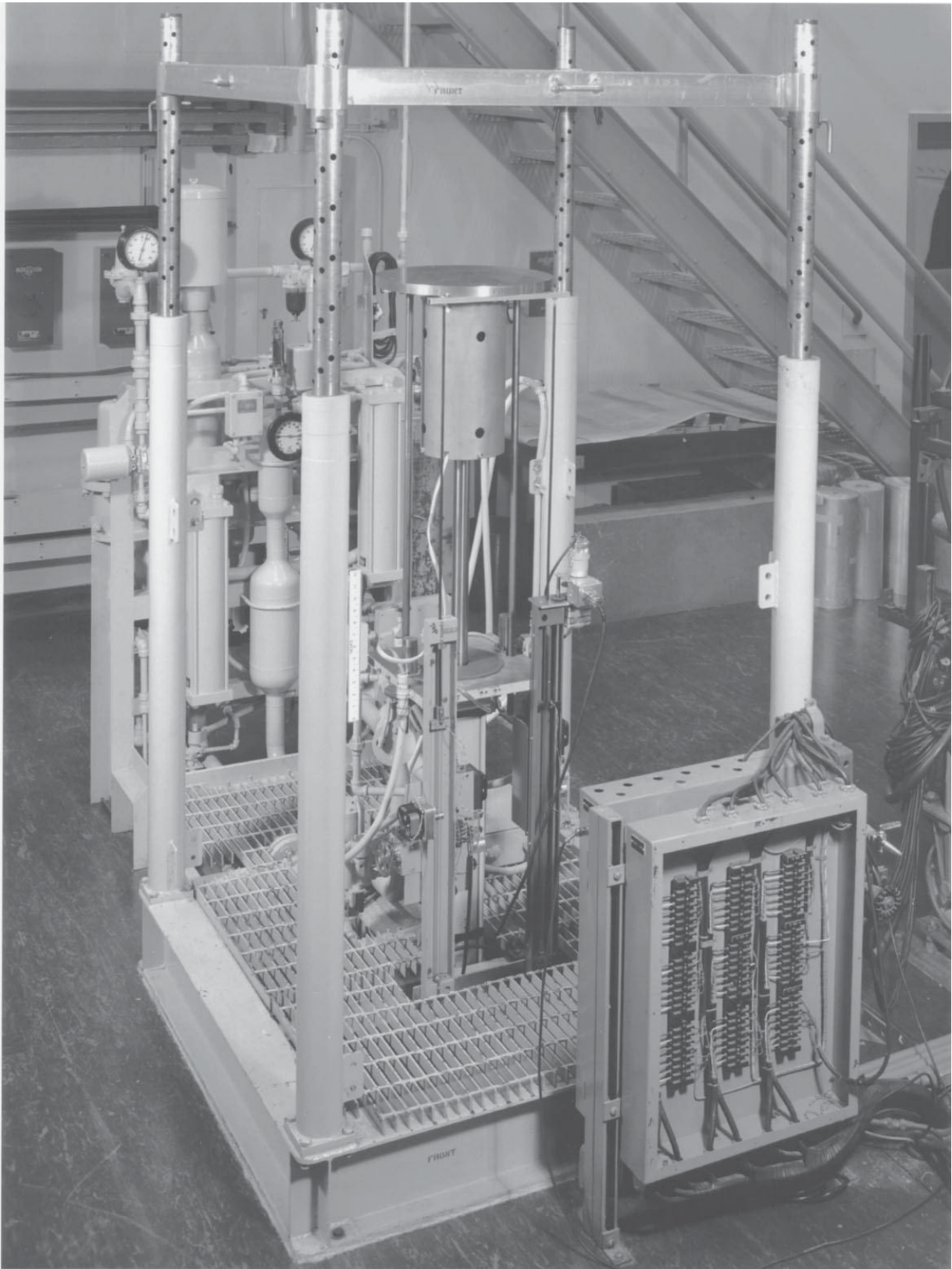


Figure 2. Photograph of the Vertical Assembly Machine with the Movable Table Up.
(The upper support shown in this photograph was not used in these measurements.)

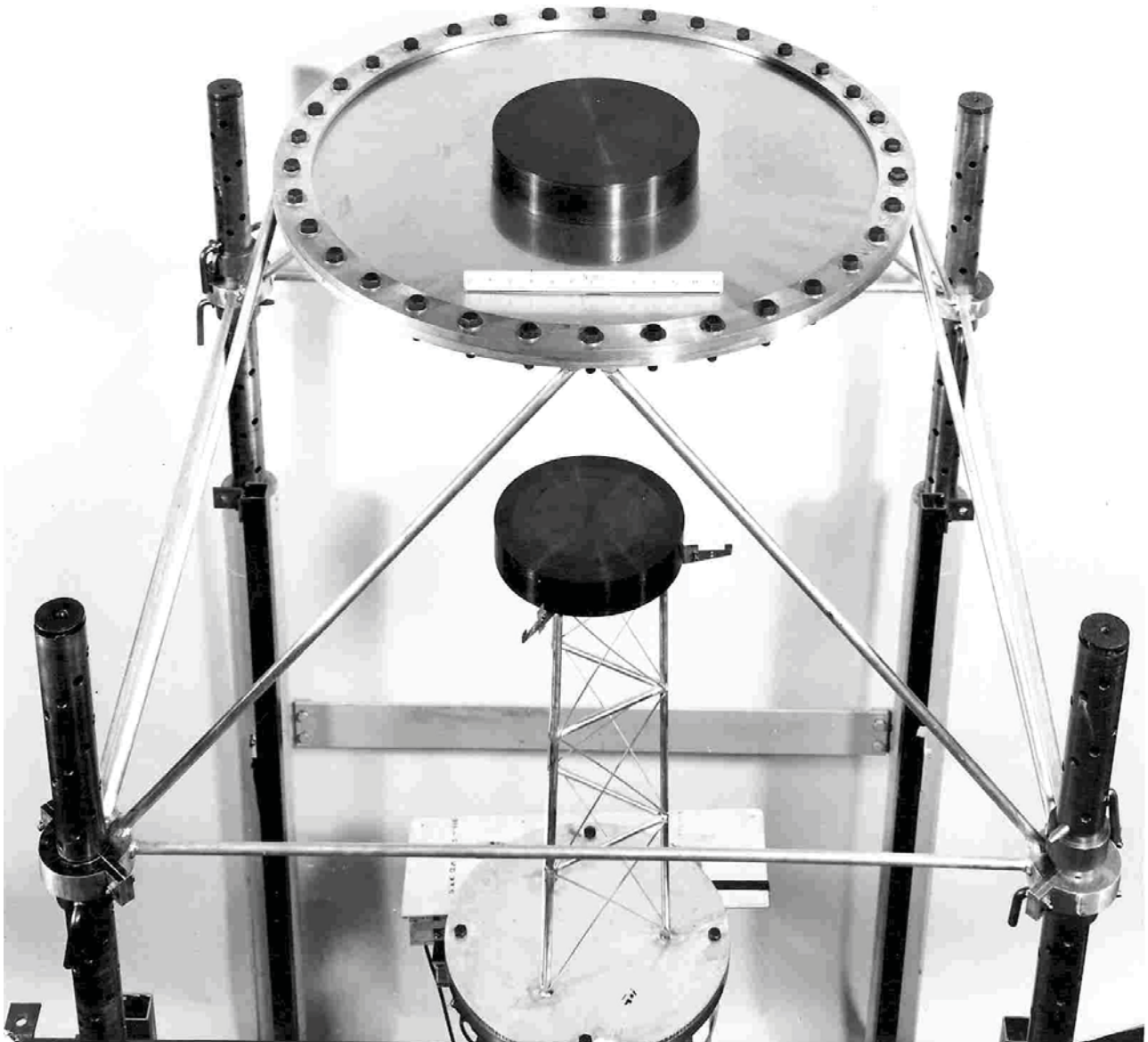


Figure 3. A Typical Uranium Metal Assembly of Two Interacting 11-inch-Diameter Cylinders at Close Spacing on the Vertical Assembly Machine.^a

(Similar supports were used in these measurements and are described in Appendix E.)

^a Photo 39380, Oak Ridge National Laboratory photo of a bare uranium assembly. This same support structure was used for internally Be moderated, unreflected uranium metal annuli and top-Be-reflected experiments.

1.2.2 Stack Height of Discs – Assembly heights at different angular locations for the experiment were measured to within ± 0.001 inches by stacking them on a precision flat surface and measuring the distance between the upper surface of uranium and the precision flat surface. Multiple measurements were performed with all parts assembled in the same vertical order and angular orientation that they were in the critical experiment. Measured heights of the three uranium metal discs stacked on top of the diaphragm are given in Table 1. The beryllium reflector stack was also measured and the heights are also reported in Table 1. The average stack heights were calculated and reported in the original logbooks. The standard deviation has been calculated using the original data.

Table 1. Stack Height (in.) Measurements.

Measurement	Top Stack of Uranium	Beryllium
1	2.630	5.570
2	2.631	5.570
3	2.6305	5.570
4	2.630	5.570
5	2.630	5.570
6	2.6315	5.573
7	2.630	5.571
8	2.630	5.573
9	2.631	5.575
10	--	5.574
11	--	5.572
Average	2.630	5.572
1 σ	0.001	0.002

1.2.3 Assembly Alignment

Radial Alignment of Upper Section: For assembly of the upper section, uranium metal was added to the top of the Type 304L stainless steel diaphragm. Uranium was positioned, with a ruler, the appropriate distance from the inside of the aluminum clamping ring, which held the 0.010-inch-thick stainless diaphragm. The location of the material was continuously adjusted with a precise high-quality level in one direction and then the level was rotated 90° on the top of the uranium. If the assembly was not exactly centered on the diaphragm, it would not be precisely level because of the sag in the diaphragm as it was loaded. Two precisely machined steel blocks (± 0.0001 inches) were used to squeeze the outside radial surface of the uranium metal until it was aligned. An edge of the machined block was then held at one outside radial location, squeezing the uranium together until no light was visible between the machined block and the uranium metal. This process was repeated 90° from the position of the original adjustment, rechecked again at the original position, and small adjustments made if necessary. This process continued until the outside radii of the parts were precisely aligned and the upper section assembly was complete. The squeezing procedure was performed by one individual while another person observed the light coming through small

gaps between the blocks and the uranium metal.^a The alignment of outer radii of the upper or lower section was less than ± 0.001 inches. Of course, if two positions 90° apart are adjusted, the positions at 180° and 270° can be off only by the difference in the diameters of the outside parts.

Radial Alignment of Lower Section: For the lower section, uranium was centrally located on the lower support stand and the same procedure was used except that the leveling of the parts was accomplished by shimming with aluminum foil (various thicknesses of aluminum foil were available). The foil was placed between the three 120° upper edges of the lower support stand and the lowest parts.

Radial Alignment Accuracy Summary: Uncertainty in radial alignment of uranium metal parts on each half is ± 0.001 inches.

Lateral Alignment of Upper Section with the Lower Section: For these experiments, the alignment of the upper and lower sections was adjusted and verified using the Lateral Alignment Fixture shown in Figure 4. There were two identical fixtures used for lateral alignment between the upper section and the lower section. They were U-shaped and were machined out of 0.375-inch-thick aluminum. The end pieces were carefully machined by the Y-12 shops to be perpendicular to the long direction of the fixture and coplanar with each other. When leveled properly, the front face of the $4 \times 4 \times \frac{1}{2}$ -inch-thick end pieces were vertical and in the same plane to within ± 0.001 inches. In use, the lower side of the upper leg rested on the top surface of the clamping ring for the diaphragm. The fixture was perpendicular to the outer radial surface and was moved inward until it touched the uranium of the top section. The leveling screws were adjusted until the fixture was level.

The second fixture was placed 90° apart from the first in a similar manner. Both fixtures were moved back slightly, and the lower section was raised until it was at the height of the lower leg of the U-shaped fixtures. Both fixtures were then nearly adjusted properly. Removal or additions of material from the upper section sometimes required small leveling adjustments. The fixtures were moved in until they touched uranium (either on the upper or the lower section). When lack of contact was observed at either of the front faces of the fixture, the lower section was lowered to the full-out position, and the position of the uranium on the lower support stand was adjusted. Finally, the lower lift table was raised and the alignment was checked.

The process was repeated several times as necessary. The final 0.005-inch adjustments were usually made by moving the upper section. This was a long and tedious procedure, which took one to two hours or more as needed but was always performed and resulted in uranium metal of the upper and lower sections being aligned within ± 0.005 inches.

Lateral Alignment Accuracy Summary: Upper and lower assembly uranium metal alignment uncertainty is ± 0.005 inches.

^a Personal communication with John T. Mihalcz, March 2010.

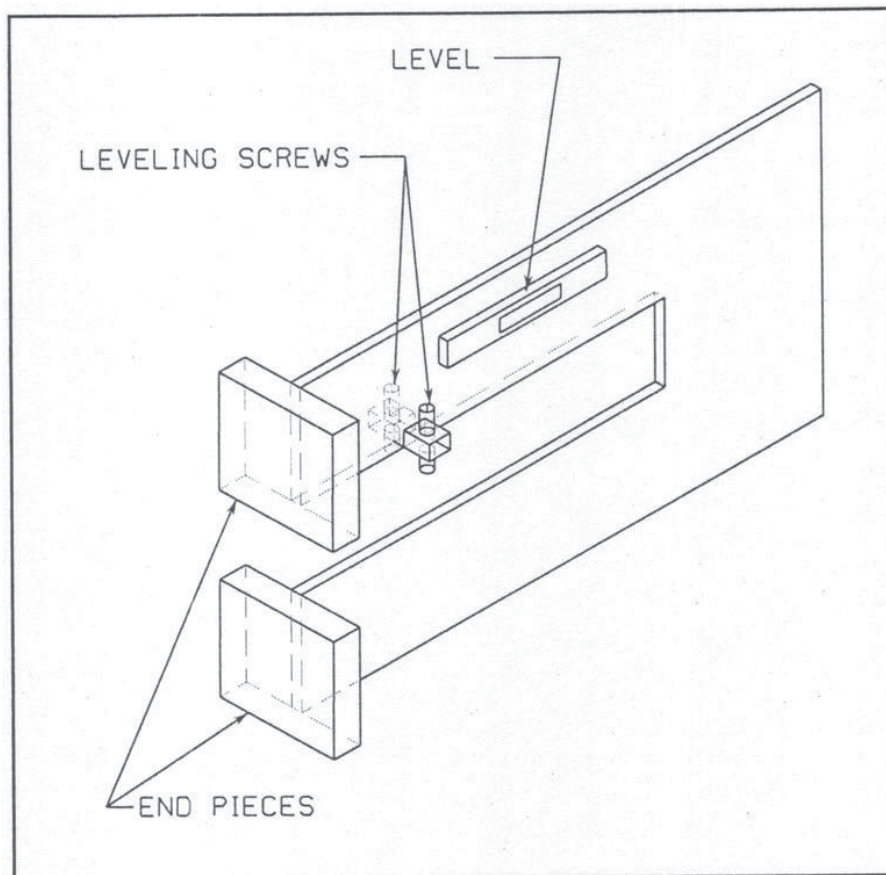


Figure 4. Sketch of Fixture for Lateral Alignment of Uranium.

1.2.4 Reactivity Effects of Support Structure – The support structure that was used to assemble these experiments was made up of the 0.010-inch-thick Type 304L stainless steel diaphragm, low-mass aluminum support stand, and two 30-inch-diameter, 2-inch-wide, 0.5-inch-thick diaphragm clamping rings bolted together. The support structure reactivity worth consisted primarily of the reactivity effects of the diaphragm, the diaphragm support rings, and the low-mass support stand. The reactivity worth of each of these three parts of the support structure was measured or estimated from other measurements.

Additional figures depicting the assembly support structure are provided in Appendix E.

A positive reactivity effect means that the reactivity of the critical assembly increased due to the inclusion of that item in the assembly. Therefore, removing that particular item from the experiment resulted in a decrease in the neutron multiplication factor. A negative reactivity effect means that the reactivity of the assembly decreased due to the item's inclusion. The Type 304L stainless steel diaphragm reduced the k_{eff} of the system since it separated uranium metal halves and introduced neutron absorbing material between them. The presence of the diaphragm support ring and low-mass support stand of the lower section resulted in a positive reactivity addition. The presence of the support ring and low-mass stand provided neutron reflection to the system. The combined reactivity effect of all other supports, such as the four vertical poles and tubing for the diaphragm support ring, was reported to be less than one cent and was not evaluated.

The reactivity of the support structure, when measured, was evaluated by assembling the system to delayed criticality or a known measured reactivity, adding additional support structure, and obtaining the reactivity of the support structure from the measured reactor period for the assembly with and without the additional

support structure. The effect of the lower support stand was estimated from other measurements with 7-in-diameter uranium experiments. To estimate the effect of the diaphragm and clamping ring, their thicknesses were doubled and the reactivity change was measured. Where multiple instruments were used to measure the reactor period, the reactivity values obtained were averaged. These effects were measured for the components listed in Table 2. The reactivity worth of the entire support structure is obtained by adding the worth of the three components of the support structure: annular diaphragm rings, stainless steel diaphragm, and low-mass support stand. Multiple measurements for the reactivity effects of the support structure were unavailable.

The worths of the diaphragm and the diaphragm support structure were measured and the worth of the low-mass stand was estimated from other experiments. The measured worth of the diaphragm includes the separation distance between the two halves of the experiment.^a

Table 2. Reactivity Effects of Removing All Support Structure.

Reactivity of Support Structure (cents) ^(a)				
Diaphragm	Rings and Diaphragm	Rings ^(b)	Low-Mass Support Stand	All Support Structure
+10.33	+8.00	-2.33	-15 ^(c)	-7

- (a) These values were obtained by comparing the worth measurements between two slightly different configurations, where the difference is the portion of the support structure being evaluated. A total of three configurations were needed to evaluate the two worth measurements (for the diaphragm and rings), where one of the configurations was that of the clean critical experiment.
- (b) The worth of the rings was obtained by taking the difference between the worth of removing the rings and diaphragm and the worth of removing just the diaphragm.
- (c) Estimated from other similar experiments.

The effective delayed-neutron fraction, β_{eff} , reported for this experiment is 0.0066. The full assembly was 9.6¢ above delayed critical (k_{eff} of 1.0006) and the assembly, as depicted in Figure 1, was 7.73¢ below delayed critical (k_{eff} of 0.9995). The experiment without any of the assembly or the diaphragm was 2.6¢ above delayed critical (k_{eff} of 1.0002).

The diaphragm bolts were not included in the experimental analysis of the support structure worth. The 304L stainless steel bolts are 0.5 in. (1.27 cm) in diameter and 1.5 in. (3.81 cm) long.^b

1.2.5 Uranium Components – The average dimensions and masses of the uranium metal parts for these experiments are given in Table 3 and come from the Y-12 database; the dimensions are measured to within 1×10^{-4} inches with an uncertainty of 5×10^{-5} inches and the masses of the parts are accurate to within 0.5 grams. All dimensional measurements for the parts were measured at 70° F at the Y-12 plant. The readout of the measuring device was calibrated to 0.0001 in. (0.000254 cm) using standards traceable back to the

^a Personal communication with John T. Mihalcz, February 2010.

^b Personal communication with John T. Mihalcz, June-July 2010.

National Bureau of Standards (now NIST). An average of more than one measurement could result in the recording of a fifth digit.^a

The average gap thickness between uranium metal parts were obtained by subtracting the sum of the heights of the individual parts in the stack from the measured stack height, and then dividing this value by the number of parts in the stack minus one. The density of each part can be obtained by dividing the reported mass of the part by the volume, which is calculated using the values provided in Table 3.

Table 3. Properties of Uranium (93.2 wt.% ²³⁵U) Metal Cylinders.

Part Number	Mass (g)	Height (in.)	Diameter (in.)
2732	11,814	1.00125	6.9960
2733	17,742	1.5026	6.99675
2734	17,742	1.50165	6.9964
2768	1,481	0.1250	6.9965

1.2.6 Beryllium Components – The nominal 7-inch-diameter reflector is comprised of a stack of five beryllium discs with nominal thicknesses of 1/2, 9/16, 1, 1.5, and 2 inches. Detailed dimensional data were not available. These beryllium discs were fabricated to nominally fit inside an annulus with 9 in. (22.86 cm) outer diameter and 7 in. (17.78 cm) inner diameter and the diameter of the discs should be within 0.001 in. (0.00254 cm) of the average of the oralloy metal discs and have the same uncertainties in machining.^b The beryllium discs were also measured at Y-12 with a measuring device that was accurate to 0.0001 in. (0.000254 cm) and traceable back to the National Bureau of Standards.^c

1.2.7 Experimental Configuration – The experimental assembly comprised of the uranium and beryllium discs with the stainless steel diaphragm provided in the reference, with the part locations identified, is shown in Figure 5.

^a Personal communication with John T. Mihalczo, March 2010.

^b Personal communications with John T. Mihalczo, October 2009 and July 2010.

^c Personal communication with John T. Mihalczo, March 2010.

HEU-MET-FAST-069

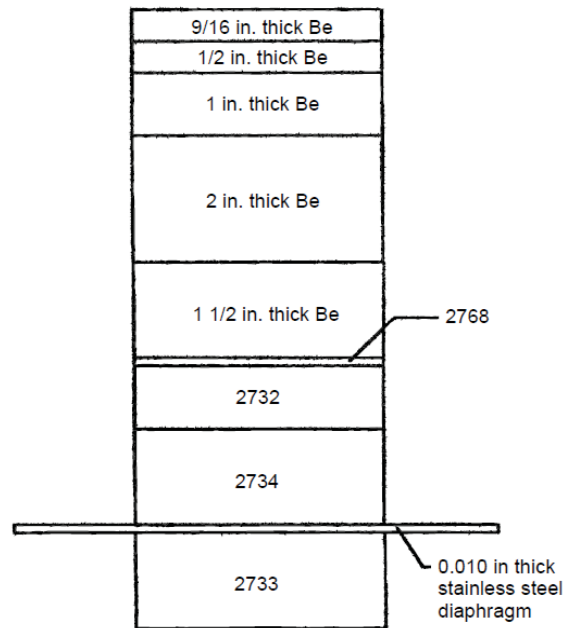


Figure 5. Schematic of the Experimental Assembly.

1.3 Description of Material Data

1.3.1 Uranium Components – The uranium metal parts for these critical experiments were carefully cast and machined at the Oak Ridge Y-12 Plant in the early 1960s. Each uranium metal part was a separate casting which was then machined. Dimensions, masses, uranium isotopics, and impurity content were measured after machining. Uranium part masses and dimensions can be found in Table 3. The total uranium mass is 48.779 kg, which is the sum of the individual part masses.

The uranium isotopics obtained from spectrographic analyses are given in Table 4. The average isotopic contents of the uranium are 0.95 wt.% ^{234}U , 93.17 wt.% ^{235}U and 0.24 wt.% ^{236}U with an average impurity content of ~500 ppm. The uncertainty in the measured values for ^{234}U , ^{235}U , and ^{236}U are 5×10^{-3} wt.%. The ^{238}U values were obtained by subtracting the sum of the other three from 100%.

The impurities from the 11 spectrographic analyses performed are given in Table 5 for uranium parts; only average and variation information exist.^a These 11 randomly sampled uranium parts include discs and annular parts. As such, the information presented is a representative average of the impurity content in all uranium parts. These values are consistent with the nominal impurity content of highly enriched uranium metal at the Oak Ridge Y-12 Plant at the time the parts were made (i.e., 99.95 g of U per 100 g of material). Oxygen and nitrogen content was assumed by the experimentalist to be 20 and 30 ppm, respectively, consistent with highly enriched uranium produced at the time of these experiments.^b

The HEU parts were coated annually in a very thin film of lightweight fluorocarbon oil to decrease oxidation removal. This oil has negligible effect upon the experiment conditions. After oiling, the parts were wiped with a dry rag to remove most of the oil. The alloy parts were then handled by leather gloves, which further reduced the oil on the surface.^c

Table 4. Uranium Disc Isotopic Content.^(a)

Part Number	^{234}U (wt.%)	^{235}U (wt.%)	^{236}U (wt.%)	^{238}U (wt.%) ^(b)
2732	0.95	93.17	0.21	5.67
2733	0.96	93.15	0.26	5.63
2734	0.95	93.18	0.24	5.63
2768	0.92	93.14	0.26	5.68

(a) Mass spectrographic analysis, unless noted otherwise.

(b) By difference from 100% pure uranium.

^a J. T. Mihalcz, "Graphite and Polyethylene Reflected Uranium-Metal Cylinders and Annuli," Union Carbide Corporation Nuclear Division, Oak Ridge Y-12 Plant, Y-DR-81 (1972).

^b [HEU-MET-FAST-076](#).

^c Personal communication with John T. Mihalcz, June 2010.

Table 5. Measured Impurity Content of Uranium Metal Cylinders, Annuli, and Plates.^(a)

Element ^(a)	Parts per Million by Weight (ppm) ^(b)	Variation (ppm)	Standard Deviation (ppm) ^(c)
Ag	8	3-25	3.2
Ba	< 0.01 ^(d)	-	0.005
Bi	164	81-311	52.9
C	< 10	-	2.4
Ca	0.1	-	0.05
Cd	< 1	-	0.5
Co	5	2-15	1.9
Cr	7	4-12	1.9
Cu	25	10-40	8
K	< 0.2	0.2-0.8	0.1
Li	< 2	-	1
Mg	3	2-3	1.7
Mn	56	25-89	17.1
Mo	< 1	< 1 – 1	0.5
Na	27	15-50	7.7
Ni	100	-	10
Sb	38	10-80	17.4
Ti	1	-	0.5

- (a) Mass spectrographic analysis except for oxygen and nitrogen using data in J. T. Mihalczo, "Graphite and Polyethylene Reflected Uranium-Metal Cylinders and Annuli," Union Carbide Corporation Nuclear Division, Oak Ridge Y-12 Plant, Y-DR-81 (April 28, 1972). Oxygen and nitrogen content was assumed by the principal experimentalist to be 20 and 30 ppm, respectively, consistent with highly enriched uranium produced at the time of these experiments. Total impurity content is consistent with stated values at that time of 500 ppm which gives 99.95 grams of U per 100 grams of material. Minor differences in the impurities exist between values listed in Table 5 and the impurity values provided in [HEU-MET-FAST-051](#).
- (b) Except for the values shown as less than the detection limit, impurity data are average values from 11 randomly sampled uranium parts.
- (c) Personal communication, J. A. Mullens to John Mihalczo in [HEU-MET-FAST-076](#), June 2004.
- (d) Less than (<) indicates lower detection limit and not necessarily that the impurity is present.

1.3.2 Beryllium Components – The measured mass of the beryllium stack is 6.433 kg with an average calculated density of 1.831 g/cm³. The beryllium discs were machined at the Y-12 Plant from material obtained from Brush Beryllium and had the reported average, or expected, impurities shown in Table 6 and would have been machined and measured with the same accuracy and precision as the uranium discs.^a The individual masses of each beryllium disc are reported in the logbook^b and summarized in Table 7.

^a Personal communication with John T. Mihalczo, November 2009.

^b Page 1 of ORNL logbook 13R (East Cell -- Logbook 2).

Table 6. Material Density and Impurities of Unmachined Beryllium.^(a)

Density (g/cm ³)	1.854 ^(b)
Impurity	wt. %
BeO	1.93
Al	0.06
C	0.12
Fe	0.13
Mg	0.02
Bi	0.05
B	0.001
Cd	0.0002
Dy	0.0001
Br	0.00005
Gd	0.0001
Ni	0.0001
Sm	0.0001
Total	2.31165

- (a) Personal communication with John T. Mihalczo, October 2009. These are the properties of the raw material delivered to Y-12 for fabrication into discs.
- (b) The reported material density is greater than the density calculated with the measured mass and approximate dimensions of the beryllium discs used in the experiment. The density of pure beryllium is reported to be 1.8477 g/cm³ with a commercial grade density between 1.82 and 1.85 g/cm³, which would be typical of material obtained from Brush Beryllium (K. A. Walsh, et al., *Beryllium Chemistry and Processing*, ASM International, Materials Park, OH, p. 27 (2009)).

Table 7. Individual Masses of Beryllium Discs.

Thickness (in)	Mass (g)
2	2314
1.5	1741
1	1159
9/16	646
1/2	573
Total	6433

1.3.3 Temperature – Room and assembly temperature measurements were not recorded during the course of the experiments. The ORCEF operated in a controlled environment.^a The fission rate in the measurements corresponded to usually much less than 0.01 watts, so there was no appreciable heating of the experiment components. The dimensions of the uranium were measured at 70 °F and the experiments were performed at 72 °F. The reactivity coefficient for a temperature change for these assemblies is approximately $-1\text{¢}/^{\circ}\text{C}$.^b

1.4 Supplemental Experimental Measurements

No additional supplemental experimental measurements were performed.

^a Personal communication with John T. Mihalcz, February 2010.

^b Personal communication with John T. Mihalcz, March 2010.

2.0 EVALUATION OF EXPERIMENTAL DATA

Monte Carlo n-Particle (MCNP) version 5.1.51 calculations were utilized to estimate the biases and uncertainties associated with the experimental results in this evaluation. MCNP is a general-purpose, continuous-energy, generalized-geometry, time-dependent, coupled n-particle Monte Carlo transport code.^a The Evaluated Neutron Data File library, ENDF/B-VII.0,^b was utilized in analysis of the experiment and benchmark model biases and uncertainties. The statistical uncertainty in k_{eff} and Δk_{eff} is 0.00004 and 0.00006, respectively. Calculations were performed with 1,050 generations with 250,000 neutrons per generation. The k_{eff} estimates did not include the first 50 generations and are the result of 250,000,000 neutron histories.

The detailed benchmark model provided in Section 3 was utilized with perturbations of the model parameters to estimate uncertainties in k_{eff} due to uncertainties in parameter values defining the benchmark configuration. Where applicable, comparison of the upper and lower perturbation k_{eff} values to evaluate the uncertainty in the k_{eff} eigenvalue were utilized to minimize correlation effects, if any, induced by comparing all perturbations to the original benchmark model configuration, as discussed elsewhere.^c

Unless specifically stated otherwise, all uncertainty values in this section correspond to 1σ . When the change in k_{eff} between the base case and the perturbed model, or two perturbed models, is less than the statistical uncertainty of the Monte Carlo results, the changes in the variable are amplified, if possible, and the calculations repeated. The resulting calculated change is then scaled back corresponding to the actual uncertainty, assuming that it is linear, which should be adequate for these changes in k_{eff} . Linearity was evaluated and found to apply, within statistical uncertainty, to the scaled perturbations.

Uncertainties less than or equal to 0.00005 are treated as negligible. When calculated uncertainties in Δk_{eff} are less than or equal to their statistical uncertainties, and an increased parameter scaling cannot be performed, the statistical uncertainties are added to the calculated uncertainty to assess the magnitude of the total uncertainty; however, the absolute magnitude of any uncertainty combined in this way is less than or equal to 0.00005, therefore they are treated as negligible.

Room return effects with its associated uncertainty are addressed in Section 3.1.3.1.

The total evaluated uncertainty in k_{eff} for this experiment is provided in Table 10. The square root of the sum of the squares of all the individual uncertainties assessed in this section is used to obtain the total uncertainty to be applied towards the benchmark eigenvalue.

When evaluating parameters such as part diameters, heights, and masses, all parts of a given type are perturbed at the same time: e.g., the diameter of all HEU annuli are simultaneously increased or decreased. Then the calculated uncertainty is reduced by the square root of the number of components perturbed. All uncertainties are treated as 100% random, without any systematic component. Systematic uncertainties were either not reported, or believed to be negligible. The measurement uncertainties are approximately the same as the uncertainty in the standards that were used for measurement calibration. However, even if all uncertainties were treated as 100% systematic, the total uncertainty in the experiment would not increase significantly.

^a X-5 Monte Carlo Team, "MCNP – a General Monte Carlo n-Particle Transport Code, version 5," LA-UR-03-1987, Los Alamos National Laboratory (2003).

^b M. B. Chadwick, et al., "ENDF/B-VII.0: Next Generation Evaluated Nuclear Data Library for Nuclear Science and Technology," *Nucl. Data Sheets*, **107**: 2931-3060 (2006).

^c D. Mennerdahl, "Statistical Noise for Nuclear Criticality Safety Specialists," *Trans. Am. Nucl. Soc.*, **101**: 465-466 (2009).

2.1 Experimental Measurements

2.1.1 Temperature – This experiment was performed at a room temperature of ~ 295 K. Part measurements were performed at a room temperature of ~ 294 K. The uncertainty in each of these two temperatures is unknown. Any variations in temperature for the experiment and room environment were small. Heating effects in the experiment components were negligible. The temperature reactivity coefficient is approximately $-1\phi/^{\circ}\text{C}$. It is assumed that a temperature variation of 2°C (1σ) adequately describes the temperature uncertainty. A temperature uncertainty of $\pm 2^{\circ}\text{C}$ in k_{eff} results in a Δk_{eff} of ± 0.00013 .

2.1.2 Experiment Reproducibility – The experimenter indicated that to completely dismantle a system and reassemble it on a different day, the reactivity differences are $\sim 2\phi$ or less. The experimenter indicated that reproducibility of experiments performed with the vertical lift is even better. The corresponding uncertainty of $\pm 0.00013 \Delta k_{\text{eff}}$ is treated as a 1σ uncertainty.

The uncertainty in the actual measurement of the reactivity, which is determined by positive period measurements, is considered very accurate. There is some uncertainty in fitting data and evaluation of the period. Careful measurements and rigorous fitting procedures can yield estimate uncertainties of ~ 0.2 pcm, which is negligible.^a It is assumed that uncertainty in the actual measurement of the reactivity is already included in the reproducibility uncertainty already discussed in the previous paragraph.

2.1.3 Measured Reactivity of Support Structure Removal – Reactivity values for the worth of the support structure are given in Table 2. Multiple measurements to assess the uncertainty in the support structure worth were not performed. Previous benchmarks in this series ([HEU-MET-FAST-051](#), [HEU-MET-FAST-071](#), and [HEU-MET-FAST-076](#)) assumed a 1σ standard deviation of 10% of each measured value of the support structure worth and the delayed critical measurement worth was sufficient. A slightly more rigorous approach is utilized in this evaluation.

The worth measurement of the rings and diaphragm were obtained using a modified experiment from the clean critical experimental configuration. Each of these configurations would have a repeatability uncertainty of $\sim 2\phi$ (as discussed in the previous section). It is assumed that a similar uncertainty would apply in the configurations used to estimate the worth of the low-mass support stand. Therefore the uncertainty in the adjustment for the removal of the assembly support structure from the experiment configuration would be obtained by taking the square root of the number of measured worths (diaphragm with rings and low-mass support structure), multiplied by the square root of the number of experiment configurations needed to evaluate a given measured worth, and multiplied by the reproducibility uncertainty for a single configuration: $\sqrt{2} \times \sqrt{2} \times 2\phi$.

The calculated k_{eff} uncertainty associated with the uncertainty in the measured reactivity for support structure removal is ± 0.00026 .

2.1.4 Effective Delayed Neutron Fraction, β_{eff} – This parameter was reported by the experimenters to be 0.0066. Typically the uncertainty in β_{eff} is around 5%, which results in a Δk_{eff} of approximately ± 0.00002 , which is considered negligible (≤ 0.00005). This uncertainty was obtained by taking the difference between the experimental eigenvalue calculated for the actual experiment using the reported delayed neutron fraction, and an eigenvalue calculated using the delayed neutron fraction increased by an additional 5%.

Calculations were performed to verify the reported value of 0.0066 using ENDF/B-VII.0, JEFF-3.1, and JENDL-3.3. MCNP Monte Carlo calculations performed for the detailed benchmark model in Section 3 and results provided in Section 4 were repeated with neutron production from delayed neutrons disabled

^a Personal communication with Dick McKnight, July 2010.

(TOTNU card set to “no”). Comparison of the calculated eigenvalues, using the equation below,^a provides an estimated β_{eff} value. The average of the calculated results from the three cross section sets is 0.00657 ± 0.00003 and is within the typical uncertainty of the reported value.

$$\beta_{eff} = 1 - \frac{k_{prompt}}{k_{eff}}.$$

2.2 Geometrical Properties

The measurement uncertainties in the stack heights can be calculated using the standard deviation of the average from multiple measurements, which are typically about ± 0.001 inches (± 0.00254 cm). The manufacturing tolerances of the Y-12 parts are ± 0.0001 inches (± 0.000254 cm). When multiple measurements of the dimensions of a part were taken, the average was typically within ± 0.00005 inches (± 0.000127 cm) of all the individual measurements.^b

There may be effects on the system k_{eff} values associated with correlations between uncertainties in stack heights, gap thicknesses, and the height of the individual parts. However, except for the k_{eff} uncertainty in the uranium stack height, the individual evaluated uncertainties in k_{eff} are negligible. Therefore, a possible increase in the uncertainty in k_{eff} due to correlation, if any, between the individual uncertainties is considered negligible.

2.2.1 Uranium Discs

2.2.1.1 Diameter

The diameter of each uranium disc was measured after machining at the Y-12 Plant to an accuracy of 0.0001 inches (0.000254 cm) at several locations (~ 8) and then averaged. All measurements were at 70° Fahrenheit and are traceable back to the National Bureau of Standards. The uncertainty in the diameter of each of the disc is reported as ± 0.00005 inches (± 0.000127 cm). To find the effect of this diametral uncertainty on the k_{eff} value, the diameters of the discs (Table 3) were adjusted by a factor of 100 times the reported uncertainty. In order to keep the uranium mass of the experiment constant, the density of each of the uranium discs was adjusted accordingly. Effectively the entire uranium volume in the system was expanded and contracted while maintaining the total uranium mass constant. Diameters were simultaneously increased by 0.0127 cm to find an upper perturbation k_{eff} value and then simultaneously decreased to find a lower perturbation k_{eff} value. Half of the difference between the upper and lower perturbation k_{eff} values was used to represent the variation in k_{eff} due to perturbing the disc diameters by 0.0127 cm. The calculated difference in k_{eff} is 0.00079 . The 1σ uncertainty in k_{eff} associated with the uncertainty in the diameter of the uranium discs is found from the following formula, where Δk_{eff} is one-half the difference between the upper and lower perturbation k_{eff} values, 4 is the number of uranium discs, and 100 is the parameter scaling factor:

$$\frac{\Delta k_{eff}}{100\sqrt{4}}.$$

The calculated k_{eff} uncertainty associated with the uncertainty in the diameter of the uranium discs is < 0.00001 , which is negligible (≤ 0.00005).

^a R. K. Meulekamp and S. C. van der Marck, “Calculating the Effective Delayed Neutron Fraction with Monte Carlo,” *Nucl. Sci. Eng.*, **152**, 142-148 (2006).

^b Personal communication with John T. Mihalcz, March 2010.

2.2.1.2 Height

The height of each uranium discs was measured after machining at the Y-12 Plant to an accuracy of 0.0001 inches (0.000254 cm) at several radial locations (~8) and then averaged. All measurements were at 70° Fahrenheit and are traceable back to the National Bureau of Standards. The uncertainty in the height of each uranium disc is reported as ± 0.00005 inches (± 0.000127 cm). To find the effect of this uncertainty on the k_{eff} value, the heights of the discs (Table 3) were adjusted by a factor of 10 times the reported uncertainty, while reducing the effective gap thicknesses between each component. The measured stack height was conserved. In order to keep the uranium mass of the experiment constant, the density of each of the uranium parts was adjusted accordingly. Effectively the entire uranium volume in the system was expanded and contracted while maintaining the total uranium mass constant. Heights were simultaneously increased by 0.00127 cm to find an upper perturbation k_{eff} value and then simultaneously decreased to find a lower perturbation k_{eff} value. Half of the difference between the upper and lower perturbation k_{eff} values was used to represent the variation in k_{eff} due to perturbing the disc heights by 0.00127 cm. The calculated difference in k_{eff} is 0.00011. The 1σ uncertainty in k_{eff} associated with the uncertainty in the heights of the uranium discs is found from the following formula, where Δk_{eff} is one-half the difference between the upper and lower perturbation k_{eff} values, 4 is the number of uranium discs, and 10 is the parameter scaling factor:

$$\frac{\Delta k_{\text{eff}}}{10\sqrt{4}}.$$

The calculated k_{eff} uncertainty associated with the uncertainty in the individual heights of the uranium discs is 0.00001, which is negligible.

2.2.1.3 Stack Height

The stack height of the three uranium discs placed above the stainless steel diaphragm was measured nine times and had a standard deviation of the average of ± 0.001 in. (± 0.00254 cm), which is also the uncertainty of the measurement device for taking stack height measurements. To find the effect of this uncertainty on the k_{eff} value, the stack height of these discs (Table 1) was adjusted by increasing the effective gap thicknesses between each component. The stack height was increased by 0.0254 cm (a factor of 10 times the reported uncertainty) to find an upper perturbation k_{eff} value. The difference between the upper perturbation k_{eff} value and the benchmark model k_{eff} value was used to represent the variation in k_{eff} due to perturbing the disc stack height by 0.0254 cm. The calculated difference in k_{eff} is -0.00124. The 1σ uncertainty in k_{eff} associated with the uncertainty in the measured stack height of the uranium discs is found from the following formula, where Δk_{eff} is the difference between the upper perturbation and benchmark model k_{eff} values, and 10 is the parameter scaling factor:

$$\frac{\Delta k_{\text{eff}}}{10}.$$

The calculated k_{eff} uncertainty associated with the uncertainty in the uranium disc stack height is 0.00012.

2.2.2 Beryllium Discs

2.2.2.1 Diameter

The diameter of each beryllium disc is stated to be approximately the same as the average diameter of the uranium discs, which is 6.996444 inches (17.7709671 cm). The uncertainty in the diameter of each of the uranium parts is reported as ± 0.00005 inches (± 0.000127 cm). However, twice that uncertainty is assumed to apply to the beryllium discs because of the lack of reported information. To find the effect of this

diametral uncertainty on the k_{eff} value, the diameters of the discs were adjusted by a factor of 100 times the assumed uncertainty. In order to keep the beryllium mass of the experiment constant, the density of each of the beryllium discs was adjusted accordingly. Effectively the entire beryllium volume in the system was expanded and contracted while maintaining the total beryllium mass constant. Diameters were simultaneously increased by 0.0254 cm to find an upper perturbation k_{eff} value and then simultaneously decreased to find a lower perturbation k_{eff} value. Half of the difference between the upper and lower perturbation k_{eff} values was used to represent the variation in k_{eff} due to perturbing the disc diameters by 0.0254 cm. The calculated difference in k_{eff} is 0.00015. The 1σ uncertainty in k_{eff} associated with the uncertainty in the diameter of the beryllium discs is found from the following formula, where Δk_{eff} is one-half the difference between the upper and lower perturbation k_{eff} values, 5 is the number of beryllium discs, and 100 is the parameter scaling factor:

$$\frac{\Delta k_{\text{eff}}}{100\sqrt{5}}.$$

The calculated k_{eff} uncertainty associated with the uncertainty in the diameters of the beryllium discs is <0.00001 , which is negligible (≤ 0.00005).

2.2.2.2 Height

Nominal heights were reported for the beryllium discs. The uncertainty in the height of each uranium disc is reported as ± 0.00005 inches (± 0.000127 cm). However, twice that uncertainty is assumed to apply to the beryllium discs because of the lack of reported information. To find the effect of this uncertainty on the k_{eff} value, the heights of the discs (Table 7) were adjusted by a factor of 10 times the assumed uncertainty, while reducing the effective gap thicknesses between each component. The measured stack height was conserved. In order to keep the beryllium mass of the experiment constant, the density of each of the beryllium discs was adjusted accordingly. Effectively the entire beryllium volume in the system was expanded and contracted while maintaining the total beryllium mass constant. Heights were simultaneously increased by 0.00254 cm to find an upper perturbation k_{eff} value and then simultaneously decreased to find a lower perturbation k_{eff} value. Half of the difference between the upper and lower perturbation k_{eff} values was used to represent the variation in k_{eff} due to perturbing the disc heights by 0.0254 cm. The calculated difference in k_{eff} is 0.00013. The 1σ uncertainty in k_{eff} associated with the uncertainty in the heights of the beryllium discs is found from the following formula, where Δk_{eff} is one-half the difference between the upper and lower perturbation k_{eff} values, 5 is the number of beryllium discs, and 10 is the parameter scaling factor:

$$\frac{\Delta k_{\text{eff}}}{10\sqrt{5}}.$$

The calculated k_{eff} uncertainty associated with the uncertainty in the individual heights of the beryllium discs is 0.00001, which is negligible (≤ 0.00005).

2.2.2.3 Stack Height

The stack height of the five beryllium discs placed on top of the uranium disc stack was measured eleven times and had a standard deviation of the average of ± 0.002 in. (± 0.00508 cm). The uncertainty of the measurement device for taking stack height measurements is ± 0.001 in. (± 0.00254 cm), which is less than the deviation in the stack height measurement. To find the effect of this uncertainty on the k_{eff} value, the stack height of these discs (Table 1) was adjusted by increasing the effective gap thicknesses between each component. The stack height was increased by 0.0508 cm (a factor of 10 times the measurement uncertainty) to find an upper perturbation k_{eff} value. The difference between the upper perturbation k_{eff} value and the

benchmark model k_{eff} value was used to represent the variation in k_{eff} due to perturbing the disc stack height by 0.0508 cm. The calculated difference in k_{eff} is -0.00024. The 1σ uncertainty in k_{eff} associated with the uncertainty in the measured stack height of the beryllium discs is found from the following formula, where Δk_{eff} is the difference between the upper perturbation and benchmark model k_{eff} values, and 10 is the parameter scaling factor:

$$\frac{\Delta k_{eff}}{10}.$$

The calculated k_{eff} uncertainty associated with the uncertainty in the beryllium disc stack height is 0.00002, which is negligible (≤ 0.00005).

2.2.3 Lateral Assembly Alignment – Lateral alignment measurements were made to within ± 0.005 inches (± 0.0127 cm). To find the effect of this uncertainty on the k_{eff} value, the lower disc was moved laterally (in a model) by a factor of 10 times the reported uncertainty. The lower disc was moved (in a model) a distance of 0.127 cm in the horizontal direction to find an upper perturbation k_{eff} value. The difference between the upper perturbation k_{eff} value and the benchmark model k_{eff} value was used to represent the variation in k_{eff} due to perturbing the lateral assembly alignment by 0.127 cm. The calculated difference in k_{eff} is -0.00009. The 1σ uncertainty in k_{eff} associated with the uncertainty in the lateral alignment is found from the following formula, where Δk_{eff} is the difference between the upper perturbation and benchmark model k_{eff} values, and 10 is the parameter scaling factor:

$$\frac{\Delta k_{eff}}{10\sqrt{3}}.$$

This uncertainty is treated as a bounding uncertainty with uniform probability; therefore, the final uncertainty is divided by the square root of three. The calculated uncertainty in the lateral assembly alignment is 0.00001, which is negligible (≤ 0.00005).

2.2.4 Vertical Assembly Alignment – The uncertainty of axial symmetry was not considered in this evaluation since it is embedded within the uranium and beryllium diameter uncertainties.

2.2.5 Gaps between Parts – The uncertainty in gap heights was not considered in this evaluation since it is embedded within the uranium and beryllium disc stack height uncertainties.

For the benchmark model and uncertainty analysis, the total height of the gaps between the beryllium discs was obtained by taking the difference between the measured stack height and the summation of the heights of the five beryllium discs. The total gap height was then divided by five, to represent the number of gaps between the beryllium discs plus the gap between the beryllium disc stack and the uranium disc stack. The gaps heights for the beryllium disc stack were calculated to be 0.0019 in. (0.004826 cm).

The total height of the gaps between the stack of three uranium discs was obtained by taking the difference between the measured stack height and the summation of the heights of the three uranium discs. The total gap height was then divided by three, to represent the number of gaps between the uranium discs plus the gap between the uranium disc stack and the stainless steel diaphragm. The gap heights for the uranium disc stack were calculated to be ~ 0.0007 in. (0.001778 cm).

The fourth uranium disc was not included in the stack height measurements or gap height calculations. No gap was recorded between the fourth uranium disc and the steel diaphragm.

The measured worth of the diaphragm includes the separation distance between the two halves of the experiment. Therefore, when the diaphragm is removed from the model, the distance between the parts adjacent to the diaphragm location is brought closer together.^a Only the gaps that would have existed between the diaphragm and the uranium discs would remain, and the thickness of 0.010 in. (0.0254 cm) that represents the diaphragm thickness would be eliminated. The diaphragm is believed to deform to meet the contours of the uranium discs; removal of the diaphragm would also reduce the gap between the adjacent uranium discs. Therefore no gap is used between the diaphragm and the bottom uranium disc, and only the effective gap obtained for the three uranium discs above the diaphragm is retained.^b

2.2.6 Assembly Separation – The uncertainty for the separation of the upper and lower assemblies is based upon accuracy of measurement when bringing the two experiment halves into contact, ± 0.001 in. (± 0.00254 cm). This uncertainty, however, would be included within the measurement uncertainty of the worth of the stainless steel diaphragm.

2.3 Compositional Variations

2.3.1 Uranium Discs

2.3.1.1 Mass

The uranium mass of each part measured at the Y-12 Plant is traceable back to the Bureau of Standards to less than 0.5 gram accuracy and then rounded to the nearest gram. The uncertainty for the mass of each uranium disc is ± 0.5 g. A mass measurement of multiple uranium discs was not performed. To find the effect of this uncertainty on the k_{eff} value, the masses of the discs (Table 3) were adjusted by a factor of 10 times the reported uncertainty. In order to keep the uranium volume of the experiment constant, the density of each of the uranium discs was adjusted accordingly. Uranium masses were simultaneously increased by 5 g to find an upper perturbation k_{eff} value and then simultaneously decreased to find a lower perturbation k_{eff} value. Half of the difference between the upper and lower perturbation k_{eff} values was used to represent the variation in k_{eff} due to perturbing the disc masses by 5 g. The calculated difference in k_{eff} is 0.00032. The 1σ uncertainty in k_{eff} associated with the uncertainty in the mass of the uranium discs is found from the following formula, where Δk_{eff} is one-half the difference between the upper and lower perturbation k_{eff} values, 4 is the number of uranium discs, and 10 is the parameter scaling factor:

$$\frac{\Delta k_{eff}}{10\sqrt{4}}.$$

The calculated k_{eff} uncertainty associated with the uncertainty in the mass of the uranium discs is 0.00002, which is negligible (≤ 0.00005).

2.3.1.2 Isotopic Content

Based on the accuracy of isotopic ratios from the mass spectrometry laboratory at the Y-12 Plant, uncertainty for the uranium isotopic content is ± 0.005 wt.% for ^{234}U , ^{235}U , and ^{236}U . The ^{238}U content was obtained by subtracting the sum of the ^{234}U , ^{235}U , and ^{236}U contents from one. The effect of this uncertainty on the k_{eff} value was determined by adjusting the isotopic content of the uranium parts (Table 4) by a factor of 10 times the reported maximum uncertainty. An upper perturbation k_{eff} value was found by simultaneously increasing the isotopic contents of ^{234}U , ^{235}U , and ^{236}U by 0.05 wt.% and adjusting the ^{238}U isotopic content accordingly.

^a Personal communication with John T. Mihalcz, February 2010.

^b Personal communication with John T. Mihalcz, July 2010.

The isotopic contents of ^{234}U , ^{235}U , and ^{236}U were then simultaneously decreased by 0.05 wt.%, again with the ^{238}U content adjusted, to find the lower perturbation k_{eff} value. Half of the difference between the upper and lower perturbation k_{eff} values was used to represent the variation in k_{eff} due to perturbing the isotopic content by 0.05 wt.%. The calculated difference in k_{eff} is 0.00049. The 1σ uncertainty in k_{eff} associated with the uncertainty in the isotopic content of the uranium discs is found from the following formula, where Δk_{eff} is one-half the difference between the upper and lower perturbation k_{eff} values, 4 is the number of uranium discs, and 10 is the parameter scaling factor:

$$\frac{\Delta k_{\text{eff}}}{10\sqrt{4}}.$$

The calculated k_{eff} uncertainty associated with the uncertainty in the isotopic content of the uranium discs is 0.00002, which is negligible (≤ 0.00005). Since uncertainty in ^{234}U , ^{235}U , and ^{236}U are not perfectly correlated (if one value is off by 0.05 wt.%), the variability in ^{238}U is probably overestimated. However, the effect of uncertainty in isotopic content of uranium is a small contributor to the overall uncertainty in k_{eff} .

A second study was performed to evaluate the effect of increasing the ^{235}U content by 0.05 wt.% and decreasing the ^{234}U and ^{236}U contents by 0.025 wt.% apiece (maintaining the ^{238}U content constant) to obtain an upper perturbation k_{eff} value. The reverse adjustments in wt.% were performed to obtain a lower perturbation k_{eff} value. Half of the difference between the upper and lower perturbation k_{eff} values was used to represent the variation in k_{eff} due to perturbing the isotopic content. The calculated difference in k_{eff} is 0.00011. The 1σ uncertainty in k_{eff} associated with the uncertainty in the isotopic content of the uranium discs is found from the previous formula. The calculated k_{eff} uncertainty associated with the uncertainty in the isotopic content of the uranium discs is <0.00001 , which is negligible (≤ 0.00005).

Typically, the isotopic content of all components in a system would be varied individually so as to isolate any parts with significant merit. As this is a small system and relatively large perturbations of the combined isotopic content yield a negligible change in k_{eff} , all isotopic contents were adjusted simultaneously.

2.3.1.3 Impurities

The uranium impurities listed in Table 5 are given as the average of a spectrographic analysis from randomly sampled components for each impurity (assuming the values to be normally distributed) or listed as less than a minimum value. In the latter case, they are less than the detectable limit. The impurity content, as specified in Table 5, is accepted as the nominal composition. For impurities below a detectable limit, the content is selected as half the detectable limit and the other half representing the 1σ uncertainty; therefore the uncertainty represents a 100% uncertainty in the detection limit. A summary of the nominal impurity composition is found in Table 8. The oxygen and nitrogen content was included at the experimentalist-specified quantities of 20 and 30 ppm, respectively. A 1σ uncertainty of half their value was assumed.

Table 8. Impurity Content of Uranium Metal Discs.

Element	Parts per Million by Weight (ppm)	Standard Deviation (ppm)
Ag	8	3.2
Ba	0.005	0.005
Bi	164	52.9
C	5	2.4
Ca	0.1	0.05
Cd	0.5	0.5
Co	5	1.9
Cr	7	1.9
Cu	25	8
K	0.1	0.1
Li	1	1
Mg	3	1.7
Mn	56	17.1
Mo	0.5	0.5
Na	27	7.7
Ni	100	10
Sb	38	17.4
Ti	1	0.5
O	20	10
N	30	15

The impurities were simultaneously increased by 3σ to find an upper perturbation k_{eff} value and then simultaneously decreased to find a lower perturbation k_{eff} value. Impurity limits were not reduced below a quantity of zero. The weight fraction of the uranium metal was adjusted, as appropriate, to compensate for the adjustments in impurity content. Half of the difference between the upper and lower perturbation k_{eff} values was used to represent the variation in k_{eff} due to perturbing the uranium impurity by 3σ . The calculated difference in k_{eff} is 0.00009. The 1σ uncertainty in k_{eff} associated with the uncertainty in the impurity content of the uranium discs is found from the following formula, where Δk_{eff} is one-half the difference between the upper and lower perturbation k_{eff} values and 3 is the parameter scaling factor:

$$\frac{\Delta k_{\text{eff}}}{3}.$$

The calculated k_{eff} uncertainty associated with the uncertainty in the impurity content of the uranium discs is 0.00003, which is negligible (≤ 0.00005).

2.3.2 Beryllium Discs

The density of the beryllium is not directly evaluated as an uncertainty in this benchmark evaluation. The beryllium discs were weighed with the same precision as the uranium discs. Therefore the mass is believed to be a more accurate measurement than the reported density. While the dimensions of the beryllium discs were not recorded in detail but machined with the same precision as the uranium discs, the larger assumed uncertainty in these measurements account for additional density variation. The mass densities of the beryllium discs vary between 1.819 and 1.842 g/cm³ with an average mass density of 1.832 g/cm³, which is approximately what is obtained from a mass measurement of the entire stack (Section 1.3.2). The reported density of 1.854 g/cm³ in Table 6 for the original stock material is believed to be incorrect. However, since

the material was later machined at Y-12 and subsequently weighed and measured, the calculated mass density values are believed to appropriately represent the beryllium discs used in this experiment.

The uncertainties in the mass and dimensions of the beryllium discs were evaluated and determined to be negligible.

2.3.2.1 Mass

The uncertainty for the mass of each beryllium disc is ± 0.5 g. To find the effect of this uncertainty on the k_{eff} value, the mass of the discs were adjusted by a factor of 10 times the measurement uncertainty. Beryllium masses (Table 7) were simultaneously increased by 5 g to find an upper perturbation k_{eff} value and then simultaneously decreased to find a lower perturbation k_{eff} value. Half of the difference between the upper and lower perturbation k_{eff} values was used to represent the variation in k_{eff} due to perturbing the disc masses by 5 g. The calculated difference in k_{eff} is 0.00014. The 1σ uncertainty in k_{eff} associated with the uncertainty in the mass of the beryllium discs is found from the following formula, where Δk_{eff} is one-half the difference between the upper and lower perturbation k_{eff} values, 5 is the number of beryllium discs, and 10 is the parameter scaling factor:

$$\frac{\Delta k_{\text{eff}}}{10\sqrt{5}}.$$

The calculated k_{eff} uncertainty associated with the uncertainty in the mass of the beryllium discs is 0.00001, which is negligible (≤ 0.00005).

2.3.2.2 Impurities

The beryllium impurities listed in Table 6 are given as the average impurity quantities. The impurity content, as specified in Table 9, is accepted as the nominal composition. The amount of oxygen contained in the BeO impurity is computed and also treated as an impurity (Table 9). To find the effect of this uncertainty on the k_{eff} value, the impurity content is adjusted by a factor of 100% of the average quantity. This uncertainty is then treated as a bounding uncertainty with uniform probability; therefore, the final uncertainty is divided by the square root of three.

Table 9. Nominal Beryllium Impurities.

Impurity	wt. %
O	1.23458
Al	0.06
C	0.12
Fe	0.13
Mg	0.02
Bi	0.05
B	0.001
Cd	0.0002
Dy	0.0001
Br	0.00005
Gd	0.0001
Ni	0.0001
Sm	0.0001
Total	1.61623 ^(a)

(a) The total quantity of impurities does not add up to the original amount of 2.31165 wt.% because the beryllium in BeO is not included.

The impurities were simultaneously doubled to find an upper perturbation k_{eff} value and then simultaneously removed to find a lower perturbation k_{eff} value. The weight fraction of the beryllium metal was adjusted, as appropriate, to compensate for the adjustments in impurity content. Half of the difference between the upper and lower perturbation k_{eff} values was used to represent the variation in k_{eff} due to perturbing the beryllium impurity by 100%. The calculated difference in k_{eff} is 0.00046. The 1σ uncertainty associated with the impurity content of the beryllium discs is found from the following formula, where Δk_{eff} is one-half the difference between the upper and lower perturbation k_{eff} values:

$$\frac{\Delta k_{eff}}{\sqrt{3}}.$$

The calculated k_{eff} uncertainty associated with the uncertainty in the impurity content of the beryllium discs is 0.00026.

2.4 Total Experimental Uncertainty

The total uncertainty for the experiment was calculated by taking the square root of the sum of the squares of all the individual uncertainties discussed in this section; they are summarized in Table 10. These uncertainties make this an acceptable benchmark experiment.

Table 10. Total Experimental Uncertainty.

Perturbed Parameter	Parameter Value	1 σ Uncertainty	Case 1 Δk_{eff}
Temperature (K)	294	± 2	0.00013
Experiment reproducibility (ϕ)	--	± 2	0.00013
Measured reactivity worth (ϕ)	--	$\pm \sqrt{2} \times \sqrt{2} \times 2$	0.00026
β_{eff}	0.0066	$\pm 5\%$	Negligible
Uranium diameter (cm)	Figure 7	± 0.000127	Negligible
Uranium height (cm)	Figure 7	± 0.000127	Negligible
Uranium stack height (cm)	Table 1	+0.00254	0.00012
Beryllium diameter (cm)	Figure 7	± 0.000254	Negligible
Beryllium height (cm)	Figure 7	± 0.000254	Negligible
Beryllium stack height (cm)	Table 1	+0.00508	Negligible
Lateral assembly alignment (cm)	0	± 0.0127	Negligible
Vertical assembly alignment (cm)	Not Applicable – See Section 2.2.4		
Gaps between parts (cm)	Not Applicable – See Section 2.2.5		
Assembly separation (cm)	Not Applicable – See Section 2.2.6		
Uranium mass (g)	Table 3	± 0.5	Negligible
Uranium isotopic content (wt.%)	Table 4	± 0.005	Negligible
Uranium impurities (ppm)	Table 8		Negligible
Beryllium mass (g)	Table 7	± 0.5	Negligible
Beryllium impurities (wt.%)	Table 9		0.00026
Total	--	--	0.00043

3.0 BENCHMARK SPECIFICATIONS

3.1 Description of Models

Two benchmark models were developed to represent the HEU metal cylinder with beryllium top reflector experiment (Figure 6). The detailed benchmark model represents, as much as possible, the experiment described in Reference 1. Some approximation is necessary to estimate the height of gaps between the individual components of the experiment; however, uncertainty in the gap height is negligible (see Sections 2.2.1.3, 2.2.2.3, and 2.2.5). The simple benchmark model reduces the experiment to a basic cylindrical structure comprised of two single materials: HEU and beryllium.

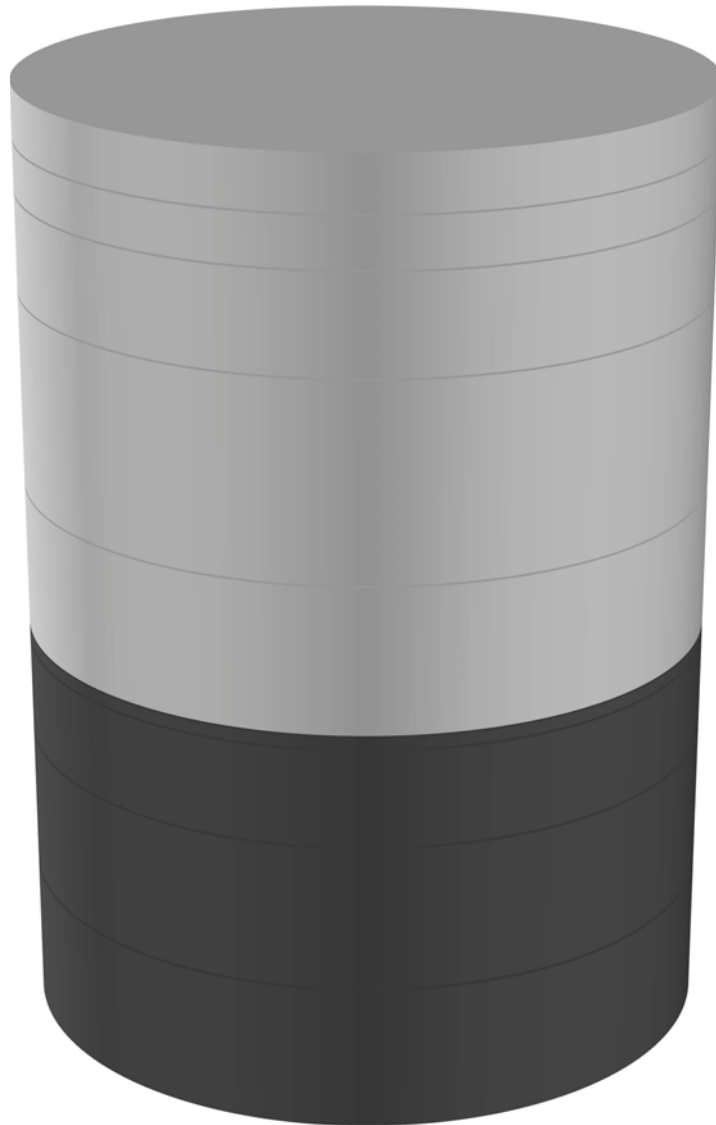


Figure 6. Stack of HEU Metal Discs Top-Reflected by Beryllium Discs.

3.1.1 Detailed Model – The detailed benchmark model is comprised of a stack of four HEU metal discs. The HEU stack is top-reflected with a stack of beryllium discs. Small gaps exist between each component of the experiment and each component has unique dimensions and composition that reproduce, as closely as possible, the actual component dimensions and compositions (see Figure 7). A discussion of the gaps between discs is provided in Section 2.2.5. The experimental assembly, including the stainless steel diaphragm and the room itself, are not included in the detailed benchmark model.

Very small gaps exist between the components of the experiment, as the top and bottom surfaces of the discs are not perfectly smooth. However, it is not easy to exactly model the imperfect surfaces of the experiment components. The measured stack height and individual heights of each part are preserved in the detailed benchmark model. To preserve the stack height, small gaps must be placed between the discs. These gap heights are exaggerated in Figure 7 so that the gap heights can be easily noticed. The effect of eliminating the gaps between parts is quite small compared to effects such as adjusting the overall stacked height dimension of the experiment.

3.1.2 Simple Model – The simple benchmark model consists of a single HEU metal cylinder with a height of 10.4775 cm (4-1/8 in.) with a single beryllium cylinder coaxially placed on top. The height of the beryllium is 14.12875 cm (5-9/16 in.) and both cylinders have a diameter of 17.78 cm (7 in.). There is no gap present between the uranium and beryllium cylinders. Total mass for the beryllium and uranium is conserved in the simple model. There is no stainless steel diaphragm or experimental assembly structure in the simple benchmark model. The simple model dimensions are chosen to correspond to the nominal experiment dimensions.

3.1.3 Bias Assessment

3.1.3.1 Room Return Effects

The properties and dimensions of the room in which the experiment was performed were not provided in Reference 1, but they are well known and available from many other East Cell, ORCEF experiment reports. The dimensions were obtained from a similar benchmark report: [HEU-MET-FAST-076](#). Room return effects were estimated using the room and experiment placement dimensions provided in Section 1.2 and assuming that the other concrete wall, floor, and ceiling thicknesses are 2 feet. The concrete was modeled as Oak Ridge Concrete with a density of 2.3 g/cm³ and the room containing air with a density of 1.2 kg/m³. The use of either Oak Ridge Concrete or Magnuson Concrete would provide similar results as shown in [HEU-MET-FAST-076](#). Both concretes were prepared using crushed limestone instead of sand due to the unavailability of sand at the time.^a

The effective bias in neglecting room return effects was determined to be $-0.00036 \pm 0.00006 \Delta k_{\text{eff}}$. This worth is equivalent to $-5.5 \pm 0.9\%$ using a β_{eff} of 0.0066 ± 0.00033 (assumed uncertainty of 5%). This bias was evaluated using KENO-VI, and a room return worth of $-2.2 \pm 1.1\%$ was determined. The results are within 2σ . Because the primary analysis of this benchmark is being performed with MCNP5 calculations, that value will be used to represent the effective bias in neglecting room return effects.

3.1.3.2 Support Structure Removal

The benchmark models do not include the support structure of the experimental assembly or the stainless steel diaphragm. Removal of the support structure materials was included in the experimental assessment of the reported eigenvalue and the uncertainty in their worth is discussed in Section 2.2.2.

^a Personal communication with John T. Mihalcz, February 2010.

The diaphragm bolts were not included in the experimental analysis of the support structure worth.^a A calculation was performed to evaluate a “ring” of steel material where the bolts would have been located in the actual experiment. The calculated bias was negligible.

3.1.3.3 Temperature

The temperature reactivity coefficient is reported by the experimenter to be approximately $-1\text{¢}/^{\circ}\text{C}$. The parts were measured at $\sim 294\text{ K}$ and the original experiments were performed at $\sim 295\text{ K}$. The uncertainty in either of these two temperatures is unknown. The benchmark model uses dimensions as measured at room temperature conditions, $\sim 294\text{ K}$, using ENDF/B-VII.0 cross sections evaluated at 300 K . No bias for temperature effects was included in the benchmark model, however an uncertainty in the temperature of the experiments and evaluation are provided in Section 2.1.1.

3.1.3.4 Model Simplification

Additional simplifications were performed to facilitate the application of a simple model in place of the detailed model. Simplifications include the removal of impurities from the uranium and beryllium discs (for the impurity of BeO, only the oxygen in BeO is removed, and the beryllium is assumed to be beryllium metal), development of a cylinder of stacked beryllium discs with uniform material properties, and development of a cylinder of stacked uranium discs with uniform material properties. The diameter is adjusted to 17.78 cm (7 in.) for both stacked disc simplifications. The beryllium stack has a total height of 14.12875 cm ($5\text{-}9/16\text{ in.}$), and the uranium stack height is 10.4775 cm ($4\text{-}1/8\text{ in.}$). There are no gaps between the individual discs in a stack, as they are modeled as a single homogenous cylinder. These adjustments in dimensions were performed to match the approximate measurement descriptions for the experiment. The density of the individual stacks was computed using the total measured mass of each stack divided by the total adjusted volume. The mass density of the beryllium and uranium cylinders is 1.8338 and 18.7509 g/cm^3 , respectively. The weight fraction of isotopes in the uranium disc stack was weighted by the mass of the individual discs in the stack. Results for these simplifications are shown in Table 11.

The effect of incorporating all of these simplifications into a single benchmark model was assessed using ENDF/B-VII.0, JEFF-3.1,^b and JENDL-3.3^c neutron cross section libraries. Results, including the total simplification bias, are shown in Table 12. There are two competing effects when homogenizing the benchmark models: removal of the interstitial gaps between parts, and increasing the surface area to volume ratio while conserving mass. The removal of the gaps increases k_{eff} by eliminating any streaming paths while the homogenization of the model to meet the nominal dimensions of the experiment provided by the experimenter reduces k_{eff} . In this experiment, the competing effects are nearly equal, and the net difference in neutron leakage between the simple and detailed models is quite small (Appendix C).

^a Personal communication with John T. Mihalcz, June 2010.

^b A. Koning, R. Forrest, M. Kellett, R. Mills, H. Henriksson, and Y. Rugama, “The JEFF-3.1 Nuclear Data Library,” JEFF Report 21, Organisation for Economic Co-operation and Development, Paris (2006).

^c K. Shibata, et al., “Japanese Evaluated Nuclear Data Library Version 3 Revision-3: JENDL-3.3,” *J. Nucl. Sci. Tech.*, **39**(11): 1125-1136 (November 2002).

Table 11. Calculated Biases for Individual Model Simplifications.

Simplification	Δk_{eff}	\pm	σ
Removal of beryllium impurities	-0.00036	\pm	0.00006
Removal of uranium impurities	-0.00015	\pm	0.00006
Homogenized stack of beryllium discs and removal of beryllium impurities	-0.00034	\pm	0.00006
Homogenized stack of uranium discs and removal of uranium impurities	0.00071	\pm	0.00006

Table 12. Calculated Biases for Combined Model Simplifications.

Neutron Cross Section Library	Δk_{eff}	\pm	σ
ENDF/B-VII.0	-0.00021	\pm	0.00006
JEFF-3.1	-0.00047	\pm	0.00006
JENDL-3.3	-0.00051	\pm	0.00006
Average	-0.00040	\pm	0.00016
Model simplification with room return effects (total bias)	-0.00076	\pm	0.00017

3.1.3.5 Total Bias Adjustment (Detailed Model)

The detailed benchmark model represents the experiment except for room return effects. Therefore the total bias adjustment for the detailed benchmark model is that reported for room return effects in Section 3.1.3.1, which is $-0.00036 \pm 0.00003 \Delta k_{\text{eff}}$.

3.1.3.6 Total Bias Adjustment (Simple Model)

The total bias for the simple model is the combination of the average bias for all simplifications except room return effects (Table 12) and the bias for neglecting room return effects (Section 3.1.3.1). The total bias value for the simple benchmark model is $-0.00066 \pm 0.00009 \Delta k_{\text{eff}}$.

3.2 Dimensions

3.2.1 Detailed Model – The detailed benchmark model is shown in Figure 7, and is labeled with part identifiers and dimensions.

3.2.1.1 Uranium Discs

The diameters, positions, and heights of the four uranium discs in the benchmark model are shown in Figure 7. Gaps between the uranium discs and other components of the experiment are also shown in the figure.

3.2.1.2 Beryllium Discs

The diameters, positions, and heights of the five beryllium discs in the benchmark model are shown in Figure 7. Gaps between the beryllium discs and other components of the experiment are also shown in the figure.

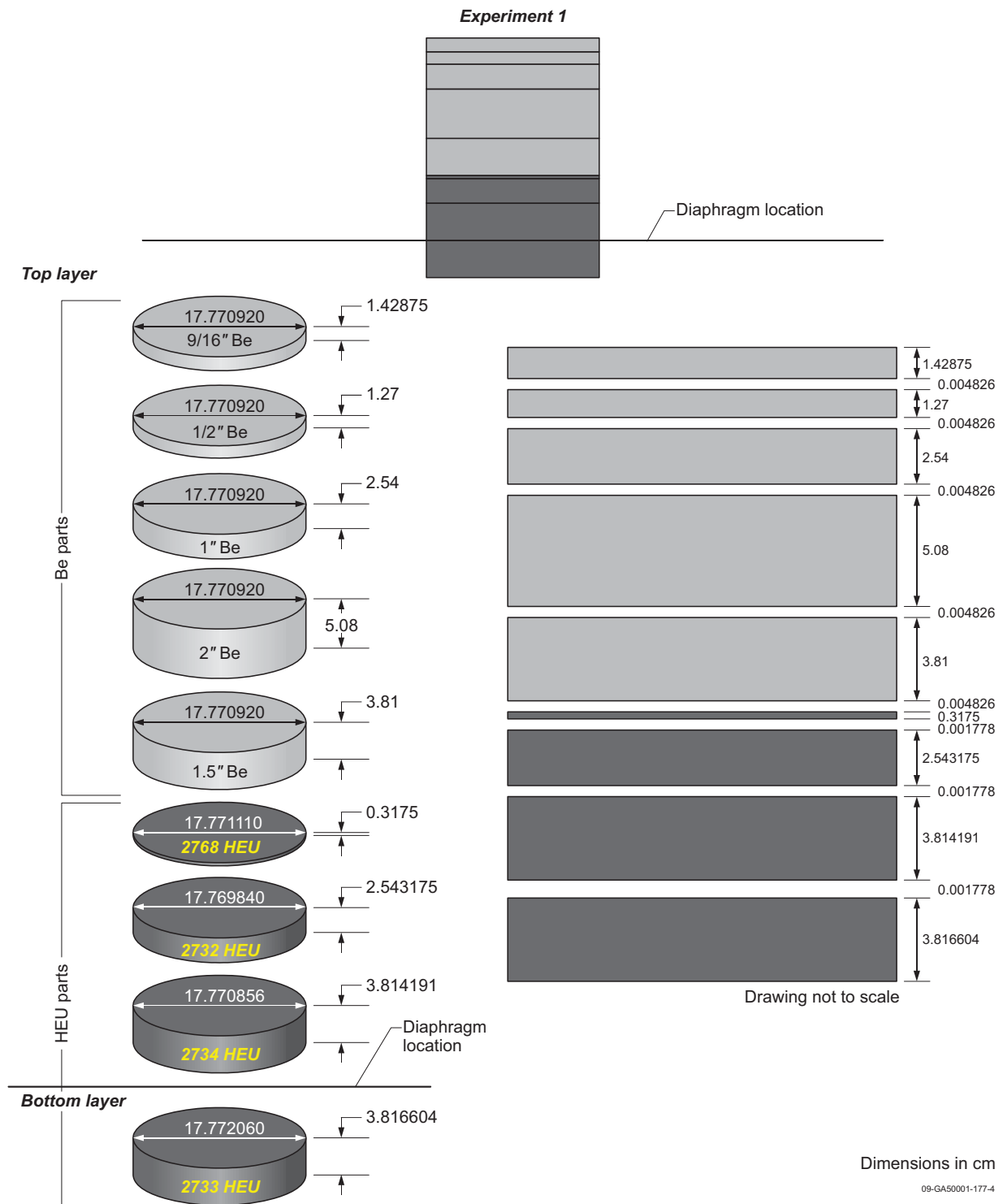
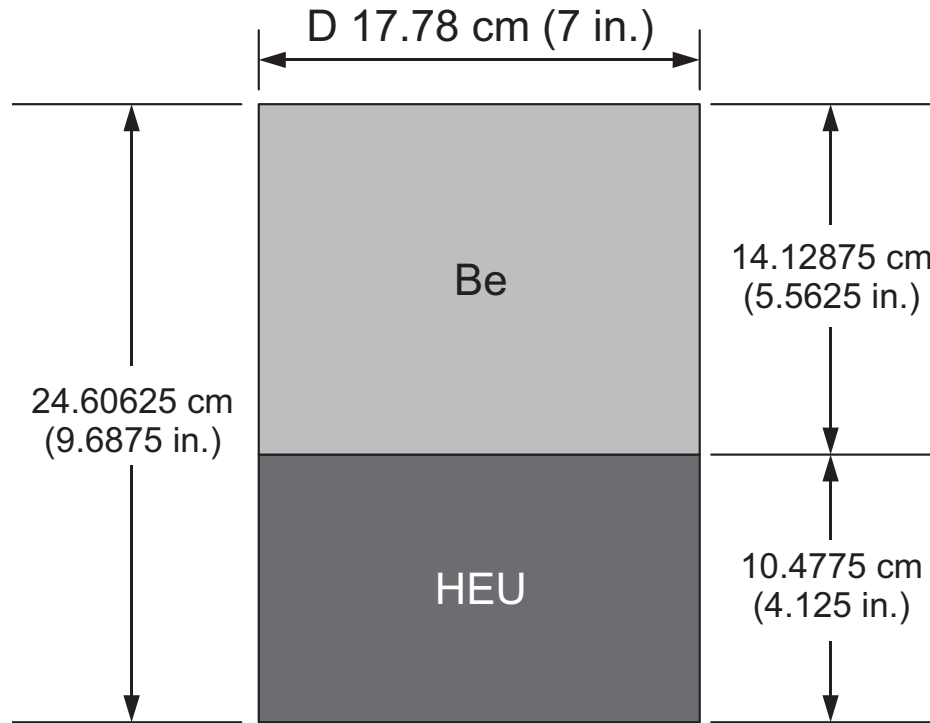


Figure 7. Detailed Benchmark Model of Oralloy and Beryllium Discs.
(Note that gap heights are quite small and visually exaggerated for the benefit of the reader.)

3.2.2 Simple Model – The simple benchmark model is shown in Figure 8, with dimensions and material labels. The simple model dimensions are chosen to correspond to the nominal experiment dimensions.



09-GA50001-177-2

Figure 8. Simple Benchmark Model of Oralloy and Beryllium Discs.

3.2.2.1 Uranium Cylinder

The uranium cylinder is 10.4775 cm (4-1/8 in.) in height with a diameter of 17.78 cm (7 in.), as shown in Figure 8.

3.2.2.2 Beryllium Cylinder

The beryllium cylinder is 14.12875 cm (5-9/16 in.) in height with a diameter of 17.78 cm (7 in.), as shown in Figure 8.

3.3 Material Data

3.3.1 Detailed Model

Material mass densities were obtained by taking the mass of the uranium, or beryllium, components divided by the volume they occupy in the benchmark model.

3.3.1.1 Uranium Discs

The atom densities of the four uranium discs are in Table 13, where part identifiers match the identifiers shown in Figure 7.

Table 13. Uranium Disc Atom Densities (a/b-cm) for the Detailed Benchmark Model.

Part Number → Material ↓	2732	2733	2734	2768
²³⁴ U	4.5765E-04	4.6267E-04	4.5821E-04	4.4496E-04
²³⁵ U	4.4692E-02	4.4702E-02	4.4751E-02	4.4855E-02
²³⁶ U	1.0030E-04	1.2424E-04	1.1477E-04	1.2468E-04
²³⁸ U	2.6854E-03	2.6677E-03	2.6697E-03	2.7009E-03
Ag	8.3658E-07	8.3696E-07	8.3760E-07	8.3992E-07
Ba	4.1070E-10	4.1089E-10	4.1120E-10	4.1234E-10
Bi	8.8522E-06	8.8562E-06	8.8630E-06	8.8875E-06
C	4.6957E-06	4.6978E-06	4.7015E-06	4.7145E-06
Ca	2.8145E-08	2.8158E-08	2.8180E-08	2.8258E-08
Cd	5.0174E-08	5.0196E-08	5.0235E-08	5.0374E-08
Co	9.5702E-07	9.5745E-07	9.5819E-07	9.6084E-07
Cr	1.5186E-06	1.5193E-06	1.5204E-06	1.5246E-06
Cu	4.4378E-06	4.4398E-06	4.4432E-06	4.4555E-06
K	2.8851E-08	2.8864E-08	2.8886E-08	2.8966E-08
Li	1.6251E-06	1.6259E-06	1.6271E-06	1.6316E-06
Mg	1.3923E-06	1.3929E-06	1.3940E-06	1.3979E-06
Mn	1.1498E-05	1.1503E-05	1.1512E-05	1.1544E-05
Mo	5.8787E-08	5.8814E-08	5.8859E-08	5.9022E-08
Na	1.3248E-05	1.3254E-05	1.3264E-05	1.3301E-05
Ni	1.9220E-05	1.9228E-05	1.9243E-05	1.9296E-05
Sb	3.5207E-06	3.5223E-06	3.5250E-06	3.5347E-06
Ti	2.3559E-07	2.3570E-07	2.3588E-07	2.3653E-07
O	1.4101E-05	1.4107E-05	1.4118E-05	1.4157E-05
N	2.4160E-05	2.4171E-05	2.4190E-05	2.4256E-05
Mass Density (g/cm ³)	18.7311	18.7396	18.7540	18.8058

3.3.1.2 Beryllium Discs

The atom densities of the five beryllium discs are shown in Table 14, where part identifiers match the identifiers shown in Figure 7.

Table 14. Beryllium Disc Atom Densities (a/b-cm) for the Detailed Benchmark Model.

Part ID → Material ↓	0.5"	9/16"	1"	1.5"	2"
Be	1.1959E-01	1.1984E-01	1.2094E-01	1.2112E-01	1.2073E-01
Al	2.4360E-05	2.4412E-05	2.4636E-05	2.4672E-05	2.4594E-05
B	1.0133E-06	1.0154E-06	1.0248E-06	1.0262E-06	1.0230E-06
Bi	2.6209E-06	2.6265E-06	2.6507E-06	2.6545E-06	2.6461E-06
Br	6.8547E-09	6.8694E-09	6.9325E-09	6.9425E-09	6.9205E-09
C	1.0944E-04	1.0968E-04	1.1069E-04	1.1084E-04	1.1049E-04
Cd	1.9490E-08	1.9532E-08	1.9711E-08	1.9740E-08	1.9677E-08
Dy	6.7412E-09	6.7556E-09	6.8176E-09	6.8275E-09	6.8059E-09
Fe	2.5500E-05	2.5555E-05	2.5790E-05	2.5827E-05	2.5745E-05
Gd	6.9662E-09	6.9811E-09	7.0453E-09	7.0554E-09	7.0331E-09
Mg	9.0141E-06	9.0334E-06	9.1164E-06	9.1295E-06	9.1006E-06
Ni	1.8665E-08	1.8705E-08	1.8877E-08	1.8904E-08	1.8844E-08
O	8.4529E-04	8.4709E-04	8.5488E-04	8.5611E-04	8.5340E-04
Sm	7.2855E-09	7.3010E-09	7.3681E-09	7.3787E-09	7.3554E-09
Mass Density (g/cm ³)	1.8190	1.8229	1.8397	1.8423	1.8365

3.3.2 Simple Model

3.3.2.1 Uranium Cylinder

The atomic composition of the uranium cylinder is in Table 15. The average isotopic weight fraction of the uranium cylinder was obtained by taking the sum of the mass-weighted isotopic weight fraction of each uranium disc in the experiment. The density of the uranium cylinder is obtained by dividing the total uranium mass by the volume of the modeled cylinder; the density is then multiplied by the factor 0.999508795 to account for the removal of impurities (Table 8). The mass density of the uranium cylinder is 18.7509 g/cm³.

Table 15. Uranium Cylinder Composition.

Material	Wt. %	Atom Density (a/b-cm)
²³⁴ U	0.953	4.5958E-04
²³⁵ U	93.165	4.4736E-02
²³⁶ U	0.241	1.1523E-04
²³⁸ U	5.641	2.6745E-03

3.3.2.2 Beryllium Cylinder

The atomic composition of the beryllium cylinder is in Table 16. The mass density of the beryllium cylinder is 1.8338 g/cm³. The beryllium density is obtained by dividing the total beryllium mass by the volume of the modeled cylinder; the density is then multiplied by the factor 0.9838377 to account for the removal of impurities (Table 9). The beryllium reported in the impurity BeO is retained in the simple benchmark model as beryllium metal. The oxygen is considered an impurity and removed.

Table 16. Beryllium Cylinder Composition.

Material	Atom Density (a/b-cm)
Be	1.2056E-01 ^(a)

(a) Includes beryllium from BeO.

3.4 Temperature Data

The temperature of both detailed and simple benchmark models is at room temperature, 294 K.

3.5 Experimental and Benchmark Model k_{eff}

The experimental k_{eff} value for the full assembly is 1.0006 ± 0.0004 . The adjusted experimental eigenvalue for just the stack of uranium and beryllium discs is 1.0002 ± 0.0004 .

3.5.1 Detailed Model – The k_{eff} value for the detailed benchmark model, adjusted for room return and temperature effects, is 0.9998 ± 0.0004 .

3.5.2 Simple Model – The k_{eff} value for the simple benchmark model, adjusted for room return effects, temperature effects, and model simplifications, is 0.9994 ± 0.0004 .

4.0 RESULTS OF SAMPLE CALCULATIONS

Results were calculated using MCNP5 and ENDF/B-V.2,^a -VI.8,^b -VII.0, JEFF-3.1, and JENDL-3.3 neutron cross section libraries with the input decks and specifications provided in Appendix A. An additional analysis using KENO-VI and KENO-V.a^c for the detailed and simple benchmark models, respectively, and ENDF/B-VII.0 neutron cross section library (both continuous energy, like in MCNP5, and 238-group) was performed; the input decks and specifications are also provided in Appendix A. A comparison of the neutron spectral data between the detailed and simple models is provided in Appendix C. The cross section data for ¹⁶O is used for ¹⁸O in the input decks.

4.1 Detailed Benchmark Model

The calculated results for the detailed benchmark model are reported in Table 17. There is variability in the calculated results for the different libraries, with ENDF/B-VII.0 and JEFF-3.1 both calculating below the expected benchmark value and JENDL-3.3 above. The greatest difference between MCNP results with different cross sections $\sim 0.64\% \Delta k_{\text{eff}}$. The differences are much greater than the evaluated uncertainty for the benchmark experiment. The number of sigmas between the benchmark eigenvalue and the calculated eigenvalues is between 5 and 11 due to the small amount of uncertainty in the benchmark experiment itself. There is not a significant difference between the MCNP and KENO results.

Table 17. Comparison of Detailed Benchmark Eigenvalues.

Analysis Code	Neutron Cross Section Library	Calculated			Benchmark			$\frac{C-E}{E}(\%)$
		k_{eff}	\pm	σ	k_{eff}	\pm	σ	
MCNP5	ENDF/B-V.2	0.99661	\pm	0.00004	0.9998	\pm	0.0004	-0.35
	ENDF/B-VI.8	0.99629	\pm	0.00004				-0.35
	ENDF/B-VII.0	0.99802	\pm	0.00004				-0.18
	JEFF-3.1	0.99578	\pm	0.00004				-0.40
	JENDL-3.3	1.00217	\pm	0.00004				0.24
KENO-VI	ENDF/B-VII.0 (continuous energy) ^(a)	0.99770	\pm	0.00007				-0.21
	ENDF/B-VII.0 (238-group)	0.99764	\pm	0.00005				-0.22

(a) These results were obtained using a slightly different KENO-VI input deck than what is described in Section 3 and provided in Appendix A; the gap thickness between the bottom two HEU discs is twice that used in the benchmark model. There is no significant effect in the calculated results.

^a R. Kinsey, Ed., ENDF/B Summary Documentation, BNL-NCS-17542 (ENDF-201), 3rd ed., Brookhaven National Laboratory (1979).

^b H. D. Lemmel, P. K. McLaughlin, and V. G. Pronyaev, "ENDF/B-VI Release 8 (Last Release of ENDF/B-VI) the U.S. Evaluated Nuclear Data Library for Neutron Reaction Data," IAEA-NDS-100 Rev. 11, International Atomic Energy Agency, Vienna (November 2001).

^c "SCALE: A Modular Code System for Performing Standardized Computer Analyses," ORNL/TM-2005/39, version 6 (January 2009).

4.2 Simple Benchmark Model

The calculated results for the simple benchmark model are reported in Table 18. Comments discussed in the previous section regarding the detailed benchmark model also apply to the simple benchmark model. The number of sigmas between the benchmark eigenvalue and the calculated eigenvalues is between 5 and 11 due to the small amount of uncertainty in the benchmark experiment itself.

Table 18. Comparison of Simple Benchmark Eigenvalues.

Analysis Code	Neutron Cross Section Library	Calculated			Benchmark			$\frac{C-E}{E}(\%)$
		k_{eff}	\pm	σ	k_{eff}	\pm	σ	
MCNP5	ENDF/B-V.2	0.99579	\pm	0.00004	0.9994	\pm	0.0004	-0.36
	ENDF/B-VI.8	0.99582	\pm	0.00004				-0.36
	ENDF/B-VII.0	0.99781	\pm	0.00004				-0.16
	JEFF-3.1	0.99531	\pm	0.00004				-0.41
	JENDL-3.3	1.00166	\pm	0.00004				0.22
KENO-V.a	ENDF/B-VII.0 (continuous energy)	0.99714	\pm	0.00005				-0.24
	ENDF/B-VII.0 (238-group)	0.99726	\pm	0.00005				-0.23

5.0 REFERENCES

1. J. T. Mihalczo and R. G. Taylor, "Experimentally Critical 7-in.-diam Highly Enriched Uranium Metal Cylinder Partially Reflected by Beryllium," *Trans. Am. Nucl. Soc.*, **82**, 169-170 (2000).

APPENDIX A: TYPICAL INPUT LISTINGS

The MCNP5 calculations were performed using the continuous energy, ENDF/B-VII.0 neutron cross section data and were performed with 1,050 generations with 250,000 neutrons per generation. The k_{eff} estimates did not include the first 50 generations and are the result of 250,000,000 neutron histories. Statistical uncertainty in k_{eff} for this number of histories is 0.00004.

Both KENO-VI and KENO-V.a calculations (for the detailed and simple benchmark models, respectively) were performed using continuous energy and 238-group, ENDF/B-VII.0 neutron cross section data. A total of 1,050 generations with 250,000 neutrons per generation (skipping the first 50 generations) were performed for a total of 250,000,000 neutron histories. Statistical uncertainty in k_{eff} using KENO is less than 0.00005.

A.1 MCNP Input Listings

A.1.1 Detailed Model

MCNP Input Listing, Table 17.

```
ORALLOY (93.2 235U) METAL CYLINDERS WITH BERYLLIUM TOP REFLECTOR
c
c John Darrell Bess - Idaho National Laboratory
c Last Updated: December 1, 2009
c
c
c Cell Cards *****
c --- HEU Cylinders -----
1 1 4.8067E-02 1 -3 -2 imp:n=1 $ Piece 2733
2 2 4.8104E-02 4 -5 -6 imp:n=1 $ Piece 2734
3 3 4.8045E-02 7 -9 -8 imp:n=1 $ Piece 2732
4 4 4.8237E-02 10 -12 -11 imp:n=1 $ Piece 2768
c
c --- Be Cylinders -----
5 5 1.2215E-01 13 -15 -14 imp:n=1 $ 1.5-inch-thick
6 6 1.2176E-01 16 -18 -17 imp:n=1 $ 2-inch-thick
7 7 1.2197E-01 19 -21 -20 imp:n=1 $ 1-inch-thick
8 8 1.2060E-01 22 -24 -23 imp:n=1 $ 0.5-inch-thick
9 9 1.2086E-01 25 -27 -26 imp:n=1 $ 9/16-inch-thick
c
c --- The Great Void -----
11 0 1 -27 -29 #1 #2 #3 #4 #5 #6 #7 #8 #9 imp:n=1 $ Lesser Void
12 0 -1:27:29 imp:n=0 $ Greater Void
c

c Surface Cards *****
c --- HEU Cylinders -----
c ----- Piece 2733 -----
1 pz 0.027178
2 cz 8.886031
3 pz 3.843782
c ----- Piece 2734 -----
4 pz 3.845560
5 cz 8.885428
6 pz 7.659751
c ----- Piece 2732 -----
7 pz 7.661529
8 cz 8.884920
9 pz 10.204704
c ----- Piece 2768 -----
10 pz 10.206482
11 cz 8.885555
12 pz 10.523982
c
c --- Be Cylinders -----
c ----- 1.5-inch-thick -----
13 pz 10.528808
14 cz 8.885460
```

NEA/NSC/DOC/(95)03/II
Volume II

HEU-MET-FAST-069

15 pz 14.338808
c ----- 2-inch-thick -----
16 pz 14.343634
17 cz 8.885460
18 pz 19.423634
c ----- 1-inch-thick -----
19 pz 19.428460
20 cz 8.885460
21 pz 21.968460
c ----- 0.5-inch-thick -----
22 pz 21.973286
23 cz 8.885460
24 pz 23.243286
c ----- 9/16-inch-thick -----
25 pz 23.248112
26 cz 8.885460
27 pz 24.676862
c
29 cz 38.100000
c

c Data Cards *****

c --- Material Cards -----

c ----- HEU Cylinders -----

c ----- Piece 2733 -----

m1 92234.00c 4.6267E-04 92235.00c 4.4702E-02 92236.00c 1.2424E-04
92238.00c 2.6677E-03 47107.00c 4.3387E-07 47109.00c 4.0309E-07
56130.00c 4.3554E-13 56132.00c 4.1500E-13 56134.00c 9.9311E-12
56135.00c 2.7086E-11 56136.00c 3.2271E-11 56137.00c 4.6151E-11
56138.00c 2.9460E-10 83209.00c 8.8562E-06 6000.00c 4.6978E-06
20040.00c 2.7297E-08 20042.00c 1.8218E-10 20043.00c 3.8013E-11
20044.00c 5.8738E-10 20046.00c 1.1263E-12 20048.00c 5.2655E-11
48106.00c 6.2746E-10 48108.00c 4.4675E-10 48110.00c 6.2695E-09
48111.00c 6.4251E-09 48112.00c 1.2112E-08 48113.00c 6.1340E-09
48114.00c 1.4421E-08 48116.00c 3.7597E-09 27059.00c 9.5745E-07
24050.00c 6.6012E-08 24052.00c 1.2730E-06 24053.00c 1.4435E-07
24054.00c 3.5931E-08 29063.00c 3.0710E-06 29065.00c 1.3688E-06
19039.00c 2.6918E-08 19040.00c 3.3770E-12 19041.00c 1.9426E-09
3006.00c 1.2340E-07 3007.00c 1.5025E-06 12024.00c 1.1003E-06
12025.00c 1.3929E-07 12026.00c 1.5336E-07 25055.00c 1.1503E-05
42092.00c 8.7279E-09 42094.00c 5.4403E-09 42095.00c 9.3631E-09
42096.00c 9.8101E-09 42097.00c 5.6167E-09 42098.00c 1.4192E-08
42100.00c 5.6638E-09 11023.00c 1.3254E-05 28058.00c 1.3090E-05
28060.00c 5.0423E-06 28061.00c 2.1918E-07 28062.00c 6.9886E-07
28064.00c 1.7798E-07 51121.00c 2.0151E-06 51123.00c 1.5072E-06
22046.00c 1.9445E-08 22047.00c 1.7536E-08 22048.00c 1.7376E-07
22049.00c 1.2751E-08 22050.00c 1.2209E-08 8016.00c 1.4102E-05
8017.00c 5.3607E-09 7014.00c 2.4082E-05 7015.00c 8.8949E-08
c Total 4.8067E-02
c

c ----- Piece 2734 -----

m2 92234.00c 4.5821E-04 92235.00c 4.4751E-02 92236.00c 1.1477E-04
92238.00c 2.6697E-03 47107.00c 4.3420E-07 47109.00c 4.0340E-07
56130.00c 4.3587E-13 56132.00c 4.1531E-13 56134.00c 9.9388E-12
56135.00c 2.7106E-11 56136.00c 3.2296E-11 56137.00c 4.6186E-11
56138.00c 2.9482E-10 83209.00c 8.8630E-06 6000.00c 4.7015E-06
20040.00c 2.7318E-08 20042.00c 1.8232E-10 20043.00c 3.8043E-11
20044.00c 5.8783E-10 20046.00c 1.1272E-12 20048.00c 5.2696E-11
48106.00c 6.2794E-10 48108.00c 4.4709E-10 48110.00c 6.2744E-09
48111.00c 6.4301E-09 48112.00c 1.2122E-08 48113.00c 6.1387E-09
48114.00c 1.4433E-08 48116.00c 3.7626E-09 27059.00c 9.5819E-07
24050.00c 6.6063E-08 24052.00c 1.2740E-06 24053.00c 1.4446E-07
24054.00c 3.5958E-08 29063.00c 3.0733E-06 29065.00c 1.3698E-06
19039.00c 2.6938E-08 19040.00c 3.3796E-12 19041.00c 1.9441E-09
3006.00c 1.2350E-07 3007.00c 1.5036E-06 12024.00c 1.1011E-06
12025.00c 1.3940E-07 12026.00c 1.5348E-07 25055.00c 1.1512E-05
42092.00c 8.7347E-09 42094.00c 5.4444E-09 42095.00c 9.3703E-09
42096.00c 9.8177E-09 42097.00c 5.6210E-09 42098.00c 1.4203E-08
42100.00c 5.6681E-09 11023.00c 1.3264E-05 28058.00c 1.3100E-05
28060.00c 5.0462E-06 28061.00c 2.1935E-07 28062.00c 6.9939E-07
28064.00c 1.7812E-07 51121.00c 2.0166E-06 51123.00c 1.5083E-06
22046.00c 1.9460E-08 22047.00c 1.7549E-08 22048.00c 1.7389E-07

NEA/NSC/DOC/(95)03/II
Volume II

HEU-MET-FAST-069

	22049.00c	1.2761E-08	22050.00c	1.2218E-08	8016.00c	1.4112E-05
	8017.00c	5.3648E-09	7014.00c	2.4100E-05	7015.00c	8.9017E-08
c	Total 4.8104E-02					
c						
c	----- Piece 2732 -----					
m3	92234.00c	4.5765E-04	92235.00c	4.4692E-02	92236.00c	1.0030E-04
	92238.00c	2.6854E-03	47107.00c	4.3368E-07	47109.00c	4.0291E-07
	56130.00c	4.3534E-13	56132.00c	4.1481E-13	56134.00c	9.9266E-12
	56135.00c	2.7073E-11	56136.00c	3.2256E-11	56137.00c	4.6130E-11
	56138.00c	2.9446E-10	83209.00c	8.8522E-06	6000.00c	4.6957E-06
	20040.00c	2.7284E-08	20042.00c	1.8210E-10	20043.00c	3.7996E-11
	20044.00c	5.8711E-10	20046.00c	1.1258E-12	20048.00c	5.2632E-11
	48106.00c	6.2717E-10	48108.00c	4.4655E-10	48110.00c	6.2667E-09
	48111.00c	6.4222E-09	48112.00c	1.2107E-08	48113.00c	6.1312E-09
	48114.00c	1.4415E-08	48116.00c	3.7580E-09	27059.00c	9.5702E-07
	24050.00c	6.5983E-08	24052.00c	1.2724E-06	24053.00c	1.4428E-07
	24054.00c	3.5915E-08	29063.00c	3.0696E-06	29065.00c	1.3682E-06
	19039.00c	2.6905E-08	19040.00c	3.3755E-12	19041.00c	1.9417E-09
	3006.00c	1.2335E-07	3007.00c	1.5018E-06	12024.00c	1.0998E-06
	12025.00c	1.3923E-07	12026.00c	1.5329E-07	25055.00c	1.1498E-05
	42092.00c	8.7240E-09	42094.00c	5.4378E-09	42095.00c	9.3589E-09
	42096.00c	9.8057E-09	42097.00c	5.6142E-09	42098.00c	1.4185E-08
	42100.00c	5.6612E-09	11023.00c	1.3248E-05	28058.00c	1.3084E-05
	28060.00c	5.0400E-06	28061.00c	2.1909E-07	28062.00c	6.9854E-07
	28064.00c	1.7790E-07	51121.00c	2.0142E-06	51123.00c	1.5065E-06
	22046.00c	1.9436E-08	22047.00c	1.7528E-08	22048.00c	1.7368E-07
	22049.00c	1.2745E-08	22050.00c	1.2204E-08	8016.00c	1.4095E-05
	8017.00c	5.3582E-09	7014.00c	2.4071E-05	7015.00c	8.8909E-08
c	Total 4.8045E-02					
c						
c	----- Piece 2768 -----					
m4	92234.00c	4.4496E-04	92235.00c	4.4855E-02	92236.00c	1.2468E-04
	92238.00c	2.7009E-03	47107.00c	4.3541E-07	47109.00c	4.0451E-07
	56130.00c	4.3708E-13	56132.00c	4.1646E-13	56134.00c	9.9662E-12
	56135.00c	2.7181E-11	56136.00c	3.2385E-11	56137.00c	4.6314E-11
	56138.00c	2.9564E-10	83209.00c	8.8875E-06	6000.00c	4.7145E-06
	20040.00c	2.7393E-08	20042.00c	1.8283E-10	20043.00c	3.8148E-11
	20044.00c	5.8945E-10	20046.00c	1.1303E-12	20048.00c	5.2842E-11
	48106.00c	6.2967E-10	48108.00c	4.4833E-10	48110.00c	6.2917E-09
	48111.00c	6.4479E-09	48112.00c	1.2155E-08	48113.00c	6.1557E-09
	48114.00c	1.4472E-08	48116.00c	3.7730E-09	27059.00c	9.6084E-07
	24050.00c	6.6246E-08	24052.00c	1.2775E-06	24053.00c	1.4486E-07
	24054.00c	3.6058E-08	29063.00c	3.0818E-06	29065.00c	1.3736E-06
	19039.00c	2.7013E-08	19040.00c	3.3890E-12	19041.00c	1.9494E-09
	3006.00c	1.2384E-07	3007.00c	1.5078E-06	12024.00c	1.1042E-06
	12025.00c	1.3979E-07	12026.00c	1.5391E-07	25055.00c	1.1544E-05
	42092.00c	8.7588E-09	42094.00c	5.4595E-09	42095.00c	9.3962E-09
	42096.00c	9.8448E-09	42097.00c	5.6366E-09	42098.00c	1.4242E-08
	42100.00c	5.6838E-09	11023.00c	1.3301E-05	28058.00c	1.3136E-05
	28060.00c	5.0601E-06	28061.00c	2.1996E-07	28062.00c	7.0133E-07
	28064.00c	1.7861E-07	51121.00c	2.0222E-06	51123.00c	1.5125E-06
	22046.00c	1.9514E-08	22047.00c	1.7598E-08	22048.00c	1.7437E-07
	22049.00c	1.2796E-08	22050.00c	1.2252E-08	8016.00c	1.4151E-05
	8017.00c	5.3796E-09	7014.00c	2.4167E-05	7015.00c	8.9263E-08
c	Total 4.8237E-02					
c						
c	----- Be Cylinders -----					
c	----- 1.5-inch-thick -----					
m5	4009.00c	1.2112E-01	13027.00c	2.4672E-05	5010.00c	2.0422E-07
	5011.00c	8.2201E-07	83209.00c	2.6545E-06	35079.00c	3.5191E-09
	35081.00c	3.4233E-09	6000.00c	1.1084E-04	48106.00c	2.4674E-10
	48108.00c	1.7568E-10	48110.00c	2.4655E-09	48111.00c	2.5267E-09
	48112.00c	4.7632E-09	48113.00c	2.4122E-09	48114.00c	5.6712E-09
	48116.00c	1.4785E-09	66156.00c	4.0965E-12	66158.00c	6.8275E-12
	66160.00c	1.5976E-10	66161.00c	1.2911E-09	66162.00c	1.7417E-09
	66163.00c	1.7000E-09	66164.00c	1.9240E-09	26054.00c	1.5096E-06
	26056.00c	2.3697E-05	26057.00c	5.4727E-07	26058.00c	7.2832E-08
	64152.00c	1.4111E-11	64154.00c	1.5381E-10	64155.00c	1.0442E-09
	64156.00c	1.4442E-09	64157.00c	1.1042E-09	64158.00c	1.7526E-09
	64160.00c	1.5423E-09	12024.00c	7.2114E-06	12025.00c	9.1295E-07
	12026.00c	1.0052E-06	28058.00c	1.2869E-08	28060.00c	4.9571E-09
	28061.00c	2.1548E-10	28062.00c	6.8706E-10	28064.00c	1.7497E-10

NEA/NSC/DOC/(95)03/II
Volume II

HEU-MET-FAST-069

```

      8016.00c 8.5578E-04 8017.00c 3.2532E-07 62144.00c 2.2653E-10
      62147.00c 1.1061E-09 62148.00c 8.2937E-10 62149.00c 1.0197E-09
      62150.00c 5.4455E-10 62152.00c 1.9738E-09 62154.00c 1.6787E-09
c      Total 1.2215E-01
mt5      Be.00t OBeO.00t
c
c ----- 2-inch-thick -----
m6      4009.00c 1.2073E-01 13027.00c 2.4594E-05 5010.00c 2.0358E-07
      5011.00c 8.1942E-07 83209.00c 2.6461E-06 35079.00c 3.5080E-09
      35081.00c 3.4125E-09 6000.00c 1.1049E-04 48106.00c 2.4596E-10
      48108.00c 1.7513E-10 48110.00c 2.4577E-09 48111.00c 2.5187E-09
      48112.00c 4.7481E-09 48113.00c 2.4046E-09 48114.00c 5.6533E-09
      48116.00c 1.4738E-09 66156.00c 4.0835E-12 66158.00c 6.8059E-12
      66160.00c 1.5926E-10 66161.00c 1.2870E-09 66162.00c 1.7362E-09
      66163.00c 1.6947E-09 66164.00c 1.9179E-09 26054.00c 1.5048E-06
      26056.00c 2.3622E-05 26057.00c 5.4554E-07 26058.00c 7.2602E-08
      64152.00c 1.4066E-11 64154.00c 1.5332E-10 64155.00c 1.0409E-09
      64156.00c 1.4397E-09 64157.00c 1.1007E-09 64158.00c 1.7470E-09
      64160.00c 1.5374E-09 12024.00c 7.1886E-06 12025.00c 9.1006E-07
      12026.00c 1.0020E-06 28058.00c 1.2828E-08 28060.00c 4.9415E-09
      28061.00c 2.1480E-10 28062.00c 6.8489E-10 28064.00c 1.7442E-10
      8016.00c 8.5308E-04 8017.00c 3.2429E-07 62144.00c 2.2581E-10
      62147.00c 1.1026E-09 62148.00c 8.2675E-10 62149.00c 1.0165E-09
      62150.00c 5.4283E-10 62152.00c 1.9676E-09 62154.00c 1.6734E-09
c      Total 1.2176E-01
mt6      Be.00t OBeO.00t
c
c ----- 1-inch-thick -----
m7      4009.00c 1.2094E-01 13027.00c 2.4636E-05 5010.00c 2.0393E-07
      5011.00c 8.2083E-07 83209.00c 2.6507E-06 35079.00c 3.5141E-09
      35081.00c 3.4184E-09 6000.00c 1.1069E-04 48106.00c 2.4639E-10
      48108.00c 1.7543E-10 48110.00c 2.4619E-09 48111.00c 2.5230E-09
      48112.00c 4.7563E-09 48113.00c 2.4087E-09 48114.00c 5.6630E-09
      48116.00c 1.4764E-09 66156.00c 4.0906E-12 66158.00c 6.8176E-12
      66160.00c 1.5953E-10 66161.00c 1.2892E-09 66162.00c 1.7392E-09
      66163.00c 1.6976E-09 66164.00c 1.9212E-09 26054.00c 1.5074E-06
      26056.00c 2.3663E-05 26057.00c 5.4648E-07 26058.00c 7.2727E-08
      64152.00c 1.4091E-11 64154.00c 1.5359E-10 64155.00c 1.0427E-09
      64156.00c 1.4422E-09 64157.00c 1.1026E-09 64158.00c 1.7500E-09
      64160.00c 1.5401E-09 12024.00c 7.2010E-06 12025.00c 9.1164E-07
      12026.00c 1.0037E-06 28058.00c 1.2851E-08 28060.00c 4.9500E-09
      28061.00c 2.1517E-10 28062.00c 6.8607E-10 28064.00c 1.7472E-10
      8016.00c 8.5455E-04 8017.00c 3.2485E-07 62144.00c 2.2620E-10
      62147.00c 1.1045E-09 62148.00c 8.2817E-10 62149.00c 1.0183E-09
      62150.00c 5.4377E-10 62152.00c 1.9710E-09 62154.00c 1.6762E-09
c      Total 1.2197E-01
mt7      Be.00t OBeO.00t
c
c ----- 0.5-inch-thick -----
m8      4009.00c 1.1959E-01 13027.00c 2.4360E-05 5010.00c 2.0164E-07
      5011.00c 8.1163E-07 83209.00c 2.6209E-06 35079.00c 3.4747E-09
      35081.00c 3.3801E-09 6000.00c 1.0944E-04 48106.00c 2.4363E-10
      48108.00c 1.7346E-10 48110.00c 2.4343E-09 48111.00c 2.4947E-09
      48112.00c 4.7030E-09 48113.00c 2.3817E-09 48114.00c 5.5995E-09
      48116.00c 1.4598E-09 66156.00c 4.0447E-12 66158.00c 6.7412E-12
      66160.00c 1.5774E-10 66161.00c 1.2748E-09 66162.00c 1.7197E-09
      66163.00c 1.6786E-09 66164.00c 1.8997E-09 26054.00c 1.4905E-06
      26056.00c 2.3398E-05 26057.00c 5.4036E-07 26058.00c 7.1911E-08
      64152.00c 1.3932E-11 64154.00c 1.5186E-10 64155.00c 1.0310E-09
      64156.00c 1.4260E-09 64157.00c 1.0902E-09 64158.00c 1.7304E-09
      64160.00c 1.5228E-09 12024.00c 7.1203E-06 12025.00c 9.0141E-07
      12026.00c 9.9246E-07 28058.00c 1.2706E-08 28060.00c 4.8945E-09
      28061.00c 2.1276E-10 28062.00c 6.7837E-10 28064.00c 1.7276E-10
      8016.00c 8.4497E-04 8017.00c 3.2121E-07 62144.00c 2.2366E-10
      62147.00c 1.0921E-09 62148.00c 8.1889E-10 62149.00c 1.0069E-09
      62150.00c 5.3767E-10 62152.00c 1.9489E-09 62154.00c 1.6574E-09
c      Total 1.2060E-01
mt8      Be.00t OBeO.00t
c
c ----- 9/16-inch-thick -----
m9      4009.00c 1.1984E-01 13027.00c 2.4412E-05 5010.00c 2.0207E-07
      5011.00c 8.1336E-07 83209.00c 2.6265E-06 35079.00c 3.4821E-09

```

Revision: 0

Date: September 30, 2010

NEA/NSC/DOC/(95)03/II
Volume II

HEU-MET-FAST-069

```
35081.00c 3.3873E-09 6000.00c 1.0968E-04 48106.00c 2.4415E-10
48108.00c 1.7383E-10 48110.00c 2.4395E-09 48111.00c 2.5001E-09
48112.00c 4.7130E-09 48113.00c 2.3868E-09 48114.00c 5.6115E-09
48116.00c 1.4629E-09 66156.00c 4.0533E-12 66158.00c 6.7556E-12
66160.00c 1.5808E-10 66161.00c 1.2775E-09 66162.00c 1.7233E-09
66163.00c 1.6821E-09 66164.00c 1.9037E-09 26054.00c 1.4937E-06
26056.00c 2.3448E-05 26057.00c 5.4151E-07 26058.00c 7.2065E-08
64152.00c 1.3962E-11 64154.00c 1.5219E-10 64155.00c 1.0332E-09
64156.00c 1.4290E-09 64157.00c 1.0925E-09 64158.00c 1.7341E-09
64160.00c 1.5261E-09 12024.00c 7.1354E-06 12025.00c 9.0334E-07
12026.00c 9.9457E-07 28058.00c 1.2734E-08 28060.00c 4.9049E-09
28061.00c 2.1321E-10 28062.00c 6.7982E-10 28064.00c 1.7313E-10
8016.00c 8.4677E-04 8017.00c 3.2189E-07 62144.00c 2.2414E-10
62147.00c 1.0944E-09 62148.00c 8.2063E-10 62149.00c 1.0090E-09
62150.00c 5.3881E-10 62152.00c 1.9530E-09 62154.00c 1.6610E-09
c      Total 1.2086E-01
mt9    Be.00t OBeO.00t
c
c --- Control Cards -----
mode  n
kcode 250000 1 50 1050
ksrc 0 0 1.908302 0 0 5.752549 0 0 8.933052 0 0 10.365146
print
```

A.1.2 Simple Model

MCNP Input Listing, Table 18.

```
ORALLOY (93.2 235U) METAL CYLINDER WITH BERYLLIUM TOP REFLECTOR (SIMPLE)
c
c John Darrell Bess - Idaho National Laboratory
c Last Updated: December 1, 2009
c
c
c Cell Cards *****
1      1  4.7986E-02 -1 -2 imp:n=1 $ HEU
2      2  1.2056E-01 -1  2 imp:n=1 $ Be
3      0              1      imp:n=0 $ Void
c

c Surface Cards *****
1      rcc  0.0 0.0 0.0 0.0 0.0 24.60625 8.89
2      pz 10.4775
c

c Data Cards *****
c --- Material Cards -----
c ----- HEU Cylinders -----
m1      92234.00c 4.5958E-04 92235.00c 4.4736E-02 92236.00c 1.1523E-04
        92238.00c 2.6745E-03
c          Total 4.7986E-02
c
c ----- Be Cylinders -----
m2      4009.00c 1.2056E-01
c          Total 1.2056E-01
mt2      Be.00t
c
c --- Control Cards -----
mode n
kcode 250000 1 50 1050
ksrc 0 0 1.908302 0 0 5.752549 0 0 8.933052 0 0 10.365146
print
```

A.2 KENO Input Listings

A.2.1 Detailed Model (KENO-VI) – 238-group

KENO Input Listing, Table 17.

```
'Input generated by GeeWiz SCALE 6.0.2 Compiled on February 18, 2009
=csas6
oralloy (93.2 235u) metal cylinders with beryllium top reflector
v7-238
read composition
u-234      1 0 0.00046267 296      end
u-235      1 0 0.044702 296      end
u-236      1 0 0.00012424 296      end
u-238      1 0 0.0026677 296      end
ag         1 0 8.3696e-07 296
          47107 51.839
          47109 48.161      end
ba         1 0 4.1089e-10 296
          56130 0.106
          56132 0.101
          56134 2.417
          56135 6.592
          56136 7.854
          56137 11.232
          56138 71.698      end
bi         1 0 8.8562e-06 296      end
c          1 0 4.6978e-06 296      end
ca         1 0 2.8158e-08 296
          20040 96.941
          20042 0.647
          20043 0.135
          20044 2.086
          20046 0.004
          20048 0.187      end
cd         1 0 5.0196e-08 296
          48106 1.25
          48108 0.89
          48110 12.49
          48111 12.8
          48112 24.13
          48113 12.22
          48114 28.73
          48116 7.49      end
co         1 0 9.5745e-07 296      end
cr         1 0 1.5193e-06 296
          24050 4.345
          24052 83.789
          24053 9.501
          24054 2.365      end
cu         1 0 4.4398e-06 296
          29063 69.17
          29065 30.83      end
k          1 0 2.8864e-08 296
          19039 93.2581
          19040 0.0117
          19041 6.7302      end
li         1 0 1.6259e-06 296
          3006 7.59
          3007 92.41      end
mg         1 0 1.3929e-06 296
          12024 78.99
          12025 10
          12026 11.01      end
mn         1 0 1.1503e-05 296      end
mo         1 0 5.8814e-08 296
          42092 14.84
          42094 9.25
          42095 15.92
          42096 16.68
          42097 9.55
```

HEU-MET-FAST-069

			42098	24.13	
			42100	9.63	end
na	1 0	1.3254e-05	296	end	
ni	1 0	1.9228e-05	296		
			28058	68.0769	
			28060	26.2231	
			28061	1.1399	
			28062	3.6345	
			28064	0.9256	end
sb	1 0	3.5223e-06	296		
			51121	57.21	
			51123	42.79	end
ti	1 0	2.357e-07	296		
			22046	8.25	
			22047	7.44	
			22048	73.72	
			22049	5.41	
			22050	5.18	end
o-16	1 0	1.4102e-05	296	end	
o-17	1 0	5.3607e-09	296	end	
n-14	1 0	2.4082e-05	296	end	
n-15	1 0	8.8949e-08	296	end	
u-234	2 0	0.00045821	296	end	
u-235	2 0	0.044751	296	end	
u-236	2 0	0.00011477	296	end	
u-238	2 0	0.0026697	296	end	
ag	2 0	8.3760e-07	296		
			47107	51.839	
			47109	48.161	end
ba	2 0	4.1120e-10	296		
			56130	0.106	
			56132	0.101	
			56134	2.417	
			56135	6.592	
			56136	7.854	
			56137	11.232	
			56138	71.698	end
bi	2 0	8.8630e-06	296	end	
c	2 0	4.7015e-06	296	end	
ca	2 0	2.8180e-08	296		
			20040	96.941	
			20042	0.647	
			20043	0.135	
			20044	2.086	
			20046	0.004	
			20048	0.187	end
cd	2 0	5.0235e-08	296		
			48106	1.25	
			48108	0.89	
			48110	12.49	
			48111	12.8	
			48112	24.13	
			48113	12.22	
			48114	28.73	
			48116	7.49	end
co	2 0	9.5819e-07	296	end	
cr	2 0	1.5204e-06	296		
			24050	4.345	
			24052	83.789	
			24053	9.501	
			24054	2.365	end
cu	2 0	4.4432e-06	296		
			29063	69.17	
			29065	30.83	end
k	2 0	2.8886e-08	296		
			19039	93.2581	
			19040	0.0117	
			19041	6.7302	end
li	2 0	1.6271e-06	296		
			3006	7.59	
			3007	92.41	end
mg	2 0	1.394e-06	296		

HEU-MET-FAST-069

			12024	78.99	
			12025	10	
			12026	11.01	end
mn	2 0	1.1512e-05	296	end	
mo	2 0	5.8859e-08	296		
			42092	14.84	
			42094	9.25	
			42095	15.92	
			42096	16.68	
			42097	9.55	
			42098	24.13	
			42100	9.63	end
na	2 0	1.3264e-05	296	end	
ni	2 0	1.9243e-05	296		
			28058	68.0769	
			28060	26.2231	
			28061	1.1399	
			28062	3.6345	
			28064	0.9256	end
sb	2 0	3.5250e-06	296		
			51121	57.21	
			51123	42.79	end
ti	2 0	2.3588e-07	296		
			22046	8.25	
			22047	7.44	
			22048	73.72	
			22049	5.41	
			22050	5.18	end
o-16	2 0	1.4112e-05	296	end	
o-17	2 0	5.3648e-09	296	end	
n-14	2 0	2.41e-05	296	end	
n-15	2 0	8.9017e-08	296	end	
u-234	3 0	0.00045765	296	end	
u-235	3 0	0.044692	296	end	
u-236	3 0	0.0001003	296	end	
u-238	3 0	0.0026854	296	end	
ag	3 0	8.3658e-07	296		
			47107	51.839	
			47109	48.161	end
ba	3 0	4.1070e-10	296		
			56130	0.106	
			56132	0.101	
			56134	2.417	
			56135	6.592	
			56136	7.854	
			56137	11.232	
			56138	71.698	end
bi	3 0	8.8522e-06	296	end	
c	3 0	4.6957e-06	296	end	
ca	3 0	2.8145e-08	296		
			20040	96.941	
			20042	0.647	
			20043	0.135	
			20044	2.086	
			20046	0.004	
			20048	0.187	end
cd	3 0	5.0174e-08	296		
			48106	1.25	
			48108	0.89	
			48110	12.49	
			48111	12.8	
			48112	24.13	
			48113	12.22	
			48114	28.73	
			48116	7.49	end
co	3 0	9.5702e-07	296	end	
cr	3 0	1.5186e-06	296		
			24050	4.345	
			24052	83.789	
			24053	9.501	
			24054	2.365	end
cu	3 0	4.4378e-06	296		

NEA/NSC/DOC/(95)03/II
Volume II

HEU-MET-FAST-069

			29063 69.17	
			29065 30.83	end
k	3 0 2.8851e-08	296		
			19039 93.2581	
			19040 0.0117	
			19041 6.7302	end
li	3 0 1.6251e-06	296		
			3006 7.59	
			3007 92.41	end
mg	3 0 1.3923e-06	296		
			12024 78.99	
			12025 10	
			12026 11.01	end
mn	3 0 1.1498e-05	296	end	
mo	3 0 5.8787e-08	296		
			42092 14.84	
			42094 9.25	
			42095 15.92	
			42096 16.68	
			42097 9.55	
			42098 24.13	
			42100 9.63	end
na	3 0 1.3248e-05	296	end	
ni	3 0 1.9220e-05	296		
			28058 68.0769	
			28060 26.2231	
			28061 1.1399	
			28062 3.6345	
			28064 0.9256	end
sb	3 0 3.5207e-06	296		
			51121 57.21	
			51123 42.79	end
ti	3 0 2.3559e-07	296		
			22046 8.25	
			22047 7.44	
			22048 73.72	
			22049 5.41	
			22050 5.18	end
o-16	3 0 1.4095e-05	296	end	
o-17	3 0 5.3582e-09	296	end	
n-14	3 0 2.4071e-05	296	end	
n-15	3 0 8.8909e-08	296	end	
u-234	4 0 0.00044496	296	end	
u-235	4 0 0.044855	296	end	
u-236	4 0 0.00012468	296	end	
u-238	4 0 0.0027009	296	end	
ag	4 0 8.3992e-07	296		
			47107 51.839	
			47109 48.161	end
ba	4 0 4.1234e-10	296		
			56130 0.106	
			56132 0.101	
			56134 2.417	
			56135 6.592	
			56136 7.854	
			56137 11.232	
			56138 71.698	end
bi	4 0 8.8875e-06	296	end	
c	4 0 4.7145e-06	296	end	
ca	4 0 2.8258e-08	296		
			20040 96.941	
			20042 0.647	
			20043 0.135	
			20044 2.086	
			20046 0.004	
			20048 0.187	end
cd	4 0 5.0374e-08	296		
			48106 1.25	
			48108 0.89	
			48110 12.49	
			48111 12.8	
			48112 24.13	

HEU-MET-FAST-069

				48113	12.22	
				48114	28.73	
				48116	7.49	end
co	4	0	9.6084e-07	296	end	
cr	4	0	1.5246e-06	296		
				24050	4.345	
				24052	83.789	
				24053	9.501	
				24054	2.365	end
cu	4	0	4.4555e-06	296		
				29063	69.17	
				29065	30.83	end
k	4	0	2.8966e-08	296		
				19039	93.2581	
				19040	0.0117	
				19041	6.7302	end
li	4	0	1.6316e-06	296		
				3006	7.59	
				3007	92.41	end
mg	4	0	1.3979e-06	296		
				12024	78.99	
				12025	10	
				12026	11.01	end
mn	4	0	1.1544e-05	296	end	
mo	4	0	5.9022e-08	296		
				42092	14.84	
				42094	9.25	
				42095	15.92	
				42096	16.68	
				42097	9.55	
				42098	24.13	
				42100	9.63	end
na	4	0	1.3301e-05	296	end	
ni	4	0	1.9296e-05	296		
				28058	68.0769	
				28060	26.2231	
				28061	1.1399	
				28062	3.6345	
				28064	0.9256	end
sb	4	0	3.5347e-06	296		
				51121	57.21	
				51123	42.79	end
ti	4	0	2.3653e-07	296		
				22046	8.25	
				22047	7.44	
				22048	73.72	
				22049	5.41	
				22050	5.18	end
o-16	4	0	1.4151e-05	296	end	
o-17	4	0	5.3796e-09	296	end	
n-14	4	0	2.4167e-05	296	end	
n-15	4	0	8.9263e-08	296	end	
bebound	5	0	0.12112	296	end	
al	5	0	2.4672e-05	296	end	
b	5	0	1.0262e-06	296		
				5010	19.9	
				5011	80.1	end
bi	5	0	2.6545e-06	296	end	
br	5	0	6.9425e-09	296		
				35079	50.69	
				35081	49.31	end
c	5	0	0.00011084	296	end	
cd	5	0	1.974e-08	296		
				48106	1.25	
				48108	0.89	
				48110	12.49	
				48111	12.8	
				48112	24.13	
				48113	12.22	
				48114	28.73	
				48116	7.49	end
dy	5	0	6.8275e-09	296		

HEU-MET-FAST-069

			66156	0.06	
			66158	0.1	
			66160	2.34	
			66161	18.91	
			66162	25.51	
			66163	24.9	
			66164	28.18	end
fe	5	0	2.5827e-05	296	
			26054	5.845	
			26056	91.754	
			26057	2.119	
			26058	0.282	end
gd	5	0	7.0554e-09	296	
			64152	0.2	
			64154	2.18	
			64155	14.8	
			64156	20.47	
			64157	15.65	
			64158	24.84	
			64160	21.86	end
mg	5	0	9.1295e-06	296	
			12024	78.99	
			12025	10	
			12026	11.01	end
ni	5	0	1.8904e-08	296	
			28058	68.0769	
			28060	26.2231	
			28061	1.1399	
			28062	3.6345	
			28064	0.9256	end
o-16	5	0	0.00085578	296	end
o-17	5	0	3.2532e-07	296	end
sm	5	0	7.3787e-09	296	
			62144	3.07	
			62147	14.99	
			62148	11.24	
			62149	13.82	
			62150	7.38	
			62152	26.75	
			62154	22.75	end
bebound	6	0	0.12073	296	end
al	6	0	2.4594e-05	296	end
b	6	0	1.023e-06	296	
			5010	19.9	
			5011	80.1	end
bi	6	0	2.6461e-06	296	end
br	6	0	6.9205e-09	296	
			35079	50.69	
			35081	49.31	end
c	6	0	0.00011049	296	end
cd	6	0	1.9677e-08	296	
			48106	1.25	
			48108	0.89	
			48110	12.49	
			48111	12.8	
			48112	24.13	
			48113	12.22	
			48114	28.73	
			48116	7.49	end
dy	6	0	6.8059e-09	296	
			66156	0.06	
			66158	0.1	
			66160	2.34	
			66161	18.91	
			66162	25.51	
			66163	24.9	
			66164	28.18	end
fe	6	0	2.5745e-05	296	
			26054	5.845	
			26056	91.754	
			26057	2.119	
			26058	0.282	end

HEU-MET-FAST-069

gd	6 0 7.0331e-09 296	64152 0.2 64154 2.18 64155 14.8 64156 20.47 64157 15.65 64158 24.84 64160 21.86	end
mg	6 0 9.1006e-06 296	12024 78.99 12025 10 12026 11.01	end
ni	6 0 1.8844e-08 296	28058 68.0769 28060 26.2231 28061 1.1399 28062 3.6345 28064 0.9256	end
o-16	6 0 0.00085308 296	end	
o-17	6 0 3.2429e-07 296	end	
sm	6 0 7.3554e-09 296	62144 3.07 62147 14.99 62148 11.24 62149 13.82 62150 7.38 62152 26.75 62154 22.75	end
bebound	7 0 0.12094 296	end	
al	7 0 2.4636e-05 296	end	
b	7 0 1.0248e-06 296	5010 19.9 5011 80.1	end
bi	7 0 2.6507e-06 296	end	
br	7 0 6.9325e-09 296	35079 50.69 35081 49.31	end
c	7 0 0.00011069 296	end	
cd	7 0 1.9711e-08 296	48106 1.25 48108 0.89 48110 12.49 48111 12.8 48112 24.13 48113 12.22 48114 28.73 48116 7.49	end
dy	7 0 6.8176e-09 296	66156 0.06 66158 0.1 66160 2.34 66161 18.91 66162 25.51 66163 24.9 66164 28.18	end
fe	7 0 2.579e-05 296	26054 5.845 26056 91.754 26057 2.119 26058 0.282	end
gd	7 0 7.0453e-09 296	64152 0.2 64154 2.18 64155 14.8 64156 20.47 64157 15.65 64158 24.84 64160 21.86	end
mg	7 0 9.1164e-06 296	12024 78.99 12025 10 12026 11.01	end

HEU-MET-FAST-069

ni	7 0 1.8877e-08 296	28058 68.0769	
		28060 26.2231	
		28061 1.1399	
		28062 3.6345	
		28064 0.9256	end
o-16	7 0 0.00085455 296	end	
o-17	7 0 3.2485e-07 296	end	
sm	7 0 7.3681e-09 296	62144 3.07	
		62147 14.99	
		62148 11.24	
		62149 13.82	
		62150 7.38	
		62152 26.75	
		62154 22.75	end
bebound	8 0 0.11959 296	end	
al	8 0 2.436e-05 296	end	
b	8 0 1.0133e-06 296	5010 19.9	
		5011 80.1	end
bi	8 0 2.6209e-06 296	end	
br	8 0 6.8547e-09 296	35079 50.69	
		35081 49.31	end
c	8 0 0.00010944 296	end	
cd	8 0 1.949e-08 296	48106 1.25	
		48108 0.89	
		48110 12.49	
		48111 12.8	
		48112 24.13	
		48113 12.22	
		48114 28.73	
		48116 7.49	end
dy	8 0 6.7412e-09 296	66156 0.06	
		66158 0.1	
		66160 2.34	
		66161 18.91	
		66162 25.51	
		66163 24.9	
		66164 28.18	end
fe	8 0 2.55e-05 296	26054 5.845	
		26056 91.754	
		26057 2.119	
		26058 0.282	end
gd	8 0 6.9662e-09 296	64152 0.2	
		64154 2.18	
		64155 14.8	
		64156 20.47	
		64157 15.65	
		64158 24.84	
		64160 21.86	end
mg	8 0 9.0141e-06 296	12024 78.99	
		12025 10	
		12026 11.01	end
ni	8 0 1.8665e-08 296	28058 68.0769	
		28060 26.2231	
		28061 1.1399	
		28062 3.6345	
		28064 0.9256	end
o-16	8 0 0.00084497 296	end	
o-17	8 0 3.2121e-07 296	end	
sm	8 0 7.2855e-09 296	62144 3.07	
		62147 14.99	
		62148 11.24	

HEU-MET-FAST-069

```

62149 13.82
62150 7.38
62152 26.75
62154 22.75    end
bebound      9 0 0.11984 296    end
al           9 0 2.4412e-05 296    end
b           9 0 1.0154e-06 296
5010 19.9
5011 80.1    end
bi           9 0 2.6265e-06 296    end
br           9 0 6.8694e-09 296
35079 50.69
35081 49.31    end
c           9 0 0.00010968 296    end
cd           9 0 1.9532e-08 296
48106 1.25
48108 0.89
48110 12.49
48111 12.8
48112 24.13
48113 12.22
48114 28.73
48116 7.49    end
dy           9 0 6.7556e-09 296
66156 0.06
66158 0.1
66160 2.34
66161 18.91
66162 25.51
66163 24.9
66164 28.18    end
fe           9 0 2.5555e-05 296
26054 5.845
26056 91.754
26057 2.119
26058 0.282    end
gd           9 0 6.9811e-09 296
64152 0.2
64154 2.18
64155 14.8
64156 20.47
64157 15.65
64158 24.84
64160 21.86    end
mg           9 0 9.0334e-06 296
12024 78.99
12025 10
12026 11.01    end
ni           9 0 1.8705e-08 296
28058 68.0769
28060 26.2231
28061 1.1399
28062 3.6345
28064 0.9256    end
o-16        9 0 0.00084677 296    end
o-17        9 0 3.2189e-07 296    end
sm           9 0 7.301e-09 296
62144 3.07
62147 14.99
62148 11.24
62149 13.82
62150 7.38
62152 26.75
62154 22.75    end
end composition
read parameter
gen=1050
npg=250000
nsk=50
htm=yes
end parameter
read geometry

```

HEU-MET-FAST-069

```
global unit 1
com='global unit 1'
cylinder 1 8.886031 3.843782 0.027178
cylinder 2 8.885428 7.659751 3.84556
cylinder 3 8.88492 10.204704 7.661529
cylinder 4 8.885555 10.523982 10.206482
cylinder 5 8.885484 14.338808 10.528808
cylinder 6 8.885484 19.423634 14.343634
cylinder 7 8.885484 21.968460 19.428460
cylinder 8 8.885484 23.243286 21.973286
cylinder 9 8.885484 24.676862 23.248112
cylinder 10 38.1 24.676862 0.025400
media 1 1 1
media 2 1 2
media 3 1 3
media 4 1 4
media 5 1 5
media 6 1 6
media 7 1 7
media 8 1 8
media 9 1 9
media 0 1 -1 -2 -3 -4 -5 -6 -7 -8 -9 10
boundary 10
end geometry
end data
end
```

A.2.2 Simple Model (KENO-V.a) – continuous energy

KENO Input Listing, Table 18.

```
'Input generated by GeeWiz SCALE 6.0.2 Compiled on January 30, 2009
=csas5
oralloy (93.2 235u) metal cylinder with beryllium top reflector (simple)
ce_v7_endf
read composition
  u-234      1 0 0.00045958 296  end
  u-235      1 0 0.044736 296  end
  u-236      1 0 0.00011523 296  end
  u-238      1 0 0.0026745 296  end
  bebound    2 0 0.12056 296  end
end composition
read parameter
  gen=1050
  npg=250000
  nsk=50
  htm=yes
end parameter
read geometry
global unit 1
  zcylinder 1 1      8.89  10.4775      0
  zcylinder 2 1      8.89  24.60625     0
end geometry
end data
end
```


APPENDIX B: DETAILED MODEL VARIANT

B.1 Description of Model Variant

A variant of the detailed benchmark model provided in Section 3 includes the stainless steel diaphragm (Figure B.1). This model was utilized in the evaluation of the uncertainties.

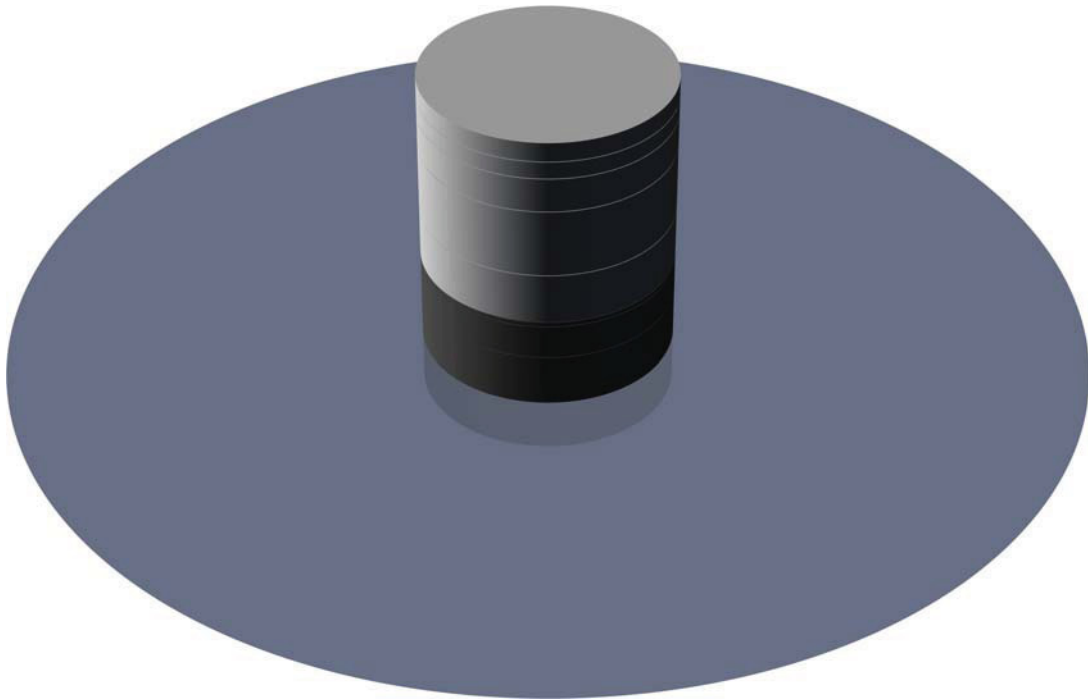


Figure B.1. Oralloy Metal Cylinder with Beryllium Top Reflector and Stainless Steel Diaphragm.

B.2 Additional Dimensions

The detailed benchmark model provided in Figure 7 has been modified to include the stainless steel diaphragm (Figure B.2). The stainless steel diaphragm that separates the bottommost uranium disc from the remainder of the experiment is 0.0254-cm thick and 76.2 cm in diameter.

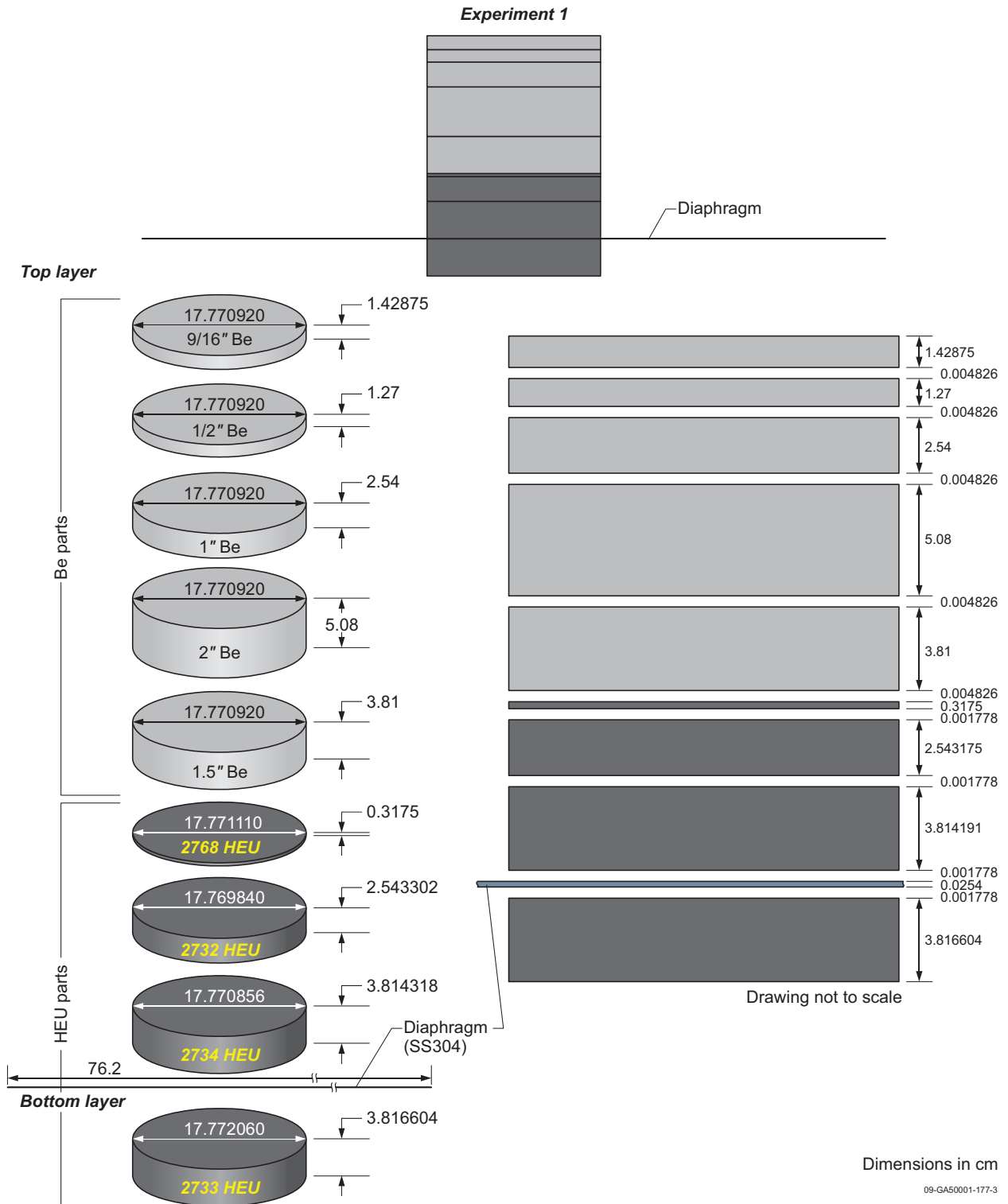


Figure B.2. Detailed Model Variant of Oralloy and Beryllium Discs with Stainless Steel Diaphragm.

B.3 Additional Material Data

The atomic composition of the stainless steel 304L diaphragm is shown in Table B.1. The mass density of the steel is 7.95 g/cm^3 .

Table B.1. Stainless Steel 304L Composition.

Material	Average Wt. % ^(a)	Atom Density (a/b-cm)
Fe	69.4475	5.9537E-02
Cr	19	1.7494E-02
Ni	10	8.1569E-03
Mn	1	8.7145E-04
Si	0.5	8.5232E-04
C	0.015	5.9791E-05
P	0.0225	3.4778E-05
S	0.015	2.2396E-05
Total	100.0000	8.7029E-02

(a) R. H. Perry, D. W. Green, and J. O. Maloney, "Perry's Chemical Engineers' Handbook," 7th ed., McGraw-Hill, New York, NY (1997).

B.4 Temperature Data

The temperature of the detailed model variant is also 294 K.

B.5 Experimental and Model k_{eff}

The experimental k_{eff} value for the full assembly is 1.0006 ± 0.0003 . The adjusted experimental eigenvalue for the stack of uranium and beryllium discs with the stainless steel diaphragm is 0.9995 ± 0.0003 .

B.5.1 Detailed Model – The expected k_{eff} value for the detailed model variant, adjusted for room return effects, is 0.9990 ± 0.0003 .

B.6 Calculation of Diaphragm Worth

The stainless steel diaphragm is not included in the detailed or simple benchmark models. The worth of the diaphragm was experimentally determined to be -10.33% . No uncertainty was provided, therefore an assumed uncertainty of 10% provides a worth uncertainty of $\pm 1.03\%$. The calculated effect for removal of the steel diaphragm is $-0.00067 \pm 0.00006 \Delta k_{\text{eff}}$. The calculated worth of the diaphragm is $-10.15 \pm 1.00\%$ (using a β_{eff} of 0.0066 ± 0.00033 with an assumed uncertainty of 5%), which is comparable to the experimental value.

There was insufficient information to adequately calculate the worth of the other assembly components.

B.7 Results of Sample Calculations for Detailed Benchmark Model Variant

Computational codes and libraries used for the analysis of the detailed and simple benchmark models (Section 4) were also employed in the evaluation of the detailed model variant that includes the stainless steel diaphragm. The calculated results are shown in Table B.2, with calculate neutron spectral data in Tables B.3 and B.4.

Table B.2. Comparison of Detailed Model Variant Eigenvalues.

Analysis Code	Neutron Cross Section Library	Calculated			Benchmark	$\frac{C-E}{E}(\%)$
		Δk_{eff}	\pm	σ		
MCNP5	ENDF/B-V.2	0.99548	\pm	0.00004	0.9991 \pm 0.0004	-0.37
	ENDF/B-VI.8	0.99552	\pm	0.00004		-0.36
	ENDF/B-VII.0	0.99737	\pm	0.00004		-0.18
	JEFF-3.1	0.99503	\pm	0.00004		-0.41
	JENDL-3.3	1.00135	\pm	0.00004		0.21
KENO-VI	ENDF/B-VII.0 (continuous energy)	0.99694	\pm	0.00005		-0.22
	ENDF/B-VII.0 (238-group)	0.99687	\pm	0.00006		-0.23

Table B.3. Neutron Spectral Data for Detailed Model Variant (MCNP).

Neutron Cross Section Library	ENDF/B-VII.0	JEFF-3.1	JENDL-3.3
k_{eff}	0.99737	0.99502	1.00135
$\pm\sigma_k$	0.00004	0.00004	0.00004
Neutron Leakage (%) ^(a)	54.34	54.40	54.06
Fission Fraction, by Energy (%)	Thermal (<0.625 eV)	0.00	0.06
	Intermediate	7.49	7.67
	Fast (>100 keV)	92.51	92.27
Fission Fraction, by Isotope (%)	²³⁴ U	0.73	0.75
	²³⁵ U	98.29	98.26
	²³⁶ U	0.08	0.08
	²³⁸ U	0.90	0.91
Average Number of Neutrons Produced per Fission	2.592	2.590	2.597
Energy of Average Neutron Lethargy Causing Fission (MeV)	0.717	0.715	0.727

(a) The neutron leakage is calculated using the neutron balance tables provided in the MCNP output file. The weight fraction of neutrons lost due to escaping the boundaries of the benchmark model are divided by the total weight fraction of neutron loss.

Table B.4. Neutron Spectral Data for Detailed Model Variant (KENO-VI).

Neutron Cross Section Library	ENDF/B-VII.0 (continuous energy)	ENDF/B-VII.0 (238-group)
k_{eff}	0.99694	0.996865
$\pm\sigma_k$	0.00005	0.000055
Average Number of Neutrons Produced per Fission	2.59212 ± 0.00001	2.59165 ± 0.00001
Energy of Average Neutron Lethargy Causing Fission (MeV)	0.71538 ± 0.00007	0.71534 ± 0.00008
Mean Free Path (cm)	1.90193 ± 0.00007	1.90566 ± 0.00007

B.8 MCNP Input Listing for Detailed Model Variant

```

ORALLOY (93.2 235U) METAL CYLINDERS WITH BERYLLIUM TOP HAT
c
c John Darrell Bess - Idaho National Laboratory
c Last Updated: December 1, 2009
c
c
c Cell Cards *****
c --- HEU Cylinders -----
1      1  4.8067E-02  1  -3  -2 imp:n=1 $ Piece 2733
2      2  4.8104E-02  4  -5  -6 imp:n=1 $ Piece 2734
3      3  4.8045E-02  7  -9  -8 imp:n=1 $ Piece 2732
4      4  4.8237E-02 10 -12 -11 imp:n=1 $ Piece 2768
c
c --- Be Cylinders -----
5      5  1.2215E-01 13 -15 -14 imp:n=1 $ 1.5-inch-thick
6      6  1.2176E-01 16 -18 -17 imp:n=1 $ 2-inch-thick
7      7  1.2197E-01 19 -21 -20 imp:n=1 $ 1-inch-thick
8      8  1.2060E-01 22 -24 -23 imp:n=1 $ 0.5-inch-thick
9      9  1.2086E-01 25 -27 -26 imp:n=1 $ 9/16-inch-thick
c
c --- SS304L Disc -----
10     10  8.7029E-02 28 -30 -29 imp:n=1
c
c --- The Great Void -----
11     0  1 -27 -29 #1 #2 #3 #4 #5 #6 #7 #8 #9 #10 imp:n=1 $ Lesser Void
12     0  -1:27:29                                imp:n=0 $ Greater Void
c

c Surface Cards *****
c --- HEU Cylinders -----
c ----- Piece 2733 -----
1      pz  0.000000
2      cz  8.886031
3      pz  3.816604
c ----- Piece 2734 -----
4      pz  3.845560
5      cz  8.885428
6      pz  7.659751
c ----- Piece 2732 -----
7      pz  7.661529
8      cz  8.884920
9      pz 10.204704
c ----- Piece 2768 -----
10     pz 10.206482
11     cz  8.885555
12     pz 10.523982
c
c --- Be Cylinders -----
c ----- 1.5-inch-thick -----
13     pz 10.528808
14     cz  8.885460
15     pz 14.338808
c ----- 2-inch-thick -----
16     pz 14.343634
17     cz  8.885460
18     pz 19.423634
c ----- 1-inch-thick -----
19     pz 19.428460
20     cz  8.885460
21     pz 21.968460
c ----- 0.5-inch-thick -----
22     pz 21.973286
23     cz  8.885460
24     pz 23.243286
c ----- 9/16-inch-thick -----
25     pz 23.248112
26     cz  8.885460
27     pz 24.676862
c

```

NEA/NSC/DOC/(95)03/II
Volume II

HEU-MET-FAST-069

```
c --- SS304L Disc -----
28 pz 3.818382
29 cz 38.100000
30 pz 3.843782
c

c Data Cards *****
c --- Material Cards -----
c ----- HEU Cylinders -----
c ----- Piece 2733 -----
m1 92234.00c 4.6267E-04 92235.00c 4.4702E-02 92236.00c 1.2424E-04
    92238.00c 2.6677E-03 47107.00c 4.3387E-07 47109.00c 4.0309E-07
    56130.00c 4.3554E-13 56132.00c 4.1500E-13 56134.00c 9.9311E-12
    56135.00c 2.7086E-11 56136.00c 3.2271E-11 56137.00c 4.6151E-11
    56138.00c 2.9460E-10 83209.00c 8.8562E-06 6000.00c 4.6978E-06
    20040.00c 2.7297E-08 20042.00c 1.8218E-10 20043.00c 3.8013E-11
    20044.00c 5.8738E-10 20046.00c 1.1263E-12 20048.00c 5.2655E-11
    48106.00c 6.2746E-10 48108.00c 4.4675E-10 48110.00c 6.2695E-09
    48111.00c 6.4251E-09 48112.00c 1.2112E-08 48113.00c 6.1340E-09
    48114.00c 1.4421E-08 48116.00c 3.7597E-09 27059.00c 9.5745E-07
    24050.00c 6.6012E-08 24052.00c 1.2730E-06 24053.00c 1.4435E-07
    24054.00c 3.5931E-08 29063.00c 3.0710E-06 29065.00c 1.3688E-06
    19039.00c 2.6918E-08 19040.00c 3.3770E-12 19041.00c 1.9426E-09
    3006.00c 1.2340E-07 3007.00c 1.5025E-06 12024.00c 1.1003E-06
    12025.00c 1.3929E-07 12026.00c 1.5336E-07 25055.00c 1.1503E-05
    42092.00c 8.7279E-09 42094.00c 5.4403E-09 42095.00c 9.3631E-09
    42096.00c 9.8101E-09 42097.00c 5.6167E-09 42098.00c 1.4192E-08
    42100.00c 5.6638E-09 11023.00c 1.3254E-05 28058.00c 1.3090E-05
    28060.00c 5.0423E-06 28061.00c 2.1918E-07 28062.00c 6.9886E-07
    28064.00c 1.7798E-07 51121.00c 2.0151E-06 51123.00c 1.5072E-06
    22046.00c 1.9445E-08 22047.00c 1.7536E-08 22048.00c 1.7376E-07
    22049.00c 1.2751E-08 22050.00c 1.2209E-08 8016.00c 1.4102E-05
    8017.00c 5.3607E-09 7014.00c 2.4082E-05 7015.00c 8.8949E-08
c      Total 4.8067E-02
c
c ----- Piece 2734 -----
m2 92234.00c 4.5821E-04 92235.00c 4.4751E-02 92236.00c 1.1477E-04
    92238.00c 2.6697E-03 47107.00c 4.3420E-07 47109.00c 4.0340E-07
    56130.00c 4.3587E-13 56132.00c 4.1531E-13 56134.00c 9.9388E-12
    56135.00c 2.7106E-11 56136.00c 3.2296E-11 56137.00c 4.6186E-11
    56138.00c 2.9482E-10 83209.00c 8.8630E-06 6000.00c 4.7015E-06
    20040.00c 2.7318E-08 20042.00c 1.8232E-10 20043.00c 3.8043E-11
    20044.00c 5.8783E-10 20046.00c 1.1272E-12 20048.00c 5.2696E-11
    48106.00c 6.2794E-10 48108.00c 4.4709E-10 48110.00c 6.2744E-09
    48111.00c 6.4301E-09 48112.00c 1.2122E-08 48113.00c 6.1387E-09
    48114.00c 1.4433E-08 48116.00c 3.7626E-09 27059.00c 9.5819E-07
    24050.00c 6.6063E-08 24052.00c 1.2740E-06 24053.00c 1.4446E-07
    24054.00c 3.5958E-08 29063.00c 3.0733E-06 29065.00c 1.3698E-06
    19039.00c 2.6938E-08 19040.00c 3.3796E-12 19041.00c 1.9441E-09
    3006.00c 1.2350E-07 3007.00c 1.5036E-06 12024.00c 1.1011E-06
    12025.00c 1.3940E-07 12026.00c 1.5348E-07 25055.00c 1.1512E-05
    42092.00c 8.7347E-09 42094.00c 5.4444E-09 42095.00c 9.3703E-09
    42096.00c 9.8177E-09 42097.00c 5.6210E-09 42098.00c 1.4203E-08
    42100.00c 5.6681E-09 11023.00c 1.3264E-05 28058.00c 1.3100E-05
    28060.00c 5.0462E-06 28061.00c 2.1935E-07 28062.00c 6.9939E-07
    28064.00c 1.7812E-07 51121.00c 2.0166E-06 51123.00c 1.5083E-06
    22046.00c 1.9460E-08 22047.00c 1.7549E-08 22048.00c 1.7389E-07
    22049.00c 1.2761E-08 22050.00c 1.2218E-08 8016.00c 1.4112E-05
    8017.00c 5.3648E-09 7014.00c 2.4100E-05 7015.00c 8.9017E-08
c      Total 4.8104E-02
c
c ----- Piece 2732 -----
m3 92234.00c 4.5765E-04 92235.00c 4.4692E-02 92236.00c 1.0030E-04
    92238.00c 2.6854E-03 47107.00c 4.3368E-07 47109.00c 4.0291E-07
    56130.00c 4.3534E-13 56132.00c 4.1481E-13 56134.00c 9.9266E-12
    56135.00c 2.7073E-11 56136.00c 3.2256E-11 56137.00c 4.6130E-11
    56138.00c 2.9446E-10 83209.00c 8.8522E-06 6000.00c 4.6957E-06
    20040.00c 2.7284E-08 20042.00c 1.8210E-10 20043.00c 3.7996E-11
    20044.00c 5.8711E-10 20046.00c 1.1258E-12 20048.00c 5.2632E-11
    48106.00c 6.2717E-10 48108.00c 4.4655E-10 48110.00c 6.2667E-09
    48111.00c 6.4222E-09 48112.00c 1.2107E-08 48113.00c 6.1312E-09
    48114.00c 1.4415E-08 48116.00c 3.7580E-09 27059.00c 9.5702E-07
```

NEA/NSC/DOC/(95)03/II
Volume II

HEU-MET-FAST-069

24050.00c	6.5983E-08	24052.00c	1.2724E-06	24053.00c	1.4428E-07
24054.00c	3.5915E-08	29063.00c	3.0696E-06	29065.00c	1.3682E-06
19039.00c	2.6905E-08	19040.00c	3.3755E-12	19041.00c	1.9417E-09
3006.00c	1.2335E-07	3007.00c	1.5018E-06	12024.00c	1.0998E-06
12025.00c	1.3923E-07	12026.00c	1.5329E-07	25055.00c	1.1498E-05
42092.00c	8.7240E-09	42094.00c	5.4378E-09	42095.00c	9.3589E-09
42096.00c	9.8057E-09	42097.00c	5.6142E-09	42098.00c	1.4185E-08
42100.00c	5.6612E-09	11023.00c	1.3248E-05	28058.00c	1.3084E-05
28060.00c	5.0400E-06	28061.00c	2.1909E-07	28062.00c	6.9854E-07
28064.00c	1.7790E-07	51121.00c	2.0142E-06	51123.00c	1.5065E-06
22046.00c	1.9436E-08	22047.00c	1.7528E-08	22048.00c	1.7368E-07
22049.00c	1.2745E-08	22050.00c	1.2204E-08	8016.00c	1.4095E-05
8017.00c	5.3582E-09	7014.00c	2.4071E-05	7015.00c	8.8909E-08
c Total 4.8045E-02					
c					
c ----- Piece 2768 -----					
m4	92234.00c	4.4496E-04	92235.00c	4.4855E-02	92236.00c 1.2468E-04
	92238.00c	2.7009E-03	47107.00c	4.3541E-07	47109.00c 4.0451E-07
	56130.00c	4.3708E-13	56132.00c	4.1646E-13	56134.00c 9.9662E-12
	56135.00c	2.7181E-11	56136.00c	3.2385E-11	56137.00c 4.6314E-11
	56138.00c	2.9564E-10	83209.00c	8.8875E-06	6000.00c 4.7145E-06
	20040.00c	2.7393E-08	20042.00c	1.8283E-10	20043.00c 3.8148E-11
	20044.00c	5.8945E-10	20046.00c	1.1303E-12	20048.00c 5.2842E-11
	48106.00c	6.2967E-10	48108.00c	4.4833E-10	48110.00c 6.2917E-09
	48111.00c	6.4479E-09	48112.00c	1.2155E-08	48113.00c 6.1557E-09
	48114.00c	1.4472E-08	48116.00c	3.7730E-09	27059.00c 9.6084E-07
	24050.00c	6.6246E-08	24052.00c	1.2775E-06	24053.00c 1.4486E-07
	24054.00c	3.6058E-08	29063.00c	3.0818E-06	29065.00c 1.3736E-06
	19039.00c	2.7013E-08	19040.00c	3.3890E-12	19041.00c 1.9494E-09
	3006.00c	1.2384E-07	3007.00c	1.5078E-06	12024.00c 1.1042E-06
	12025.00c	1.3979E-07	12026.00c	1.5391E-07	25055.00c 1.1544E-05
	42092.00c	8.7588E-09	42094.00c	5.4595E-09	42095.00c 9.3962E-09
	42096.00c	9.8448E-09	42097.00c	5.6366E-09	42098.00c 1.4242E-08
	42100.00c	5.6838E-09	11023.00c	1.3301E-05	28058.00c 1.3136E-05
	28060.00c	5.0601E-06	28061.00c	2.1996E-07	28062.00c 7.0133E-07
	28064.00c	1.7861E-07	51121.00c	2.0222E-06	51123.00c 1.5125E-06
	22046.00c	1.9514E-08	22047.00c	1.7598E-08	22048.00c 1.7437E-07
	22049.00c	1.2796E-08	22050.00c	1.2252E-08	8016.00c 1.4151E-05
	8017.00c	5.3796E-09	7014.00c	2.4167E-05	7015.00c 8.9263E-08
c Total 4.8237E-02					
c					
c ----- Be Cylinders -----					
c ----- 1.5-inch-thick -----					
m5	4009.00c	1.2112E-01	13027.00c	2.4672E-05	5010.00c 2.0422E-07
	5011.00c	8.2201E-07	83209.00c	2.6545E-06	35079.00c 3.5191E-09
	35081.00c	3.4233E-09	6000.00c	1.1084E-04	48106.00c 2.4674E-10
	48108.00c	1.7568E-10	48110.00c	2.4655E-09	48111.00c 2.5267E-09
	48112.00c	4.7632E-09	48113.00c	2.4122E-09	48114.00c 5.6712E-09
	48116.00c	1.4785E-09	66156.00c	4.0965E-12	66158.00c 6.8275E-12
	66160.00c	1.5976E-10	66161.00c	1.2911E-09	66162.00c 1.7417E-09
	66163.00c	1.7000E-09	66164.00c	1.9240E-09	26054.00c 1.5096E-06
	26056.00c	2.3697E-05	26057.00c	5.4727E-07	26058.00c 7.2832E-08
	64152.00c	1.4111E-11	64154.00c	1.5381E-10	64155.00c 1.0442E-09
	64156.00c	1.4442E-09	64157.00c	1.1042E-09	64158.00c 1.7526E-09
	64160.00c	1.5423E-09	12024.00c	7.2114E-06	12025.00c 9.1295E-07
	12026.00c	1.0052E-06	28058.00c	1.2869E-08	28060.00c 4.9571E-09
	28061.00c	2.1548E-10	28062.00c	6.8706E-10	28064.00c 1.7497E-10
	8016.00c	8.5578E-04	8017.00c	3.2532E-07	62144.00c 2.2653E-10
	62147.00c	1.1061E-09	62148.00c	8.2937E-10	62149.00c 1.0197E-09
	62150.00c	5.4455E-10	62152.00c	1.9738E-09	62154.00c 1.6787E-09
c Total 1.2215E-01					
mt5	Be.00t OBeO.00t				
c					
c ----- 2-inch-thick -----					
m6	4009.00c	1.2073E-01	13027.00c	2.4594E-05	5010.00c 2.0358E-07
	5011.00c	8.1942E-07	83209.00c	2.6461E-06	35079.00c 3.5080E-09
	35081.00c	3.4125E-09	6000.00c	1.1049E-04	48106.00c 2.4596E-10
	48108.00c	1.7513E-10	48110.00c	2.4577E-09	48111.00c 2.5187E-09
	48112.00c	4.7481E-09	48113.00c	2.4046E-09	48114.00c 5.6533E-09
	48116.00c	1.4738E-09	66156.00c	4.0835E-12	66158.00c 6.8059E-12
	66160.00c	1.5926E-10	66161.00c	1.2870E-09	66162.00c 1.7362E-09
	66163.00c	1.6947E-09	66164.00c	1.9179E-09	26054.00c 1.5048E-06

NEA/NSC/DOC/(95)03/II
Volume II

HEU-MET-FAST-069

26056.00c	2.3622E-05	26057.00c	5.4554E-07	26058.00c	7.2602E-08
64152.00c	1.4066E-11	64154.00c	1.5332E-10	64155.00c	1.0409E-09
64156.00c	1.4397E-09	64157.00c	1.1007E-09	64158.00c	1.7470E-09
64160.00c	1.5374E-09	12024.00c	7.1886E-06	12025.00c	9.1006E-07
12026.00c	1.0020E-06	28058.00c	1.2828E-08	28060.00c	4.9415E-09
28061.00c	2.1480E-10	28062.00c	6.8489E-10	28064.00c	1.7442E-10
8016.00c	8.5308E-04	8017.00c	3.2429E-07	62144.00c	2.2581E-10
62147.00c	1.1026E-09	62148.00c	8.2675E-10	62149.00c	1.0165E-09
62150.00c	5.4283E-10	62152.00c	1.9676E-09	62154.00c	1.6734E-09
c Total 1.2176E-01					
mt6 Be.00t OBeO.00t					
c					
c ----- 1-inch-thick -----					
m7	4009.00c	1.2094E-01	13027.00c	2.4636E-05	5010.00c 2.0393E-07
	5011.00c	8.2083E-07	83209.00c	2.6507E-06	35079.00c 3.5141E-09
	35081.00c	3.4184E-09	6000.00c	1.1069E-04	48106.00c 2.4639E-10
	48108.00c	1.7543E-10	48110.00c	2.4619E-09	48111.00c 2.5230E-09
	48112.00c	4.7563E-09	48113.00c	2.4087E-09	48114.00c 5.6630E-09
	48116.00c	1.4764E-09	66156.00c	4.0906E-12	66158.00c 6.8176E-12
	66160.00c	1.5953E-10	66161.00c	1.2892E-09	66162.00c 1.7392E-09
	66163.00c	1.6976E-09	66164.00c	1.9212E-09	26054.00c 1.5074E-06
	26056.00c	2.3663E-05	26057.00c	5.4648E-07	26058.00c 7.2727E-08
	64152.00c	1.4091E-11	64154.00c	1.5359E-10	64155.00c 1.0427E-09
	64156.00c	1.4422E-09	64157.00c	1.1026E-09	64158.00c 1.7500E-09
	64160.00c	1.5401E-09	12024.00c	7.2010E-06	12025.00c 9.1164E-07
	12026.00c	1.0037E-06	28058.00c	1.2851E-08	28060.00c 4.9500E-09
	28061.00c	2.1517E-10	28062.00c	6.8607E-10	28064.00c 1.7472E-10
	8016.00c	8.5455E-04	8017.00c	3.2485E-07	62144.00c 2.2620E-10
	62147.00c	1.1045E-09	62148.00c	8.2817E-10	62149.00c 1.0183E-09
	62150.00c	5.4377E-10	62152.00c	1.9710E-09	62154.00c 1.6762E-09
c Total 1.2197E-01					
mt7 Be.00t OBeO.00t					
c					
c ----- 0.5-inch-thick -----					
m8	4009.00c	1.1959E-01	13027.00c	2.4360E-05	5010.00c 2.0164E-07
	5011.00c	8.1163E-07	83209.00c	2.6209E-06	35079.00c 3.4747E-09
	35081.00c	3.3801E-09	6000.00c	1.0944E-04	48106.00c 2.4363E-10
	48108.00c	1.7346E-10	48110.00c	2.4343E-09	48111.00c 2.4947E-09
	48112.00c	4.7030E-09	48113.00c	2.3817E-09	48114.00c 5.5995E-09
	48116.00c	1.4598E-09	66156.00c	4.0447E-12	66158.00c 6.7412E-12
	66160.00c	1.5774E-10	66161.00c	1.2748E-09	66162.00c 1.7197E-09
	66163.00c	1.6786E-09	66164.00c	1.8997E-09	26054.00c 1.4905E-06
	26056.00c	2.3398E-05	26057.00c	5.4036E-07	26058.00c 7.1911E-08
	64152.00c	1.3932E-11	64154.00c	1.5186E-10	64155.00c 1.0310E-09
	64156.00c	1.4260E-09	64157.00c	1.0902E-09	64158.00c 1.7304E-09
	64160.00c	1.5228E-09	12024.00c	7.1203E-06	12025.00c 9.0141E-07
	12026.00c	9.9246E-07	28058.00c	1.2706E-08	28060.00c 4.8945E-09
	28061.00c	2.1276E-10	28062.00c	6.7837E-10	28064.00c 1.7276E-10
	8016.00c	8.4497E-04	8017.00c	3.2121E-07	62144.00c 2.2366E-10
	62147.00c	1.0921E-09	62148.00c	8.1889E-10	62149.00c 1.0069E-09
	62150.00c	5.3767E-10	62152.00c	1.9489E-09	62154.00c 1.6574E-09
c Total 1.2060E-01					
mt8 Be.00t OBeO.00t					
c					
c ----- 9/16-inch-thick -----					
m9	4009.00c	1.1984E-01	13027.00c	2.4412E-05	5010.00c 2.0207E-07
	5011.00c	8.1336E-07	83209.00c	2.6265E-06	35079.00c 3.4821E-09
	35081.00c	3.3873E-09	6000.00c	1.0968E-04	48106.00c 2.4415E-10
	48108.00c	1.7383E-10	48110.00c	2.4395E-09	48111.00c 2.5001E-09
	48112.00c	4.7130E-09	48113.00c	2.3868E-09	48114.00c 5.6115E-09
	48116.00c	1.4629E-09	66156.00c	4.0533E-12	66158.00c 6.7556E-12
	66160.00c	1.5808E-10	66161.00c	1.2775E-09	66162.00c 1.7233E-09
	66163.00c	1.6821E-09	66164.00c	1.9037E-09	26054.00c 1.4937E-06
	26056.00c	2.3448E-05	26057.00c	5.4151E-07	26058.00c 7.2065E-08
	64152.00c	1.3962E-11	64154.00c	1.5219E-10	64155.00c 1.0332E-09
	64156.00c	1.4290E-09	64157.00c	1.0925E-09	64158.00c 1.7341E-09
	64160.00c	1.5261E-09	12024.00c	7.1354E-06	12025.00c 9.0334E-07
	12026.00c	9.9457E-07	28058.00c	1.2734E-08	28060.00c 4.9049E-09
	28061.00c	2.1321E-10	28062.00c	6.7982E-10	28064.00c 1.7313E-10
	8016.00c	8.4677E-04	8017.00c	3.2189E-07	62144.00c 2.2414E-10
	62147.00c	1.0944E-09	62148.00c	8.2063E-10	62149.00c 1.0090E-09
	62150.00c	5.3881E-10	62152.00c	1.9530E-09	62154.00c 1.6610E-09

HEU-MET-FAST-069

```

c          Total 1.2086E-01
mt9       Be.00t  OBeO.00t
c
c ----- SS304L Disc -----
m10  26054.00c 3.4799E-03 26056.00c 5.4628E-02 26057.00c 1.2616E-03
      26058.00c 1.6789E-04 24050.00c 7.6013E-04 24052.00c 1.4658E-02
      24053.00c 1.6621E-03 24054.00c 4.1374E-04 28058.00c 5.5530E-03
      28060.00c 2.1390E-03 28061.00c 9.2981E-05 28062.00c 2.9646E-04
      28064.00c 7.5500E-05 25055.00c 8.7145E-04 14028.00c 7.8609E-04
      14029.00c 3.9916E-05 14030.00c 2.6313E-05 6000.00c 5.9791E-05
      15031.00c 3.4778E-05 16032.00c 2.1261E-05 16033.00c 1.7021E-07
      16034.00c 9.6080E-07 16036.00c 4.4792E-09
c          Total 8.7029E-02
mt10     Fe.00t
c
c --- Control Cards -----
mode  n
kcode 250000 1 50 1050
ksrc 0 0 1.908302 0 0 5.752549 0 0 8.933052 0 0 10.365146
print

```

B.9 KENO Input Listing for Detailed Model Variant

```

'Input generated by GeeWiz SCALE 6.0.2 Compiled on February 18, 2009
=csas6
oralloy (93.2 235u) metal cylinders with beryllium top reflector
ce_v7_endf
read composition
u-234      1 0 0.00046267 296  end
u-235      1 0 0.044702 296  end
u-236      1 0 0.00012424 296  end
u-238      1 0 0.0026677 296  end
ag          1 0 8.3696e-07 296
                                     47107 51.839
                                     47109 48.161  end
ba          1 0 4.1089e-10 296
                                     56130 0.106
                                     56132 0.101
                                     56134 2.417
                                     56135 6.592
                                     56136 7.854
                                     56137 11.232
                                     56138 71.698  end
bi          1 0 8.8562e-06 296  end
c           1 0 4.6978e-06 296  end
ca          1 0 2.8158e-08 296
                                     20040 96.941
                                     20042 0.647
                                     20043 0.135
                                     20044 2.086
                                     20046 0.004
                                     20048 0.187  end
cd          1 0 5.0196e-08 296
                                     48106 1.25
                                     48108 0.89
                                     48110 12.49
                                     48111 12.8
                                     48112 24.13
                                     48113 12.22
                                     48114 28.73
                                     48116 7.49  end
co          1 0 9.5745e-07 296  end
cr          1 0 1.5193e-06 296
                                     24050 4.345
                                     24052 83.789
                                     24053 9.501
                                     24054 2.365  end
cu          1 0 4.4398e-06 296
                                     29063 69.17
                                     29065 30.83  end
k           1 0 2.8864e-08 296
                                     19039 93.2581

```

Revision: 0

Date: September 30, 2010

NEA/NSC/DOC/(95)03/II
Volume II

HEU-MET-FAST-069

			19040 0.0117	
			19041 6.7302	end
li	1 0 1.6259e-06 296		3006 7.59	
			3007 92.41	end
mg	1 0 1.3929e-06 296		12024 78.99	
			12025 10	
			12026 11.01	end
mn	1 0 1.1503e-05 296		end	
mo	1 0 5.8814e-08 296		42092 14.84	
			42094 9.25	
			42095 15.92	
			42096 16.68	
			42097 9.55	
			42098 24.13	
			42100 9.63	end
na	1 0 1.3254e-05 296		end	
ni	1 0 1.9228e-05 296		28058 68.0769	
			28060 26.2231	
			28061 1.1399	
			28062 3.6345	
			28064 0.9256	end
sb	1 0 3.5223e-06 296		51121 57.21	
			51123 42.79	end
ti	1 0 2.357e-07 296		22046 8.25	
			22047 7.44	
			22048 73.72	
			22049 5.41	
			22050 5.18	end
o-16	1 0 1.4102e-05 296		end	
o-17	1 0 5.3607e-09 296		end	
n-14	1 0 2.4082e-05 296		end	
n-15	1 0 8.8949e-08 296		end	
u-234	2 0 0.00045821 296		end	
u-235	2 0 0.044751 296	end		
u-236	2 0 0.00011477 296	end		
u-238	2 0 0.0026697 296	end		
ag	2 0 8.3760e-07 296		47107 51.839	
			47109 48.161	end
ba	2 0 4.1120e-10 296		56130 0.106	
			56132 0.101	
			56134 2.417	
			56135 6.592	
			56136 7.854	
			56137 11.232	
			56138 71.698	end
bi	2 0 8.8630e-06 296	end		
c	2 0 4.7015e-06 296	end		
ca	2 0 2.8180e-08 296		20040 96.941	
			20042 0.647	
			20043 0.135	
			20044 2.086	
			20046 0.004	
			20048 0.187	end
cd	2 0 5.0235e-08 296		48106 1.25	
			48108 0.89	
			48110 12.49	
			48111 12.8	
			48112 24.13	
			48113 12.22	
			48114 28.73	
			48116 7.49	end
co	2 0 9.5819e-07 296	end		

NEA/NSC/DOC/(95)03/II
Volume II

HEU-MET-FAST-069

cr	2	0	1.5204e-06	296	24050 4.345	
					24052 83.789	
					24053 9.501	
					24054 2.365	end
cu	2	0	4.4432e-06	296	29063 69.17	
					29065 30.83	end
k	2	0	2.8886e-08	296	19039 93.2581	
					19040 0.0117	
					19041 6.7302	end
li	2	0	1.6271e-06	296	3006 7.59	
					3007 92.41	end
mg	2	0	1.394e-06	296	12024 78.99	
					12025 10	
					12026 11.01	end
mn	2	0	1.1512e-05	296	end	
mo	2	0	5.8859e-08	296	42092 14.84	
					42094 9.25	
					42095 15.92	
					42096 16.68	
					42097 9.55	
					42098 24.13	
					42100 9.63	end
na	2	0	1.3264e-05	296	end	
ni	2	0	1.9243e-05	296	28058 68.0769	
					28060 26.2231	
					28061 1.1399	
					28062 3.6345	
					28064 0.9256	end
sb	2	0	3.5250e-06	296	51121 57.21	
					51123 42.79	end
ti	2	0	2.3588e-07	296	22046 8.25	
					22047 7.44	
					22048 73.72	
					22049 5.41	
					22050 5.18	end
o-16	2	0	1.4112e-05	296	end	
o-17	2	0	5.3648e-09	296	end	
n-14	2	0	2.41e-05	296	end	
n-15	2	0	8.9017e-08	296	end	
u-234	3	0	0.00045765	296	end	
u-235	3	0	0.044692	296	end	
u-236	3	0	0.0001003	296	end	
u-238	3	0	0.0026854	296	end	
ag	3	0	8.3658e-07	296	47107 51.839	
					47109 48.161	end
ba	3	0	4.1070e-10	296	56130 0.106	
					56132 0.101	
					56134 2.417	
					56135 6.592	
					56136 7.854	
					56137 11.232	
					56138 71.698	end
bi	3	0	8.8522e-06	296	end	
c	3	0	4.6957e-06	296	end	
ca	3	0	2.8145e-08	296	20040 96.941	
					20042 0.647	
					20043 0.135	
					20044 2.086	
					20046 0.004	
					20048 0.187	end

HEU-MET-FAST-069

cd	3	0	5.0174e-08	296	
					48106 1.25
					48108 0.89
					48110 12.49
					48111 12.8
					48112 24.13
					48113 12.22
					48114 28.73
					48116 7.49 end
co	3	0	9.5702e-07	296	end
cr	3	0	1.5186e-06	296	
					24050 4.345
					24052 83.789
					24053 9.501
					24054 2.365 end
cu	3	0	4.4378e-06	296	
					29063 69.17
					29065 30.83 end
k	3	0	2.8851e-08	296	
					19039 93.2581
					19040 0.0117
					19041 6.7302 end
li	3	0	1.6251e-06	296	
					3006 7.59
					3007 92.41 end
mg	3	0	1.3923e-06	296	
					12024 78.99
					12025 10
					12026 11.01 end
mn	3	0	1.1498e-05	296	end
mo	3	0	5.8787e-08	296	
					42092 14.84
					42094 9.25
					42095 15.92
					42096 16.68
					42097 9.55
					42098 24.13
					42100 9.63 end
na	3	0	1.3248e-05	296	end
ni	3	0	1.9220e-05	296	
					28058 68.0769
					28060 26.2231
					28061 1.1399
					28062 3.6345
					28064 0.9256 end
sb	3	0	3.5207e-06	296	
					51121 57.21
					51123 42.79 end
ti	3	0	2.3559e-07	296	
					22046 8.25
					22047 7.44
					22048 73.72
					22049 5.41
					22050 5.18 end
o-16	3	0	1.4095e-05	296	end
o-17	3	0	5.3582e-09	296	end
n-14	3	0	2.4071e-05	296	end
n-15	3	0	8.8909e-08	296	end
u-234	4	0	0.00044496	296	end
u-235	4	0	0.044855	296	end
u-236	4	0	0.00012468	296	end
u-238	4	0	0.0027009	296	end
ag	4	0	8.3992e-07	296	
					47107 51.839
					47109 48.161 end
ba	4	0	4.1234e-10	296	
					56130 0.106
					56132 0.101
					56134 2.417
					56135 6.592
					56136 7.854
					56137 11.232

HEU-MET-FAST-069

				56138	71.698	end
bi	4	0	8.8875e-06	296	end	
c	4	0	4.7145e-06	296	end	
ca	4	0	2.8258e-08	296		
				20040	96.941	
				20042	0.647	
				20043	0.135	
				20044	2.086	
				20046	0.004	
				20048	0.187	end
cd	4	0	5.0374e-08	296		
				48106	1.25	
				48108	0.89	
				48110	12.49	
				48111	12.8	
				48112	24.13	
				48113	12.22	
				48114	28.73	
				48116	7.49	end
co	4	0	9.6084e-07	296	end	
cr	4	0	1.5246e-06	296		
				24050	4.345	
				24052	83.789	
				24053	9.501	
				24054	2.365	end
cu	4	0	4.4555e-06	296		
				29063	69.17	
				29065	30.83	end
k	4	0	2.8966e-08	296		
				19039	93.2581	
				19040	0.0117	
				19041	6.7302	end
li	4	0	1.6316e-06	296		
				3006	7.59	
				3007	92.41	end
mg	4	0	1.3979e-06	296		
				12024	78.99	
				12025	10	
				12026	11.01	end
mn	4	0	1.1544e-05	296	end	
mo	4	0	5.9022e-08	296		
				42092	14.84	
				42094	9.25	
				42095	15.92	
				42096	16.68	
				42097	9.55	
				42098	24.13	
				42100	9.63	end
na	4	0	1.3301e-05	296	end	
ni	4	0	1.9296e-05	296		
				28058	68.0769	
				28060	26.2231	
				28061	1.1399	
				28062	3.6345	
				28064	0.9256	end
sb	4	0	3.5347e-06	296		
				51121	57.21	
				51123	42.79	end
ti	4	0	2.3653e-07	296		
				22046	8.25	
				22047	7.44	
				22048	73.72	
				22049	5.41	
				22050	5.18	end
o-16	4	0	1.4151e-05	296	end	
o-17	4	0	5.3796e-09	296	end	
n-14	4	0	2.4167e-05	296	end	
n-15	4	0	8.9263e-08	296	end	
bebound	5	0	0.12112	296	end	
al	5	0	2.4672e-05	296	end	
b	5	0	1.0262e-06	296		
				5010	19.9	

HEU-MET-FAST-069

			5011 80.1 end
bi	5 0 2.6545e-06 296		end
br	5 0 6.9425e-09 296		
			35079 50.69
			35081 49.31 end
c	5 0 0.00011084 296		end
cd	5 0 1.974e-08 296		
			48106 1.25
			48108 0.89
			48110 12.49
			48111 12.8
			48112 24.13
			48113 12.22
			48114 28.73
			48116 7.49 end
dy	5 0 6.8275e-09 296		
			66156 0.06
			66158 0.1
			66160 2.34
			66161 18.91
			66162 25.51
			66163 24.9
			66164 28.18 end
fe	5 0 2.5827e-05 296		
			26054 5.845
			26056 91.754
			26057 2.119
			26058 0.282 end
gd	5 0 7.0554e-09 296		
			64152 0.2
			64154 2.18
			64155 14.8
			64156 20.47
			64157 15.65
			64158 24.84
			64160 21.86 end
mg	5 0 9.1295e-06 296		
			12024 78.99
			12025 10
			12026 11.01 end
ni	5 0 1.8904e-08 296		
			28058 68.0769
			28060 26.2231
			28061 1.1399
			28062 3.6345
			28064 0.9256 end
o-16	5 0 0.00085578 296		end
o-17	5 0 3.2532e-07 296		end
sm	5 0 7.3787e-09 296		
			62144 3.07
			62147 14.99
			62148 11.24
			62149 13.82
			62150 7.38
			62152 26.75
			62154 22.75 end
bebound	6 0 0.12073 296	end	
al	6 0 2.4594e-05 296		end
b	6 0 1.023e-06 296		
			5010 19.9
			5011 80.1 end
bi	6 0 2.6461e-06 296		end
br	6 0 6.9205e-09 296		
			35079 50.69
			35081 49.31 end
c	6 0 0.00011049 296		end
cd	6 0 1.9677e-08 296		
			48106 1.25
			48108 0.89
			48110 12.49
			48111 12.8
			48112 24.13

HEU-MET-FAST-069

			48113	12.22	
			48114	28.73	
			48116	7.49	end
dy	6 0 6.8059e-09	296			
			66156	0.06	
			66158	0.1	
			66160	2.34	
			66161	18.91	
			66162	25.51	
			66163	24.9	
			66164	28.18	end
fe	6 0 2.5745e-05	296			
			26054	5.845	
			26056	91.754	
			26057	2.119	
			26058	0.282	end
gd	6 0 7.0331e-09	296			
			64152	0.2	
			64154	2.18	
			64155	14.8	
			64156	20.47	
			64157	15.65	
			64158	24.84	
			64160	21.86	end
mg	6 0 9.1006e-06	296			
			12024	78.99	
			12025	10	
			12026	11.01	end
ni	6 0 1.8844e-08	296			
			28058	68.0769	
			28060	26.2231	
			28061	1.1399	
			28062	3.6345	
			28064	0.9256	end
o-16	6 0 0.00085308	296			end
o-17	6 0 3.2429e-07	296			end
sm	6 0 7.3554e-09	296			
			62144	3.07	
			62147	14.99	
			62148	11.24	
			62149	13.82	
			62150	7.38	
			62152	26.75	
			62154	22.75	end
bebound	7 0 0.12094	296			end
al	7 0 2.4636e-05	296			end
b	7 0 1.0248e-06	296			
			5010	19.9	
			5011	80.1	end
bi	7 0 2.6507e-06	296			end
br	7 0 6.9325e-09	296			
			35079	50.69	
			35081	49.31	end
c	7 0 0.00011069	296			end
cd	7 0 1.9711e-08	296			
			48106	1.25	
			48108	0.89	
			48110	12.49	
			48111	12.8	
			48112	24.13	
			48113	12.22	
			48114	28.73	
			48116	7.49	end
dy	7 0 6.8176e-09	296			
			66156	0.06	
			66158	0.1	
			66160	2.34	
			66161	18.91	
			66162	25.51	
			66163	24.9	
			66164	28.18	end
fe	7 0 2.579e-05	296			

HEU-MET-FAST-069

			26054	5.845	
			26056	91.754	
			26057	2.119	
			26058	0.282	end
gd	7 0	7.0453e-09	296		
			64152	0.2	
			64154	2.18	
			64155	14.8	
			64156	20.47	
			64157	15.65	
			64158	24.84	
			64160	21.86	end
mg	7 0	9.1164e-06	296		
			12024	78.99	
			12025	10	
			12026	11.01	end
ni	7 0	1.8877e-08	296		
			28058	68.0769	
			28060	26.2231	
			28061	1.1399	
			28062	3.6345	
			28064	0.9256	end
o-16	7 0	0.00085455	296	end	
o-17	7 0	3.2485e-07	296	end	
sm	7 0	7.3681e-09	296		
			62144	3.07	
			62147	14.99	
			62148	11.24	
			62149	13.82	
			62150	7.38	
			62152	26.75	
			62154	22.75	end
bebound	8 0	0.11959	296	end	
al	8 0	2.436e-05	296	end	
b	8 0	1.0133e-06	296		
			5010	19.9	
			5011	80.1	end
bi	8 0	2.6209e-06	296	end	
br	8 0	6.8547e-09	296		
			35079	50.69	
			35081	49.31	end
c	8 0	0.00010944	296	end	
cd	8 0	1.949e-08	296		
			48106	1.25	
			48108	0.89	
			48110	12.49	
			48111	12.8	
			48112	24.13	
			48113	12.22	
			48114	28.73	
			48116	7.49	end
dy	8 0	6.7412e-09	296		
			66156	0.06	
			66158	0.1	
			66160	2.34	
			66161	18.91	
			66162	25.51	
			66163	24.9	
			66164	28.18	end
fe	8 0	2.55e-05	296		
			26054	5.845	
			26056	91.754	
			26057	2.119	
			26058	0.282	end
gd	8 0	6.9662e-09	296		
			64152	0.2	
			64154	2.18	
			64155	14.8	
			64156	20.47	
			64157	15.65	
			64158	24.84	
			64160	21.86	end

HEU-MET-FAST-069

mg	8 0 9.0141e-06 296	12024 78.99	
		12025 10	
		12026 11.01	end
ni	8 0 1.8665e-08 296	28058 68.0769	
		28060 26.2231	
		28061 1.1399	
		28062 3.6345	
		28064 0.9256	end
o-16	8 0 0.00084497 296	end	
o-17	8 0 3.2121e-07 296	end	
sm	8 0 7.2855e-09 296	62144 3.07	
		62147 14.99	
		62148 11.24	
		62149 13.82	
		62150 7.38	
		62152 26.75	
		62154 22.75	end
bebound	9 0 0.11984 296	end	
al	9 0 2.4412e-05 296	end	
b	9 0 1.0154e-06 296	5010 19.9	
		5011 80.1	end
bi	9 0 2.6265e-06 296	end	
br	9 0 6.8694e-09 296	35079 50.69	
		35081 49.31	end
c	9 0 0.00010968 296	end	
cd	9 0 1.9532e-08 296	48106 1.25	
		48108 0.89	
		48110 12.49	
		48111 12.8	
		48112 24.13	
		48113 12.22	
		48114 28.73	
		48116 7.49	end
dy	9 0 6.7556e-09 296	66156 0.06	
		66158 0.1	
		66160 2.34	
		66161 18.91	
		66162 25.51	
		66163 24.9	
		66164 28.18	end
fe	9 0 2.5555e-05 296	26054 5.845	
		26056 91.754	
		26057 2.119	
		26058 0.282	end
gd	9 0 6.9811e-09 296	64152 0.2	
		64154 2.18	
		64155 14.8	
		64156 20.47	
		64157 15.65	
		64158 24.84	
		64160 21.86	end
mg	9 0 9.0334e-06 296	12024 78.99	
		12025 10	
		12026 11.01	end
ni	9 0 1.8705e-08 296	28058 68.0769	
		28060 26.2231	
		28061 1.1399	
		28062 3.6345	
		28064 0.9256	end
o-16	9 0 0.00084677 296	end	
o-17	9 0 3.2189e-07 296	end	

HEU-MET-FAST-069

```

sm          9 0 7.301e-09 296
              62144 3.07
              62147 14.99
              62148 11.24
              62149 13.82
              62150 7.38
              62152 26.75
              62154 22.75    end
fe          10 0 0.059537 296
              26054 5.845
              26056 91.754
              26057 2.119
              26058 0.282    end
cr          10 0 0.017494 296
              24050 4.345
              24052 83.789
              24053 9.501
              24054 2.365    end
ni          10 0 0.0081569 296
              28058 68.0769
              28060 26.2231
              28061 1.1399
              28062 3.6345
              28064 0.9256    end
mn          10 0 0.00087145 296    end
si          10 0 0.00085232 296
              14028 92.2297
              14029 4.6832
              14030 3.0871    end
c           10 0 5.9791e-05 296    end
p           10 0 3.4778e-05 296    end
s           10 0 2.2396e-05 296
              16032 94.93
              16033 0.76
              16034 4.29
              16036 0.02    end

end composition
read parameter
  gen=1050
  npg=250000
  nsk=50
  htm=yes
end parameter
read geometry
global unit 1
com='global unit 1'
cylinder 1 8.886031 3.816604 0
cylinder 2 8.885428 7.659751 3.84556
cylinder 3 8.88492 10.204704 7.661529
cylinder 4 8.885555 10.523982 10.206482
cylinder 5 8.885484 14.338808 10.528808
cylinder 6 8.885484 19.423634 14.343634
cylinder 7 8.885484 21.968460 19.428460
cylinder 8 8.885484 23.243286 21.973286
cylinder 9 8.885484 24.676862 23.248112
cylinder 10 38.1 3.843782 3.818382
cylinder 11 38.1 24.676862 0
media 1 1 1
media 2 1 2
media 3 1 3
media 4 1 4
media 5 1 5
media 6 1 6
media 7 1 7
media 8 1 8
media 9 1 9
media 10 1 10
media 0 1 -1 -2 -3 -4 -5 -6 -7 -8 -9 -10 11
boundary 11
end geometry
end data
end

```

APPENDIX C: CALCULATED SPECTRAL DATA

The neutron spectral calculations provided below were obtained from the output files for the input decks provided in Appendix A and results in Section 4. Only spectral data using the ENDF/B-VII.0, JEFF-3.1, and JENDL-3.3 neutron cross section libraries are provided here for the MCNP5 analyses and ENDF/B-VII.0 (continuous energy and 238-group) libraries for the KENO analyses. The cross sections are all continuous in the MCNP5 analyses.

C.1 MCNP-Calculated Neutron Spectral Data

C.1.1 Detailed Model

A summary of the computed neutron spectral data using MCNP5 for the detailed benchmark model is provided in Table C.1.

Table C.1. Neutron Spectral Data for Detailed Benchmark Model.

Neutron Cross Section Library	ENDF/B-VII.0	JEFF-3.1	JENDL-3.3
k_{eff}	0.99802	0.99578	1.00217
$\pm\sigma_k$	0.00004	0.00004	0.00004
Neutron Leakage (%) ^(a)	54.32	54.38	54.04
Fission Fraction, by Energy (%)	Thermal (<0.625 eV)	0.00	0.06
	Intermediate	7.48	7.66
	Fast (>100 keV)	92.51	92.28
Fission Fraction, by Isotope (%)	²³⁴ U	0.73	0.73
	²³⁵ U	98.29	98.27
	²³⁶ U	0.08	0.08
	²³⁸ U	0.90	0.91
Average Number of Neutrons Produced per Fission	2.592	2.590	2.597
Energy of Average Neutron Lethargy Causing Fission (MeV)	0.718	0.715	0.727

(a) The neutron leakage is calculated using the neutron balance tables provided in the MCNP output file. The weight fraction of neutrons lost due to escaping the boundaries of the benchmark model are divided by the total weight fraction of neutron loss.

C.1.2 Simple Model

A summary of the computed neutron spectral data using MCNP5 for the detailed benchmark model is provided in Table C.2.

Table C.2. Neutron Spectral Data for Simple Benchmark Model.

Neutron Cross Section Library	ENDF/B-VII.0	JEFF-3.1	JENDL-3.3
k_{eff}	0.99781	0.99531	1.00166
$\pm\sigma_k$	0.00004	0.00004	0.00004
Neutron Leakage (%) ^(a)	54.34	54.40	54.07
Fission Fraction, by Energy (%)	Thermal (<0.625 eV)	0.06	0.06
	Intermediate	7.42	7.64
	Fast (>100 keV)	92.51	92.30
Fission Fraction, by Isotope (%)	²³⁴ U	0.74	0.73
	²³⁵ U	98.28	98.27
	²³⁶ U	0.08	0.08
	²³⁸ U	0.90	0.91
Average Number of Neutrons Produced per Fission	2.592	2.590	2.597
Energy of Average Neutron Lethargy Causing Fission (MeV)	0.715	0.717	0.729

(a) The neutron leakage is calculated using the neutron balance tables provided in the MCNP output file. The weight fraction of neutrons lost due to escaping the boundaries of the benchmark model are divided by the total weight fraction of neutron loss.

C.1.3 Comparison of Models

A direct comparison of the results tabulated in Tables C.1 and C.2 for the detailed and simple benchmark models, respectively, shows minimal significant difference. These differences are shown in Table C.3.

It should be noted, that in the calculation of the detailed model using the ENDF/B-VII.0 library, if the effects of thermal scattering from oxygen in BeO are not included, then the fission fraction by energy for the thermal and intermediate energies are approximately identical between the calculated neutron spectra from both detailed and simple models (matching those obtained from the simple models).

Table C.3. Comparison of Benchmark Model Neutron Spectral Data.

Neutron Cross Section Library	ENDF/B-VII.0	JEFF-3.1	JENDL-3.3
Δk_{eff}	-0.00023	-0.00031	-0.00036
$\pm \sigma_{\Delta k}$	0.00006	0.00006	0.00006
Neutron Leakage (%) ^(a)	0.02	0.02	0.03
Fission Fraction, by Energy (%)	Thermal (<0.625 eV)	0.06	0.00
	Intermediate	-0.06	-0.02
	Fast (>100 keV)	0.00	0.02
Fission Fraction, by Isotope (%)	²³⁴ U	0.00	0.00
	²³⁵ U	0.00	0.00
	²³⁶ U	0.00	0.00
	²³⁸ U	0.00	0.00
Average Number of Neutrons Produced per Fission	0.000	0.000	0.000
Energy of Average Neutron Lethargy Causing Fission (MeV)	-0.003	0.002	0.002

(a) The neutron leakage is calculated using the neutron balance tables provided in the MCNP output file. The weight fraction of neutrons lost due to escaping the boundaries of the benchmark model are divided by the total weight fraction of neutron loss.

C.2 KENO-Calculated Neutron Spectral Data

C.2.1 Detailed Model

A summary of the computed neutron spectral data using KENO-VI for the detailed benchmark model is provided in Table C.4. There isn't a significant difference between the use of continuous energy or 238-group methods.

Table C.4. Neutron Spectral Data for Detailed Benchmark Model.

Neutron Cross Section Library	ENDF/B-VII.0 (continuous energy) ^(a)	ENDF/B-VII.0 (238-group)
k_{eff}	0.99769	0.997642
$\pm\sigma_k$	0.00007	0.000051
Average Number of Neutrons Produced per Fission	2.59223 \pm 0.00001	2.59176 \pm 0.00001
Energy of Average Neutron Lethargy Causing Fission (MeV)	0.71606 \pm 0.00007	0.71559 \pm 0.00008
Mean Free Path (cm)	1.90023 \pm 0.00007	1.90351 \pm 0.00006

(a) These results were obtained using a slightly different KENO-VI input deck than what is described in Section 3 and provided in Appendix A; the gap thickness between the bottom two HEU discs is twice that used in the benchmark model. There is no significant effect in the calculated results.

C.2.2 Simple Model

A summary of the computed neutron spectral data using KENO-V.a for the simple benchmark model is provided in Table C.5. There isn't a significant difference between the use of continuous energy or 238-group methods.

Table C.5. Neutron Spectral Data for Simple Benchmark Model.

Neutron Cross Section Library	ENDF/B-VII.0 (continuous energy)	ENDF/B-VII.0 (238-group)
k_{eff}	0.997137	0.997255
$\pm\sigma_k$	0.000054	0.000049
Average Number of Neutrons Produced per Fission	2.59234 \pm 0.00001	2.59187 \pm 0.00001
Energy of Average Neutron Lethargy Causing Fission (MeV)	0.717536 \pm 0.00007	0.71588 \pm 0.00008
Mean Free Path (cm)	0.90742 \pm 0.00007	0.91040 \pm 0.00007

C.2.3 Comparison of Models

A direct comparison of the results tabulated in Tables C.4 and C.5 for the detailed and simple benchmark models, respectively, shows minimal significant difference. These differences are shown in Table C.6.

Table C.6. Comparison of Benchmark Model Neutron Spectral Data.

Neutron Cross Section Library	ENDF/B-VII.0 (continuous energy) ^(a)	ENDF/B-VII.0 (238-group)
Δk_{eff}	-0.000556	-0.000387
$\pm \sigma_{\Delta k}$	0.000086	0.000071
Average Number of Neutrons Produced per Fission	0.00011 \pm 0.00002	0.00011 \pm 0.00002
Energy of Average Neutron Lethargy Causing Fission (MeV)	0.00147 \pm 0.00010	0.00028 \pm 0.00011
Mean Free Path (cm)	0.00719 \pm 0.00010	0.00689 \pm 0.00009

(a) These results were obtained using a slightly different KENO-VI input deck than what is described in Section 3 and provided in Appendix A; the gap thickness between the bottom two HEU discs is twice that used in the benchmark model. There is no significant effect in the calculated results.

C.3 Inter-Code Comparison

C.3.1 Comparison of Results between Monte Carlo Methods

A direct comparison of the results tabulated in Tables C.1, C.2, C.4, and C.5 for both simple and detailed benchmark model results calculated using MCNP5 and KENO-VI/-V.a and the continuous energy ENDF/B-VII.0 neutron cross section libraries. These differences are shown in Table C.7. There is not a significant difference between results from the two different Monte Carlo analysis methods.

Table C.7. Inter-Code Comparison of Benchmark Model Neutron Spectral Data.

Benchmark Model	Detailed	Simple
Neutron Cross Section Library	ENDF/B-VII.0 (continuous energy) ^(a)	ENDF/B-VII.0 (continuous energy)
Δk_{eff}	-0.00035	-0.00067
$\pm \sigma_{\Delta k}$	0.00008	0.00007
Average Number of Neutrons Produced per Fission	0.00023	0.00034
Energy of Average Neutron Lethargy Causing Fission (MeV)	-0.00194	0.00246

(a) These results were obtained using a slightly different KENO-VI input deck than what is described in Section 3 and provided in Appendix A; the gap thickness between the bottom two HEU discs is twice that used in the benchmark model. There is no significant effect in the calculated results.

APPENDIX D: BERYLLIUM MODERATOR/REFLECTOR WORTH

The worth of the beryllium moderator/reflector was determined by comparing this benchmark experiment with a similar bare HEU cylinder benchmark experiment evaluated in [HEU-MET-FAST-051](#) (Configuration 14). This experiment utilized many of the same HEU discs and had a diameter of 7 inches (17.78 cm). Both the beryllium-moderated/reflected experiment and the bare HEU experiment had k_{eff} eigenvalues very close to 1.0000 and a β_{eff} of 0.0066. A summary of the parts and total mass of the two experiments is provided in Table D.1. The reflector mass savings (the reduction in critical mass by addition of the beryllium top reflector to an unreflected cylinder of the same diameter) is 9.922 kg HEU. The worth of the beryllium was estimated using MCNP calculations for the configuration in this report with and without the beryllium reflector. A summary of the worth calculations using ENDF/B-VII.0, JEFF-3.1, and JENDL-3.3 neutron cross section data is provided in Table D.2. The worth of the beryllium is estimated to be $10.7 \pm 0.5\%$.

Table D.1. Comparison of Bare and Be-Reflected HEU Cylinders.

Bare HEU Cylinder ^(a)		Be-Reflected Cylinder	
Part (Type) ^(b)	Mass (g)	Part (Type) ^(b)	Mass (g)
3102 (Thin Foil)	38.5	2768 (7" Disc)	1481
3103 (Thin Foil)	38.5	2732 (7" Disc)	11814
3101 (Thin Foil)	240	2734 (7" Disc)	17742
2734 (7" Disc)	17742	2733 (7" Disc)	17742
2732 (7" Disc)	11814	--	--
2729 (7" Disc)	4440	--	--
2730 (7" Disc)	6646	--	--
2733 (7" Disc)	17742	--	--
Total	58701	Total	48779

(a) [HEU-MET-FAST-051](#) (Configuration 14).

(b) Parts listed in order from top to bottom of stack.

Table D.2. Calculated Worth of Beryllium Reflector.

Neutron Cross Section Library	Calculated Worth (ρ)	1σ
ENDF/B-VII.0	0.07019	0.00006
JEFF-3.1	0.07144	0.00006
JENDL-3.3	0.06992	0.00006
Average	0.07052	0.00081 ^(a)
Worth ($\rho\%$) ^(b)	10.68	0.54

(a) The standard deviation is of the population, and not the average of the calculated statistical uncertainties.

(b) $\beta_{\text{eff}} = 0.0066$ with an uncertainty of $\pm 5\%$.

APPENDIX E: Support Structure Assembly Schematics

Additional drawings were provided by the experimenter^a to preserve the dimensions of the support structure immediately surrounding the experiment. Figure E.1 represents the diaphragm and rings with its support structure. Figure E.2 represents the low-mass support structure. Both of these structures can be seen in Figure 3. These support structures were used in many other critical experiments with oralloy at ORCEF although the details of these support structures were not presented in the previous benchmarks: [HEU-MET-FAST-051](#), [HEU-MET-FAST-071](#), and [HEU-MET-FAST-076](#).

^a Personal communication with John T. Mihalcz, February 2010.

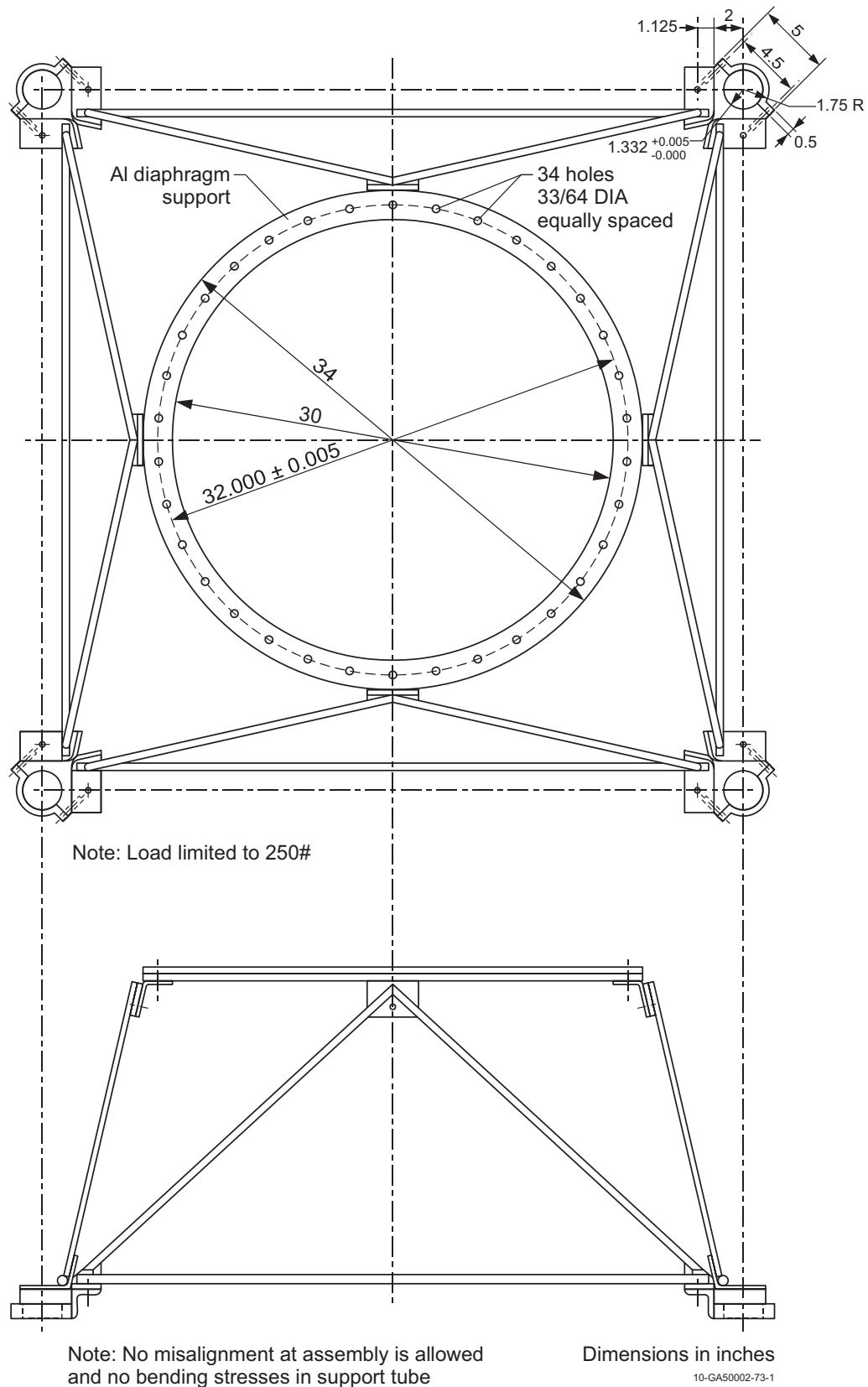
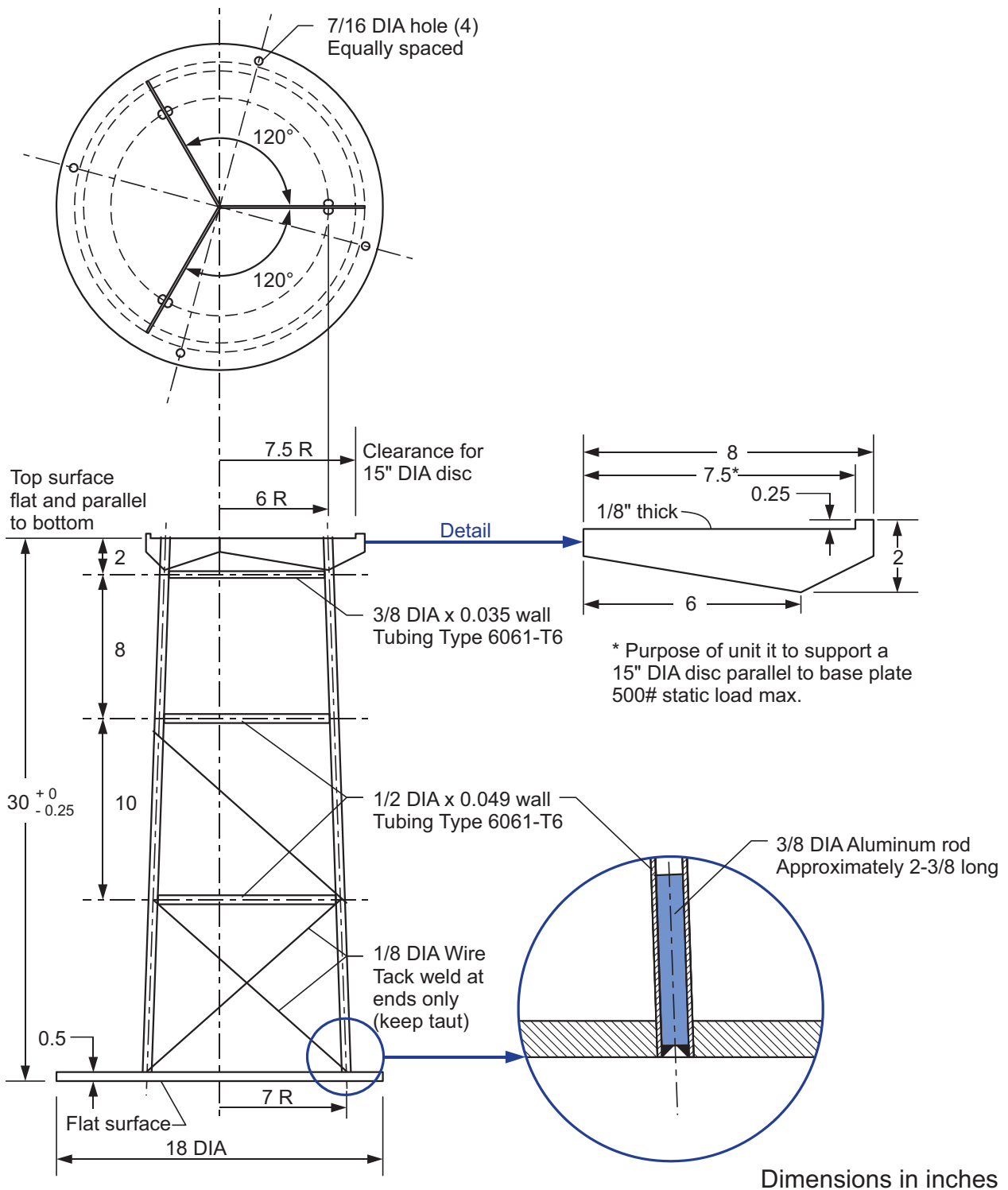


Figure E.1. Diaphragm Support Structure.



10-GA50002-73-2

Figure E.2. Low-Mass Support Structure.